WSRC-TR-96-0399
Revision 0

INTEGRATED HYDROGEOLOGICAL MODEL OF THE GENERAL SEPARATIONS AREA (U)

VOLUME 1: HYDROGEOLOGIC FRAMEWORK (U)

Andrew D. Smits, Mary K. Harris, Kelley L. Hawkins,

and Gregory P. Flach

Publication Date: August, 1997

Westinghouse Savannah River Company
Savannah River Site
Aiken, S.C. 29802

SAFETY • RESPONSIBILITY • SECURITY
SRS
SAVANNAH RIVER SITE

Prepared for the US Department of Energy Contract Number DE-AC09-96SR18500

DISCLAIMER

WSRC-TR-96-0399
Revision 0

INTEGRATED HYDROGEOLOGICAL MODEL OF THE GENERAL SEPARATIONS AREA (U)

VOLUME 1: HYDROGEOLOGIC FRAMEWORK (U)

Andrew D. Smits, Mary K. Harris, Kelley L. Hawkins,

and Gregory P. Flach

Publication Date: August, 1997

Westinghouse Savannah River Company
Savannah River Site
Aiken, S.C. 29802

SAFETY • RESPONSIBILITY • SECURITY
SRS
SAVANNAH RIVER SITE

Prepared for the US Department of Energy Contract Number DE-AC09-96SR18500

INTEGRATED HYDROGEOLOGICAL MODEL OF THE GENERAL SEPARATIONS AREA

VOLUME 1:

HYDROGEOLOGIC FRAMEWORK (U)

Authentication and Approvals:

A.D. Smits, Author, SAIC — Date: 8/4/97

M.K. Harris, Author, WSRC — Date: 8/4/97

K.L. Hawkins, Author, SAIC — Date: 8/4/97

G.P. Flach, Author, WSRC — Date: 8/4/97

J.G. Sonnenberg, Manager, WSRC/SRTC/ERTS — Date: 8/5/97

ABSTRACT

Determining lateral and vertical sedimentologic variations within hydrostratigraphic units is essential for accurate modeling of ground-water flow and contaminant transport. Data from detailed, foot-by-foot, lithologic descriptions of cores are used to construct a model of the hydrogeologic framework beneath the General Separations Area at the Savannah River Site. The model uses EarthVision® software to produce two-dimensional surfaces based on the stratigraphic boundaries picked from the geologic and geophysical data. The surfaces are used to integrate lithologic and other property data into a three-dimensional model. The three-dimensional property model can be summarized in two-dimensional maps specific to each hydrostratigraphic unit.

This report models the Gordon aquifer, the Gordon confining unit, and the "lower" aquifer zone, "tan clay" confining zone, and "upper" aquifer zone of the Water Table aquifer. The report presents structure-contour and isopach maps of each unit. Lithofacies maps include percent mud, sand-mud ratio, percent calcareous sediment, and clastic ratio. Vertical hydraulic conductivity and leakance are modeled for the Gordon confining unit and "tan clay" confining zone of the Water Table aquifer.

Lithofacies maps are a useful tool in evaluating hydrostratigraphic units when used in conjunction with whole-unit isopach maps and hydrologic maps. This information is useful for determining preferential fluid-migration pathways within aquifers or through confining units. This method relies heavily on accurate determination of unit boundaries to calculate the hydrogeological framework. Widely and evenly distributed data enhance the effectiveness of this method.

TABLE OF CONTENTS

LIST OF FIGURES

LIST OF FIGURES (Continued)

LIST OF TABLES

LIST OF PLATES

LIST OF APPENDICES

1.0 INTRODUCTION

1.1 Background

The Savannah River Site (SRS) is a U.S. Department of Energy (DOE) facility occupying 300 square miles within Aiken, Barnwell, and Allendale counties in southwestern South Carolina (Figure 1). The site was set aside in 1950 as a controlled area for production of nuclear materials for national defense. The DOE and its contractors are responsible for the operation of the SRS. Westinghouse Savannah River Company (WSRC) currently manages and operates the site.

The SRS has been the focus of numerous geological and hydrogeological investigations dating from the initial geotechnical work associated with site construction in the early 1950's. The past 10 years mark a resurgence in geological work at the SRS, primarily hydrogeological investigations related to waste-site characterization and remediation.

The General Separations Area includes the F- and H-Areas, S-Area, Z-Area (including the area formerly referred to as "Y-Area"), and the Burial Ground Complex and proposed Hazardous Waste/Mixed Waste Disposal Facility (HW/MWDF)(Figure 2). The area contains several waste sites that are undergoing environmental assessment and/or closure under State and Federal regulations. The assessment process includes evaluation of the hydrogeology of the site and modeling of ground-water flow and potential transport of contaminant releases from the waste sites. The models require an extensive knowledge of the geology of the media through which the water is moving. Subsurface geologic mapping is one method by which such knowledge may be obtained. The area has received intense geologic and hydrologic study during recent years and contains numerous borings and monitoring wells.

Westinghouse Savannah River Company's Savannah River Technology Center (WSRC-SRTC) contracted Science Applications International Corporation (SAIC) to compile a series of subsurface maps illustrating lateral variations in sediment character of the uppermost hydrostratigraphic units beneath the General Separations Area. This study will also evaluate the applicability of these maps to characterization of the specific hydrostratigraphic units and as aids in developing more accurate ground-water models (Flach and others, 1996).

1.2 Description of the Study Area

The SRS is centered 22.5 miles southeast of Augusta, Georgia, approximately 100 miles from the Atlantic Coast within the Upper Atlantic Coastal Plain Physiographic Province (Figure 1). The SRS is situated on the Aiken Plateau of the Atlantic Coastal Plain at an approximate elevation of 300 feet msl. Overall, the plateau has a highly dissected surface and is characterized by broad inter-fluvial areas with narrow, steep-sided valleys. Local relief can attain 280 feet (Siple, 1967). The Aiken plateau is generally well-drained, although many poorly drained sinks and depressions exist, especially in the "upland" unit. The SRS is bounded on the southwest by the Savannah River (Figure 1).

The study area comprises approximately 15 square miles of the central SRS known as the General Separations Area (GSA) (Figure 2). The GSA has low to moderate topographic relief and is drained by several unnamed perennial streams (Figure 3). The study area is bordered by three streams with several intermittent streams present within the area boundary. Upper Three Runs forms the northern boundary of the study area with an average elevation of 150 feet msl., Fourmile Branch forms the southern boundary with an average elevation of 200 feet msl., and McQueen Branch forms the northeastern boundary with elevations ranging from 160 to 250 feet msl. There is no natural drainage at the west margin of the area. An arbitrary boundary is established west of C Road by connecting Upper Three Runs to Fourmile Branch. The model area is shown in Figure 4. The model boundaries correspond with the mesh that is being used by WSRC-SRTC for groundwater flow and transport models.

1.3 Geology of the Study Area

The SRS is underlain by sediment of the Atlantic Coastal Plain (Figures 1 and 5). The Atlantic Coastal Plain consists of a southeast-dipping wedge of unconsolidated and semi-consolidated sediment that extends from its contact with the Piedmont Province at the Fall Line to the edge of the continental shelf (Figure 1). The sediment ranges from Late Cretaceous to Miocene in age and comprises layers of sand, muddy sand, and mud with subordinate calcareous sediment (Figure 5). The sediment rests unconformably on crystalline and sedimentary basement rock.

The mapping done in this study analyzes the units that are Tertiary in age (Figure 5). These include, in ascending order, the Lang Syne Formation, Snapp Formation, Fourmile Branch Formation, Congaree Formation, Warley Hill Formation, Santee Formation, Clinchfield Formation, Dry Branch Formation, Tobacco Road Sand, and "upland" unit. A brief discussion of these units and their relationship with the hydrostratigraphy is presented in the following section. Detailed descriptions of the geology of the SRS and GSA can be found in several recent reports (Colquhoun and others, 1983; Dennehy and others, 1989; Logan and Euler, 1989; Fallaw and others, 1990; Aadland and others, 1991; Fallaw and Price, 1995).

1.3.1 Black Mingo Group

The term "Black Mingo" was first used by Sloan (1908) for outcrops of shale along Black Mingo Creek in Georgetown and Williamsburg Counties, South Carolina. Cooke (1936) used the term to reference all Eocene rocks older than the Santee Formation (McBean Formation of older reports). Van Nieuwenhuise and Colquhoun (1982) raised the Black Mingo to group status. Overall, the Black Mingo Group is composed of quartz sand, silty clay and clay deposited in a lower delta-plain environment with marine influence (Prowell and others, 1985).

In the GSA, the Black Mingo Group includes the Sawdust Landing, Lang Syne, Snapp, and Fourmile Formations (Figure 5). The Sawdust Landing Formation was not analyzed in this study and is therefore not addressed in the following discussion.

1.3.1.1 Lang Syne Formation

The Lang Syne Formation is present in east central South Carolina (Sloan, 1908; Padgett, 1980; Colquhoun and others, 1983; Muthig and Colquhoun, 1988; Colquhoun and Muthig, 1991; Nystrom and others, 1991). This lithologic unit has historically been called the Ellenton Formation in the SRS region by Siple (1967), Prowell and others (1985), and Dennehy and others (1989). The Lang Syne Formation was correlated with and traced from its type locality to the SRS region by Nystrom and others (1989, 1991). The Lang Syne was raised to formational status by Fallaw and Price (1992, 1995) and has replaced the term Ellenton in the SRS region.

In the GSA, the Lang Syne Formation consists of dark gray and black, lignitic clay with interbedded, poorly to moderately sorted, micaceous and lignitic, muddy quartz sand and pebbly sand. The clay is commonly fissile with laminae of micaceous silt and fine sand (Fallaw and Price, 1995). The gray and black lignitic fissile clay is interpreted as lagoonal or bay deposits, while the micaceous, lignitic muddy quartz sand and pebbly sand in the vicinity of the GSA is interpreted to have been deposited in an upper delta-plain environment. Southeast of the GSA, lower delta plain and pro-delta facies are present (Fallaw and Price, 1995).

1.3.1.2 Snapp Formation

The Snapp Formation at the SRS is correlative with the Williamsburg Formation of Colquhoun and others (1983), Steele (1985), and McClelland (1987). Fallaw and Price (1995) raised the Snapp to formational status (Figure 5).

In the SRS region, the Snapp Formation consists of silty, medium-to coarse-grained quartz sand, interbedded with dark clay. Minor constituents include dark, micaceous, lignitic sand (Aadland and others, 1995). The Snapp lithology described above is indicative of deposition in a lower delta-plain environment. The interbedded clay was probably deposited in lagoonal or estuarine environments (Aadland and others, 1995). The Snapp Formation is first recognized in the southeastern part of the SRS where it attains a thickness of 50 feet. According to Aadland and others (1995), the Snapp pinches out in the northwestern part of SRS. In the study area, distribution of the Snapp is sporadic and discontinuous.

1.3.1.3 Fourmile Branch Formation

The Fourmile Branch Formation in the SRS region is equivalent to the Fishburne Formation of Gohn and others (1983). This lithologic unit was raised to formational status by Fallaw and Price (1995) (Figure 5). The unit consists of moderately to well-sorted sand, and fine to coarse-grained sand that is interbedded with thin layers of green and gray clay. Glauconite, muscovite, and iron sulfide are common accessory minerals (Fallaw and Price, 1995). According to Fallaw and Price (1995), the Fourmile Branch attains a thickness of approximately 30 feet in the northwest part of SRS and thins to the south and east, and toward the Savannah River from the central SRS. In the GSA, the unit is discontinuous and where present, is generally less than 10 feet in thickness.

1.3.2 Orangeburg Group

The Orangeburg Group (Figure 5) crops out at lower elevations within the central part of the SRS, along creek beds, and the Savannah River. The Orangeburg Group thickens from approximately 75 feet at the northwestern SRS boundary to about 150 feet near the southeastern SRS boundary (Colquhoun, 1991). Across the SRS region, the upper surface of the Orangeburg Group dips southeast at approximately 10 feet/mile. At the South Carolina coast, the Orangeburg Group is about 300 feet thick (Colquhoun and others, 1983) and represents outer-shelf depositional environments (Boylan, 1982). The dominant lithology of the Orangeburg Group includes sand, muddy and sandy limestone, calcareous mud, calcareous sand, clay, and glauconitic sand and clay. In the GSA, the Orangeburg Group includes, in ascending order, the Congaree, Warley Hill and Santee Formations (Figure 5). The sand and mud are generally unconsolidated and friable, whereas the limestone is usually moderately to well-indurated.

1.3.2.1 Congaree Formation

The term "Congaree Phase" was first introduced by Sloan (1907, 1908) to describe the shale, sands, and "buhrstone" of early and middle Eocene age overlying the "Black Mingo Phase" and underlying the "Warley Hill Phase" at Warley Creek in Calhoun County, South Carolina. Cooke and MacNeil (1952) assigned the Congaree an early middle Eocene age and raised it to formational rank, correlating it with the Tallahatta Formation of Alabama. The Congaree Formation has been traced from the Congaree valley in east-central South Carolina into the SRS area by Colquhoun and others (1982, 1983). At SRS, the Congaree crops out along Upper Three Runs near the juncture with Tinker Creek (Nystrom and Willoughby, 1982a; Willoughby, 1983, 1985, 1986; Nystrom, 1986; Nystrom and others, 1989).

At the SRS, the Congaree Formation consists of yellow, orange, tan, gray, and greenish gray, iron-stained, moderately to poorly sorted, medium to fine-grained sand with discontinuous lenses of montmorillonite-rich clay (Colquhoun and Johnson, 1968). Layers rich in pebbles, clay clasts, calcareous sand, and glauconite are present, but sporadic in their position within the formation. The base of the formation is not conformable. The Congaree and other deposits of lower middle Eocene age become increasingly calcareous between the SRS and the Atlantic coast, where they are primarily limestone (Colquhoun, and others, 1983; W.B. Harris and others, 1990; Harris and others, 1993).

Marine fossils, phosphate and glauconite indicate the Congaree Formation to be a marine-shelf deposit (Robertson and Thayer, 1992). The Congaree Formation averages 85 feet thick in the SRS area (Robertson, 1990). Robertson (1990) reported a local maximum of 110 feet for the thickness of the Congaree in this area at a location immediately south of the SRS. In the area northwest of the SRS, a unit equivalent to the Congaree is mapped as the Huber Formation (Nystrom and Willoughby, 1982a).

1.3.2.2 Warley Hill Formation

Sloan (1907) first used the term "Warley Hill Phase." Cooke and MacNeil (1952), coined the name "Warley Hill Marl" for glauconitic beds between the Congaree and McBean Formations. Pooser (1965) said that the overall lithology of the unit made the term "marl" inappropriate, and proposed the name be changed to Warley Hill Formation. Both the glauconitic sand and the clay at the top of the Congaree are assigned to the Warley Hill Formation (Fallaw and others, 1990; Fallaw and Price, 1995).

The Warley Hill Formation unconformably overlies the Congaree Formation and consists of approximately 15 feet of poorly to well-sorted quartz sand, often glauconitic, clay, sandy clay, and clayey sand (Fallaw and Price, 1995) (Figure 5). The sediment generally has a distinct dark green color due to accessory glauconite. The clay minerals that constitute the matrix of the sediment include illite and smectite (Dennehy and others, 1989). The green sand and clay beds are referred to informally as the "green clay" in many SRS reports. Northwest of the study area, the Warley Hill is missing or very thin, and the overlying Santee Formation rests unconformably on the Congaree Formation.

The lithology of the Warley Hill Formation indicates deposition in a shallow to deep clastic shelf environment, generally deeper water than the underlying Congaree Formation (Pooser, 1965). Fallaw and Price (1995) note that the presence of glauconite and the dinoflagellate assemblage are indicative of shallow marine conditions. The muddier sand in the Warley Hill indicates quieter water than that in which the Congaree was deposited (Fallaw and Price, 1995).

1.3.2.3 Santee Formation

Charles Lyell (1845) was the first to use the term "Santee" for limestone exposed along the Santee River in South Carolina. Sloan (1908) continued the use of the term, modified to "Santee Marl." The terms "McBean Formation" and "Lisbon Formation" have been applied in the past to this unit but the term "Santee" has priority (Sloan, 1908). Cooke (1936) gave the unit formational status, assigned it an upper Eocene age, and re-named it the Santee Formation. Cooke and MacNeil (1952) correlated the Santee Formation with the middle Eocene Cook Mountain Formation of the Claiborne Group.

The Santee Formation (Figure 5) consists of moderately sorted, yellow and tan sand, calcareous sand and clay, and terrigenous clay. The lithology is consistent with deposition in a shallow marine, shelf environment. The carbonate lithology of the Santee Formation includes tan to white calcilutite, calcarenite, shelly limestone, and calcareous sand and clay. The carbonate content is highly variable. Limestone is much more abundant in down-dip areas, sporadic and pod-like in the middle of the study area, and missing in up-dip areas northwest of the study area. The carbonate sediment generally represents the limit of the transgression of the carbonate platform across the continental margin. This carbonate platform first developed in early Paleocene time near the South Carolina and Georgia coasts (Colquhoun and Johnson, 1968). The average thickness of the Santee is approximately 40 to 50 feet near the center of the study area

1.3.3 Barnwell Group

The Barnwell Group (Figure 5) was previously named the Barnwell Formation by Sloan (1908). The units assigned to the Barnwell Group were originally included in the Orangeburg Group by Siple and Pooser (1965). The Barnwell was raised to group status in Georgia by Huddlestun and Hetrick (1979). The Barnwell Group comprises three formations, the Clinchfield Formation, Dry Branch Formation, and Tobacco Road Sand. Colquhoun and others (1982, 1983) and Nystrom and Willoughby (1982a, 1989b) extended group status for Barnwell strata into South Carolina.

Fallaw and Price (1995) subsequently removed group status from the Barnwell in the SRS region, and assigned the Clinchfield Formation to strata of middle Eocene age. This study does not support the interpretation of the Clinchfield made by Fallaw and Price (1995), and recognizes the Barnwell Group as defined by Huddlestun and Hetrick (1979) and Nystrom and Willoughby (1982a, 1989b).

1.3.3.1 Clinchfield Formation

The Clinchfield Formation is the lowermost formation of the Barnwell Group (Figure 5). It consists of medium-grained, well-sorted, poorly consolidated, massively bedded quartz sand (Huddlestun and Hetrick, 1979). At the SRS, this unit has only been identified where carbonate strata of the Griffins Landing Member of the Dry Branch Formation and the Santee Formation are present, with sand of the Clinchfield between them. According to Fallaw and Price (1995) the sand is tan and yellow, poorly to well-sorted, and fine to coarse-grained at the SRS.

1.3.3.2 Dry Branch Formation

The Dry Branch Formation is the middle unit of the Barnwell Group (Figure 5). The Dry Branch crops out at the SRS and is approximately 45 feet thick near the northwestern site boundary and about 77 feet near the southeastern boundary (Fallaw and Price, 1995).

Huddlestun and Hetrick (1979) divided the Dry Branch into three lithofacies: the Twiggs clay, a marine, montmorillonite-rich clay; the Irwinton Sand, a distinctly bedded sand and clay; and the Griffins Landing Member, a massive "calcareous" fossiliferous sand. The Griffins Landing Member represents the uppermost calcareous upper Eocene strata in the study area. The Griffins Landing contains the large oyster, *Crassostrea gigantissima*, and at up-dip (northwestern) locations the clay matrix appears very similar to the Twiggs Clay and is probably correlative with this unit. Distribution of the Griffins Landing is sporadic in up-dip locations, and the unit thickens to greater than 96 feet in the southern part of the SRS region.

The presence of *Crassostrea*-bearing beds indicate bay or lagoonal environments for the Griffins Landing Member. Sand of the Irwinton is interpreted to be inner neritic and barrier deposits, whereas the clay is interpreted as a lagoonal or possible bay deposit (Fallaw and Price, 1995).

1.3.3.3 Tobacco Road Sand

The Tobacco Road Sand is the uppermost unit of the Barnwell Group (Figure 5). This sandy unit varies from fine-grained and well-sorted to poorly sorted with pebbles. Variations in clay, chert, mica, carbonate, and heavy-mineral content exist locally (Huddlestun and Hetrick, 1979). Massive bedding and bioturbated strata characterize the formation (Logan and Euler, 1989).

Abundant *Ophiomorpha* and clay laminae in the Tobacco Road Formation indicate deposition in a low energy, transitional marine environment, such as a tidal flat (Fallaw and Price, 1995).

1.3.4 "Upland" Unit

The term "upland" unit has been widely used in the Coastal Plain of South Carolina for the poorly sorted, silty, clayey and pebbly sand present at higher elevations within the study area (Figure 5). At the SRS, the "upland" unit has been called the Hawthorn Formation (Siple, 1967), and the Altamaha Formation (Huddlestun, 1988; Nystrom and Willoughby, 1992; Fallaw and Price, 1995). As the age of the unit is still controversial, this report will use the informal name "upland" unit. It is believed that the unit is correlative with the Chandler Bridge Formation in the vicinity of the Atlantic Coast (Colquhoun and others, 1994).

The "upland" unit is considered by many to be a distinct unit separated from the underlying parts of the section by a significant unconformity (Nystrom and Willoughby, 1982a; Nystrom and others, 1989). Colquhoun and others (1994) demonstrate that the "upland" unit, Tobacco

Road and Dry Branch Formations are similar in texture and composition. They believe that the unit is part of the same transgressive-regressive cycle as the Tobacco Road and Dry Branch Formations. The "upland" unit represents the most inland lithofacies, and the Dry Branch represents the most seaward lithofacies of the transgressive-regressive cycle.

1.4 Hydrostratigraphy of the Study Area

The hydrostratigraphy of the SRS has been subject to several different classifications. This report incorporates the hydrostratigraphic nomenclature currently established for the SRS region by Aadland and others (1995). The nomenclature is correlated with the local lithostratigraphy in Figure 5. A thorough description and review of the hydrostratigraphy of the SRS region are available in Aadland and others (1995). This report address the up-dip part of the Floridan aquifer system and the top of the Meyers Branch confining system as defined by Aadland and others (1995)(Figure 5).

1.4.1 Meyers Branch Confining System

The Meyers Branch confining system defines the base of the Floridan aquifer system in the study area. In the GSA, the top of the Meyers Branch confining system is delineated by the laterally continuous, dense, gray to black, clay and sandy clay of the Lang Syne Formation of the Black Mingo Group (Figure 5) (Aadland and others, 1991, 1995).

1.4.2 Floridan Aquifer System

1.4.2.1 <u>Gordon Aquifer</u>

The lowermost unit that is characterized in this report is the Gordon aquifer (Figure 5). The Gordon aquifer constitutes the basal unit of the Floridan aquifer system in this part of the SRS Region. Beneath the GSA, the Gordon aquifer is made up of the loose sand and clayey sand of the Congaree Formation and, where present, the sandy parts of the underlying Fourmile Branch and Snapp Formations (Figure 5) (M.K. Harris and others, 1990; Aadland and others, 1991, 1995). The sand within the Gordon aquifer is yellowish to grayish orange and is sub- to well-rounded, moderately to poorly sorted, and medium- to coarse-grained (Plates 1 and 2). Pebbly layers and zones of iron and silica cemented sand are common. Layers of light tan to gray clay up to three feet in thickness are rare, and thin (< 6-in. thick) layers of clay are often found near the base of this unit. The Gordon aquifer contains a small amount of sporadically distributed calcareous sediment.

1.4.2.2 Gordon Confining Unit

The Gordon confining unit separates the Gordon aquifer from the Water Table aquifer. The unit is commonly referred to as the "green clay" in previous SRS literature and includes sediment of the Warley Hill Formation (Figure 5). The unit comprises layers of interbedded silty and clayey sand, sandy clay and clay. The clay is stiff to hard and often fissile (Plate 3). Glauconite is a common constituent and imparts a distinctive greenish cast to the sediment, hence the informal name "green clay" for this unit. Zones of silica-cemented sand and clay are present in some cores taken from the GSA. In the vicinity of the GSA, the Gordon confining unit includes some calcareous sediment and limestone, primarily calcarenaceous sand and clayey sand with subordinate calcarenaceous and micritic clay, and sandy micrite and limestone (Plate 4).

1.4.2.3 Water Table Aquifer

In this study, the Water Table aquifer includes the Upper Three Runs aquifer of Aadland and others (1995). The Water Table aquifer as defined inthis report, includes all sediment from the ground surface to the top of the Gordon confining unit. The Water Table aquifer includes the "upland" unit, Tobacco Road Sand, Dry Branch Formation, Clinchfield Formation, and Santee Limestone (Figure 5). For this analysis, the Water Table aquifer is locally divided into informal "lower" and "upper" aquifer zones separated by the "tan clay" confining zone. The "lower" aquifer zone and "tan clay" confining zone are equivalent to the zones established by Aadland and others (1995). For the purposes of this model, the informal "upper" aquifer zone of Aadland and others (1995), is expanded to include the vadose zone with the saturated sediment above the "tan clay" confining zone (Figure 5).

"Lower" Aquifer Zone. The "lower" aquifer zone beneath the GSA consists of the dominantly fine-grained, well-sorted sand and clayey sand of the Santee Formation and parts of the Dry Branch Formation beneath the "tan clay" confining zone (Figure 5). The bulk of the carbonate sediment beneath the GSA is contained within the Santee and lower part of the Dry Branch and is included in the "lower" aquifer zone. Descriptions of drill core indicate that the carbonate sediment in this vicinity has a dominant siliciclastic component, and consists of calcarenaceous sand, micritic sand, shelly sand and some sandy calcarenite and shelly limestone. Plates 5 through 13 illustrate sediment and rock typical of the "lower" aquifer zone.

"Tan Clay" Confining Zone. The "tan clay" confining zone is equivalent to the "tan clay" zone referred to in previous SRS reports. The "tan clay" confining zone includes sediment of the Dry Branch Formation (Figure 5). The zone contains light-yellowish tan to orange clay and sandy clay interbedded with clayey sand and sand (Plates 14 and 15). The lithology of the clay is similar to that of the Twiggs Clay Member, but individual clay layers are dispersed vertically and horizontally throughout the confining zone. Individual clay layers within the "tan clay" confining zone are probably not laterally continuous over distances greater than 100 to 200 feet (M.K. Harris and others, 1990; Aadland and others, 1991).

"Upper" Aquifer Zone. The "upper" aquifer zone consists of all sediment from the ground surface to the top of the "tan clay" confining zone. The "upper" aquifer zone includes the "upland" unit, Tobacco Road Sand, and part of the Dry Branch Formation (Figure 5). This unit is characterized by sand and clayey sand with minor intercalated clay layers (Plate 16). The sediment within the "upland" unit is commonly very dense and clayey and often contains gravely sand.

For purposes of this analysis, the "upper" aquifer zone is divided into two parts. The sediment below the water table is referred to as the saturated zone within the "upper" aquifer zone of the Water Table aquifer. The sediment above the water table is referred to as the vadose zone within the "upper" aquifer zone of the Water Table aquifer.

2.0 DISCUSSION

2.1 Database Methods

Data utilized in this analysis include SRS coordinates, elevations, geophysical logs, and drill-core descriptions. The location and elevation data are extracted from the WSRC database for use on this project. For the recently drilled borings, location and elevation data were collected from the surveyor's files maintained at SRS Building 711-1N. The SRS coordinates and elevations of the wells and borings used in this study are given in Appendix A. The study utilized down-hole geophysical data including caliper, gamma-ray and resistivity logs in delineating aquifer and confining units, correlating specific horizons from hole to hole, and in estimating the lithology of missing core intervals.

2.1.1 Data Collection

Data from detailed, foot-by-foot descriptions of continuous drill core were compiled for all the cores used in this study. The core descriptions are included in Appendix B to this report.

All core samples have been described following SRL ESSOP-2-15 (WSRC, 1990). A summary of the core description format is included with Appendix B.

The core descriptions include data on amount of core recovery; degree of induration; color; sedimentary structures; volume percent terrigenous gravel, sand, and mud; maximum and modal size of the terrigenous fraction; volume percent carbonate gravel, sand, and mud; volume percent cement; volume percent total carbonate sediment; sediment/rock name; grain sorting; volume percent porosity and dominant type; fossil types, and volume percent accessory constituents, including muscovite, glauconite, lignite, sulfides, and heavy minerals (WSRC, 1990). The rock types identified in GSA cores are listed in Appendix B.

2.1.2 Data Qualification

Boundaries or "picks" for hydrostratigraphic units beneath the GSA were initially established through previous modeling work (Thayer and others 1993). A rigorous Quality Review of the data was performed, comparing the core descriptions and geophysical logs with the list of unit boundaries. Geologists made refinements to these boundaries to ensure internal consistency between the unit boundaries and the lithology of the hydrostratigraphic units.

2.1.3 Database Structure

A relational database was constructed for this project using Paradox® (version 7.0) software. All geological and hydrological data was collected for the GSA and entered into the database. Measured values were integrated with the stratigraphic "picks" to create data output files to meet EarthVision® format and content requirements. The database is constructed so that revisions made to the subjective data (stratigraphic "picks") are documented. The database records and dates each revision to the picked boundaries, and automatically regenerates updated output files for re-loading into EarthVision®. This aspect of the database facilitates data evaluation and revision, and provides a means by which to maintain a history of the subjective data set.

2.2 Lithostratigraphic Methods

Lithostratigraphic units were picked from the geologic data according to the lithologic criteria for each unit as described in section 1.3 of this report. The unit tops are tabulated in Appendix A. Table 1 summarizes lithologic and hydrologic parameters calculated from the core descriptions. The parameters in Table 1 have been calculated by computer and used to prepare the facies maps in this report.

2.3 Hydrostratigraphic Methods

Hydrostratigraphic unit boundaries for the GSA are refined from the database produced during a previous investigation (Thayer and others, 1993). Hydrostratigraphic boundaries for cores completed since the previous report have been determined by the Savannah River Technology Center. Boundaries are determined through evaluation of:

Geophysical data. Gamma-ray logs in combination with resistivity logs are used to evaluate the potential confining properties of the strata. In general, low resistivity and high gamma-ray values indicate clay-rich sediment that impedes the flow of ground water.

Core description data. Core descriptions are used (in conjunction with the geophysical logs) to select boundaries between confining and transmissive units. Percentage of mud and estimated porosity are the primary criteria used. If core recovery is good, the foot-by-foot description is an excellent tool for determining the vertical extent of a confining or transmissive lithology.

"Picked" tops for the hydrostratigraphic units are tabulated in Appendix A.

2.4 Hydrogeologic Model

The database was used to prepare a hydrogeologic model of the GSA. The model was constructed with EarthVision® software. EarthVision® processes sets of spatial and property data by calculating minimum-tension grids to contour a "best fit" of the data. The grids can contour data in 3 dimensions (x,y,z), such as the top of a geologic unit, as two-dimensional grids, or contour data in 4-dimensions: x,y,z, and a "property." An example of a property might be the variation of the percentage of mud within a geologic unit.

2.4.1 Two-Dimensional Grid Calculation

Data for lithostratigraphic and hydrostratigraphic unit tops were exported from the Paradox® database into EarthVision®. After minor format changes, the data was processed by an algorithm, producing a two-dimensional grid of the unit top surface.

The EarthVision® model utilizes digitized x,y,z data for all U.S. Geological Survey topographic coverage of the GSA. The data was processed in the same manner as the data for the unit boundaries to produce a grid representing the topography of the study area. The high density of data points in this data set produced a two-dimensional grid of exceptional accuracy and detail. This grid was then used in subsequent two-dimensional and three-dimensional gridding to determine the extent of lithostratigraphic and hydrostratigraphic units that crop out in the study area.

2.4.2 Three-Dimensional Grid Calculation

The property data processed by EarthVision® consisted of the foot-by-foot lithologic descriptions made from continuous core samples taken from the GSA. Lithologic data was exported from the Paradox® database and formatted for use in the EarthVision® three-dimensional Minimum-Tension Gridding module. The EarthVision® software allows a wide variety of options in how the three-dimensional grids are calculated. The lithology was first processed using the two-dimensional grids of the lithostratigraphic units as limiting surfaces. This effectively prevented the model from "seeing" any lithologic information from outside the lithostratigraphic interval during the gridding process. The gridding algorithm then calculated "best fits" for each lithologic property within each lithostratigraphic unit using only the data from within the unit as delineated by the geologist and gridded by EarthVision®. This technique produces a model of the hydrogeology that is consistent with the lithostratigraphic boundaries. A model built in this manner will be more accurate for hydrogeologic analysis and groundwater modeling.

The lithologic parameters modeled using EarthVision® include percent silicate mud, percent carbonate, and the calculated sand-mud and clastic ratios. Averages of these parameters are calculated from the three-dimensional property grids over the volume of the unit. The volume is defined by the two-dimensional grids of the top and bottom of the unit. An average is calculated at each X-Y location and written as a Z value to a two-dimensional grid.

SAIC used the method presented in Sloss and others (1960) and Krumbein and Sloss (1963) to prepare the multiple-ratio facies maps presented in this report. The ratios are determined from three components. Component A includes non-clastic sediment (carbonate sediment and limestone), component B represents sand and gravel, and C represents mud (silt + clay). The ratio B/C compares coarse and fine clastic sediment and is referred to as the *sand-mud ratio* (Table 1). The ratio (B + C)/A represents the relationship between terrigenous (clastic) sediment and the non-terrigenous (non-clastic) sediment. This is the clastic ratio (Table 1). Ratio maps are contoured as continuous functions. The limits and characteristics of the lithologic types delineated by the sand-mud and clastic ratios are summarized in Table 2.

Vertical hydraulic conductivity data and leakance values from the Gordon confining unit and "tan clay" confining zone were gridded directly as two-dimensional grids. These data were compiled from laboratory measurements of undisturbed samples and grain-size analyses of sediment samples taken from GSA cores.

2.4.3 Mapping

2.4.3.1 Structure-Contour/Altitude-Contour Maps

Lithostratigraphic units were selected for mapping based on the ease with which their boundaries can be identified from core descriptions and geophysical logs, and the degree to which their lithology contrasts with adjacent units. This methodology supports the purpose of the lithostratigraphic mapping, which is to analyze and model the geometry of the lithology within the study area for application to groundwater flow modeling.

Structure-contour and altitude-contour maps were constructed for each unit using the two-dimensional grids that were calculated from the scattered data for the unit tops. Structure-contour maps illustrate the lithostratigraphic units and altitude-contour maps depict the approximate elevations of the tops of the hydrostratigraphic units. The maps are plotted using the *Contour and Basemap* module of EarthVision®. Contour intervals are chosen by individual data set so as to convey the information clearly and concisely, but virtually any level of detail is possible. An effort was made to keep the contour interval to within one-tenth of the range of the z-values. This serves to minimize the number of contour lines, yet generally maintains a level of detail suitable for interpretation of the map.

2.4.3.2 Isopach Maps

Two-dimensional grids of unit thickness (isopach grids) were calculated by first comparing the two-dimensional grids of the unit base and unit top with the two-dimensional grid of the topography. Isopach maps of vertical unit thickness were calculated from comparison of the two-dimensional grids of the unit base and unit top. A value was then written to the corresponding nodes of the resultant grid (the isopach grid) equal to the vertical distance between the base and upper surface of the unit.

The thickness of the saturated zone within the "upper" aquifer zone was calculated in the same manner as the other units, but using the water table surface as the "unit top." Similarly, the thickness of the vadose zone within the "upper" aquifer zone was calculated using the topographic surface as the "unit top."

The resultant two-dimensional isopach grids were contoured using EarthVision® in the same fashion as the structure-contour maps.

2.5 Results

The resultant maps are presented as Figures 6 through 56. Lines of section were selected to represent the hydrogeologic model in three vertical cross-sections (Figures 57 through 60). The cross-sections show the configuration of the gridded surfaces used in constructing the three-dimensional model described in Section 2.4.2.

2.5.1 Lithostratigraphic Units

Structure-contour maps were constructed for the tops of the Lang Syne Formation, Congaree Formation, Santee Formation, and Barnwell Group. Isopach maps were constructed for the Congaree Formation, Santee Formation, Barnwell Group, and the "upland" unit. The Fourmile Branch and Snapp Formations are included in the Congaree isopach owing to the patchy and discontinuous nature of these lithologic units. Due to the sporadic distribution of the Warley Hill Formation within the study area, the isopach map of the Santee Formation includes this lithologic unit. The isopach of the Barnwell Group includes the Clinchfield Formation, Dry Branch Formation, and the Tobacco Road Sand. It was not feasible to individually map each lithologic unit in the Barnwell Group due to the intertonguing of lithologic units.

Table 3 presents a summary of the two-dimensional grids calculated for the lithostratigraphic units. Due to the large number of data points for each unit is was not feasible to post the core name and/or value on each map. Lithostratigraphic tops used in the gridding are listed in Appendix A.

2.5.1.1 Lang Syne Formation

Figure 6 illustrates the structure-contour map of the top of the Lang Syne Formation. Forty-seven cores penetrated this unit within the study area. Elevations of the unit range from approximately 100 feet msl. in the northern part of the study area to -50 feet msl. in the southeastern part. There is a prominent dip to the southwest punctuated by cusps of the contours, which suggests post-depositional erosion and faulting, but may also result from the uneven distribution of data points. In the southeast part of the study areas the close spacing of the contours is probably indicative of a normal fault between cores P-27 and HPC-1, as documented by Domoracki (1995). Locations of these cores are shown on Maps C-3 and D-3 in Appendix A.

2.5.1.2 Congaree Formation

Table 3 summarizes Grids calculated for the Congaree Formation. Figure 7 illustrates the structure-contour map of the top of the Congaree Formation and Figure 8 illustrates the isopach of the unit. Elevations of the unit range from approximately 150 feet msl. in the northeastern part of the study area to 100 to 110 feet msl. in the southern parts near Fourmile Branch. Dip of the unit is primarily to the south-southeast. The dip pattern is interrupted by cusps of the contours and localized highs and lows in the central part of the study area. The overall structure contour pattern is similar to the Lang Syne. As with the underlying unit the contours are suggestive of post-depositional erosion and structural control. The close spacing of contours in the southeast is believed to represent the same fault that was observed in the top of the Lang Syne Formation between cores P-27 and HPC-1.

The isopach of the Congaree Formation (Figure 8) illustrates the variation in vertical thickness to be a function of the configuration of the top of the Lang Syne Formation (Figure 6). The contour pattern of the isopach map follows the structure-contour patterns on the top of the Lang Syne Formation, especially in the central part of the area.

2.5.1.3 Santee Formation

Figure 9 illustrates the structure-contour of the top of the Santee Formation and Figure 10 illustrates the isopach of the unit. Overall, the Santee dips to the southeast. In the central part of the area, the surface of the unit exhibits local increases in relief, in patterns remarkably similar to depression features mapped on the surface at the SRS. The variations in the configuration of the top of the Santee Formation are possibly related to dissolution of calcareous sediment at the top of the Santee unconformity. The top of the Santee represents a major unconformity at the top of the middle Eocene.

The theory of dissolution of calcareous sediment at the unconformity is supported by work done in the early 1950's by the Core of Engineers during construction of SRS (U.S. Army Corps of Engineers, 1952). Currently, there are several on-going geotechnical projects at the SRS investigating the dissolution theory (Frank Syms, 1997, personal communication). Several structural highs on the top of the Santee are present in the northern part of the study area. These high areas are thought to result from the resistance of silicified or well-cemented limestones to dissolution by groundwater.

The isopach map of the Santee (Figure 10) illustrates the variability of the thickness of the formation. Figure 16 indicates that the thickness of the Santee is a function of the configuration of the top of the Congaree Formation. There are isolated areas in the vicinity of F-Area and the Burial Grounds where the formation thickness exceeds 50 feet (Figure 10). These correspond to prominent structural lows on the top of the Congaree Formation (Figure 7).

2.5.1.4 Barnwell Group

Figure 11 illustrates structure-contours on the top of the Barnwell Group and Figure 12 illustrates the isopach of the group. The top of the Barnwell Group mimics the local topographic surface (Figure 3). The Barnwell Group crops out at lower elevations where the "upland" unit is not present, and in the stream valleys where recent erosion has stripped away sediment of the "upland" unit. The thickness of the Barnwell Group is illustrated in Figure 12. The contour patterns indicate that the Barnwell Group becomes thicker in structurally low areas on the top of the Santee Formation (Figure 9). However, the isopach does show places where the Barnwell thins; these correspond to structurally low areas of the Santee. Subsidence of the Barnwell due to dissolution of carbonate material in the underlying Santee could explain these map patterns.

2.5.1.5 "Upland" Unit

The isopach map of the "upland" unit (Figure 13) clearly demonstrates its stratigraphic position. The thickness of this unit is directly related to the current topographic surface (Figure 3). Some of the thicker areas in Figure 13 correspond to structurally low areas on the top of the Barnwell Group (Figure 11).

2.5.2 Hydrostratigraphic Units

The hydrostratigraphy is defined, in part, by the hydrologic conditions in the subsurface. Water-level measurements from GSA wells were averaged and grids calculated as two-dimensional surfaces using EarthVision®. Contour maps were generated from the two-dimensional grids for the Gordon aquifer (Figure 14) and for the "lower" and "upper" aquifer zones of the Water Table aquifer (Figures 15 and 16). The maps display a similar overall trend, with the maps of the "upper" and "lower" aquifer zones exhibiting strikingly similar patterns. This is consistent with the semi-confined and unconfined conditions described for the aquifer zones in the Water Table aquifer (Dennehy and others, 1989; Aadland and others, 1991).

The hydrology of the GSA is marked by a pronounced groundwater divide. The divide is evident in the maps for both aquifer zones of the Water Table aquifer (Figures 15 and 16). The flow direction north of the divide is north toward Upper Three Runs and south of the divide is toward Fourmile Branch along the south margin of the study area. Although the overall flow in the Gordon aquifer is north-northwest, the divergent contour pattern beneath the Burial Grounds and F-Area is similar to and coaxial with the prominent groundwater divide in the Water Table aquifer (Figures 15 and 16). The potentiometric surface of the Gordon aquifer indicates an area of higher head values centered beneath the Burial Grounds. The higher heads in the Gordon aquifer correspond with lower head values in the "lower" aquifer zone in the same area (Figure 15).

A summary of the grids calculated for the potentiometric surfaces is given in Table 4. The grids calculated for the altitude-contour maps and isopach maps of the hydrostratigraphic units are summarized in Table 5.

2.5.2.1 Meyers Branch Confining System

Locations of the data points used to grid the Meyers Branch confining system are shown in Figure 17. The configuration of the top of the Meyers Branch confining system is illustrated with altitude contours in Figure 18. The unit displays a regional dip similar to that of the Lang Syne Formation but is somewhat different in terms of the contour patterns (Figure 6). The difference in the surface configuration is due to lithologic variations in the Lang Syne Formation. Where the top of the Lang Syne Formation is sandy, the top of the Meyers Branch confining system is chosen at the top of the uppermost clay below the lithostratigraphic boundary.

2.5.2.2 Gordon Aquifer

Locations of the data points used to grid the Gordon aquifer are given in Figure 19. The configuration of the top of the unit is illustrated in Figure 20. An isopach map is presented in Figure 21. Mud distribution within the Gordon aquifer is shown in Figure 22. Figure 23 illustrates the variation in average percent carbonate. Sand/Mud ratio values are mapped in Figure 24. The highest sand/mud ratios are located south of F Area. Lithologic parameters are summarized in Table 6.

The altitude-contours on the Gordon aquifer (Figure 20) correspond somewhat to the structure contours on the top of the Congaree Formation (Figure 7). The areas of the Gordon that appear to be "lower" than corresponding areas on the Congaree are interpreted to be places where the clay near the top of the Congaree formation is included in the Gordon confining unit. The map of silicate mud percentages (Figure 22) indicates that the unit is generally thicker in areas where the average mud percentage is high.

The similarity in the isopach of the Gordon aquifer (Figure 21) with that of the Congaree Formation (Figure 8) also demonstrates the close relationship between the lithostratigraphy and hydrostratigraphy. Thicker parts of the Gordon aquifer generally correspond to thicker parts of the Congaree Formation. This is not unexpected, as the Gordon aquifer consists primarily of strata of the Congaree formation.

2.5.2.3 Gordon Confining Unit

Locations of data points used in the EarthVision® grid calculations for the Gordon confining unit are shown in Figure 25. The configuration of the top of the Gordon confining unit is shown in Figure 26 and an isopach map of the unit is presented in Figure 27. The grids calculated for lithologic parameters in the Gordon confining unit are summarized in Table 7.

The trends in the isopach of the Gordon confining unit (Figure 27) generally follow the trends in the altitude contours in Figure 26. The Gordon confining unit tends to be thicker in areas where the top is picked at a higher elevation. The altitude-contour patterns on the Gordon confining unit (Figure 26) are similar to the patterns of the structure contours on the top of the Congaree Formation (Figure 7). These similarities indicate that the Gordon confining unit is relatively continuous across the GSA, at least in terms of the interval's presence. A comparison of Figure 28 with Figures 26 and 27 indicates that the percentage of mud is only partially dependent on the thickness and/or altitude of the unit.

A map of percent carbonate in the Gordon confining unit (Figure 29) indicates several isolated patches of carbonate sediment and limestone. For the most part however, the Gordon confining unit is free of calcareous material. Calcareous influences north and east of the center of the GSA appear to be associated with decreasing sand/mud ratios (Figures 30 and 31). Vertical hydraulic conductivity and leakance distributions are shown in Figures 32 and 33. The areas of lower hydraulic conductivity and leakance values (Figures 32 and 33) correspond to areas where the average mud percentages are higher and tend to increase in areas where the Gordon confining unit is thinner (Figure 26).

2.5.2.4 Water Table Aquifer

"Lower" Aquifer Zone. The locations of data points used in EarthVision® grid calculations of the "lower" aquifer zone are given in Figure 34. The altitude-contour map and isopach for the "lower" aquifer zone are presented in Figures 35 and 36. Table 8 summarizes the calculated grids for lithologic parameters in the "lower" aquifer zone.

The variation in mud percentage within the "lower" aquifer zone is illustrated in Figure 37. The percentage of mud is highest west of the F-Area Seepage Basins, northeast of the Burial Grounds, northwest of Z-Area, and in isolated highs in the vicinity of the H-Area Seepage Basins. The mud percentage reaches minimum values in the central part of the GSA north and south of the Burial Grounds. The distribution of calcareous material is summarized in Figure 38. Sand-mud and clastic-ratio maps are presented in Figures 39 and 40.

"Tan Clay" Confining Zone. Locations of data points used to grid the "tan clay" are given in Figure 41. The configuration of the top of "tan clay" confining zone is illustrated in Figure 42 and an isopach map of the unit is presented in Figure 43. Table 9 presents a summary of the lithologic parameters used in the grid calculations.

The parts of "tan clay" confining zone containing the highest average mud percentages are concentrated north of the Burial Grounds and in the vicinity of Z-Area (Figure 44). There is an overall decrease in the mud-bed percentage southward and westward from the center of the GSA. Carbonate distribution is shown in Figure 45. A map of sand/mud ratios for "the tan clay" confining zone is shown in Figure 46. A clastic-ratio map is presented in Figure 47. The map patterns closely approximate the trends shown in the map of mud percentage (Figure 44).

Distributions of vertical hydraulic conductivity and leakance are presented in Figures 48 and 49. The hydrologic properties of the "tan clay" are somewhat correlative with the percentage of mud (Figure 44). However, lower leakance and vertical hydraulic conductivity values (Figures 48 and 49) more closely follow the trends in the isopach contours for this unit (Figure 43), indicating that the vertical thickness has a greater effect than does the percentage of mud in determining the confining properties of this unit.

Saturated Zone of the "Upper" Aquifer Zone. The locations of data points used to grid this unit are shown in Figure 50. The top of the saturated zone is defined by the water table at any given data location. Data for the water table elevations used to define the saturated zone in this report come from the database provided by WSRC for use in this study.

Variations in thickness are shown on the isopach map in Figure 51. Lithofacies maps for percent mud and sand-mud ratio are presented in Figures 52 and 53. The calculated grids of lithologic parameters within the saturated zone are summarized in Table 10.

Vadose Zone of the "Upper" Aquifer Zone. The locations of the data points used to grid this unit are shown in Figure 50. An isopach map of the vadose zone is shown in Figure 54. Lithofacies maps of mud in the vadose zone are presented in Figures 55 and 56. Table 11 presents a summary of the calculated grids for lithologic parameters in the vadose zone.

3.0 SUMMARY

Delineating the lithostratigraphy prior to analyzing the hydrostratigraphy can greatly enhance the validation of the maps of lithologic parameters calculated by EarthVision®. Vertical limits of hydrostratigraphic units do not always correspond to lithostratigraphic boundaries. Thus, the geometry of the lithostratigraphic framework is the primary factor affecting the distribution of hydrologic properties in the hydrostratigraphic units. Refining the lithostratigraphic boundaries greatly improves the resolution of the hydrogeologic analysis. The lithologic character of the hydrostratigraphic units can then be modeled more consistently, resulting in better control for modeling groundwater flow and contaminant transport within the aquifers.

An uneven distribution of control points has a profound influence on the construction of these maps. The level of detail varies significantly within these maps due to the uneven distribution of control points. Similarly, the resolution of the maps decreases down-section due to the smaller number of control points for the deeper units.

The extent of the model should be limited to an area of relatively high data density if possible. Extrapolation of the grid surfaces can create unrealistic or misleading variations near the margins of a model. The addition of "false" control points to areas of sparse data coverage could alleviate this problem. Time constraints precluded using these types of control points during this study.

The hydrostratigraphic maps show consistent trends within each unit. These trends are useful for interpreting areas of high and low permeability within hydrostratigraphic units. For example, a sand/mud ratio map can be used to interpret the distribution of sand and mud and hence the overall porosity and permeability of an aquifer unit.

Hydrostratigraphic units can be best evaluated by integrating information from lithofacies and thickness maps. For example, a map of sand/mud ratio should be used in conjunction with an isopach map of the total unit to evaluate the overall effectiveness of a confining unit.

Lithofacies maps should be used in conjunction with hydrologic maps to better interpret the hydrologic flow regime beneath a site. For example, areas of high mud content within an aquifer unit may significantly influence ground-water flow paths within that unit. Areas of high sand content may increase the overall vertical permeability of a confining unit in those areas, possibly influencing migration of contaminants between aquifer units.

The precision of these maps is greatly influenced by the amount of core recovery. Lithology for zones with no core recovery must be interpreted from geophysical data. Hence, lithologic parameters can only be generalized as "sand", "mud", "calcareous sand/mud" or "limestone". The availability of core description allows for greater resolution of the lithology.

It should be noted that the map patterns presented result, in part, from the uneven horizontal and vertical distribution of control points for the units within this area. For example, the north-central and southwestern parts of the GSA are virtually devoid of control points that penetrate through the entire hydrostratigraphic section.

4.0 REFERENCES

Aadland, R. K., Gellici, J. A, and Thayer, P.A., 1995, *Hydrogeologic Framework of West-Central South Carolina.* Report 5, Water Resources Division, South Carolina Department of Natural Resources, Columbia, SC.

Aadland, R. K., Harris, M. K. , Lewis, C. M., Gaughan, T. F., and Westbrook, T. M., 1991, *Hydrostratigraphy of the General Separations Area, Savannah River Site (SRS), South Carolina.* WSRC-RP-91-13, Westinghouse Savannah River Company, Aiken, SC 20808.

Boylan, D. C., 1982, *Stratigraphy and Depositional Environments of the Lower South Carolina Coastal Plain Between Charleston and Hilton Head Island.* M.S. Thesis, University of South Carolina.

Colquhoun, D. J., 1991, *Southeast Atlantic Transect.* American Association of Petroleum Geologists, Regional Transect Series #449.

Colquhoun, D. J., and Johnson, H. S., Jr., 1968, "Tertiary Sea-Level Fluctuation in South Carolina". *Palaeogeography, Palaeoclimatology, Palaeoecology, 5:105-126.*

Colquhoun, D. J., Oldham, R. W., Bishop, J. W., and Howell, P. D., 1982, *Updip Delineation of the Tertiary Limestone Aquifer, South Carolina.* Report No. 97, Clemson University Water-Resources Research Institute, Clemson, SC.

Colquhoun, D. J., Woollen, I. D., Van Nieuwenhuise, D. S., Padgett, G. G., Oldham, R. W., Boylan, D. C., Bishop, J. W., and Howell, P. D., 1983, *Surface and Subsurface Stratigraphy, Structure and Aquifers of the South Carolina Coastal Plain.* SCDHEC Report ISBN 0-9613154-0-7, Columbia, SC.

Colquhoun, D. J., Rine, J. M., Segall, M. P., Katuna, M. P., Cohen, A. D., and Siron, D. L., 1994, *Sedimentology and Stratigraphy of the Upland Unit.* Final Report for Task 110, SCUREF Cooperation Agreement AA00900T, Earth Sciences and Resources Institute, University of South Carolina, Columbia, SC 29201.

Colquhoun, D. J., and Muthig, M. G., 1991, "Stratigraphy and Structure of the Paleocene and Lower Eocene Black Mingo Group". *Geology of the Carolinas.* University of Tennessee Press, Knoxville, Tennessee.

Cooke, C. W., 1936, *Geology of the Coastal Plain of South Carolina.* U.S. Geological Survey Bulletin 867.

Cooke, C. W. and MacNeil, F. S., 1952, "Tertiary Stratigraphy of South Carolina". *U.S. Geological Survey Professional Paper, 243-B: l9-29.*

Dennehy, K. F., Prowell, D. C., and McMahon, P. B., 1989, *Reconnaissance Hydrogeologic Investigation of the Defense Waste Processing Facility and Vicinity, Savannah River Plant, South Carolina.* Water Resources Investigations Report 88-4221, U. S. Geological Survey, Columbia, SC.

Domoracki, W. J., 1995, *A Geophysical Investigation of Geologic Structure and Regional Tectonic Setting at the Savannah River Site, South Carolina.* Unpublished Ph.D. Dissertation, Department of Geological Sciences, Virginia Polytechnic Institute and State University.

Fallaw, W. C. and Price, V., 1995, "Stratigraphy of the Savannah River Site and Vicinity". *Southeastern Geology, 35: 21-58.*

Fallaw, W. C., Price, V., and Thayer, P., 1990, "Stratigraphy of the Savannah River Site, South Carolina". *Savannah River Region: Transition Between the Gulf and Atlantic Coastal Plains, Proceedings of the Second Bald Head Island Conference on Coastal Plains Geology,* University of North Carolina at Wilmington, pp 29-32.

Flach, G.P., Hamm, L.L., Harris, M.K., Thayer, P.A., Haselow, J.S., and Smits, A.D., 1996, *Groundwater Flow and Tritium Migration from the SRS Old Burial Ground to Fourmile Branch (U).* WSRC-TR-96-0037, Westinghouse Savannah River Company, Aiken, SC 29808.

Gohn, G. S., Hazel, J. E., Bybell, L. M., and Edwards, L .E., 1983, "The Fishburne Formation (Lower Eocene), a Newly Defined Subsurface Unit in the South Carolina Coatal Plain". U.S. *Geological Survey Bulletin 1537- C.*

Harris, W. B., Zullo, V. A., Laws, R. A. and Harris, M. K., 1990, "Paleogene Sequence Stratigraphy and Chronostratigraphy of a Core from Allendale County, South Carolina". *Geological Society of America Abstracts with Programs, 22: 17-18.*

Harris, W. B., Zullo, V. A. and Laws, R. A., 1993, "Sequence Stratigraphy of the Onshore Paleogene, Southeastern Atlantic Coastal Plain, USA". *Sequence Stratigraphy and Facies Associations*. Special Publication 18, International Association of Sedimentologists, pp 537-561.

Harris, M. K., Aadland, R. K., and Westbrook, T. M., 1990, "Lithological and Hydrological Characteristics of the Tertiary Hydrostratigraphic Systems of the General Separations Area, Savannah River Site, South Carolina". *Savannah River Region: Transition Between the Gulf and Atlantic Coastal Plains, Proceedings of the Second Bald Head Island Conference on Coastal Plains Geology*, University of North Carolina at Wilmington, pp 68-73.

Huddlestun, P. F., 1988, *A Revision of the Lithostratigraphic Units of the Coastal Plain of Georgia, the Miocene through Holocene*. Georgia Geologic Survey Bulletin 104.

Huddlestun, P. F and Hetrick, J. H., 1979, *The Stratigraphy of the Barnwell Group in Georgia:* Georgia Geologic Survey Open-File Report 80-1, pp 56-73.

Huddlestun, P. F. and Hetrick, J. H., 1986, *Upper Eocene Stratigraphy of Central and Eastern Georgia*. Georgia Geologic Survey Bulletin 95.

Krumbein, W. C., and Sloss, L. L., 1963, *Stratigraphy and Sedimentation*, 2nd ed., p 600, W. H. Freeman and Company, San Francisco.

Logan, W. R. and Euler, G. M., 1989, *Geology and Groundwater Resources of Allendale, Bamberg, and Barnwell Counties and Part of Aiken County, South Carolina*. South Carolina Water Resources Commission Report 155, Columbia, SC.

Lyell, C., 1845, "Observations on the White Limestone and Other Eocene or Older Tertiary Formations of Virginia, South Carolina, and Georgia". *Quarterly Journal of the Geological Society of London, 1: 429-442*.

McClelland, S. A., 1987, *Surface and Subsurface Stratigraphy of Cretaceous and Younger Strata Along the Savannah River From Southern Richmond County Through Burke County, Georgia*. M.S. Thesis, Department of Geology, University of South Carolina, Columbia, SC.

Muthig, M. G., and Colquhoun, D. J., 1988, "Formal Recognition of Two Members Within the Rhems Formation in Calhoun County, South Carolina". *South Carolina Geology, 32: 11-19*.

Nystrom, P. G., 1986, "Cretaceous-Tertiary Stratigraphy of the Updip Limit of the Coastal Plain Between Ward and Leesville, South Carolina". *Geological Society of America Abstracts with Programs, 18: 258.*

Nystrom, P. G., Jr. and Willoughby, R. H., 1982a, "Cretaceous, Tertiary, and Pleistocene(?) Stratigraphy of Hollow Creek and Graniteville quadrangles, Aiken County, South Carolina". *Geological Investigations Related to the Stratigraphy in the Kaolin Mining District, Aiken County, South Carolina.* Carolina Geological Society 1982 Field Trip Guidebook, South Carolina State Development Board, Division of Geology, Columbia, SC, pp. 80-113.

Nystrom, P. G., Jr. and Willoughby, R. H., 1982b, "Early Tertiary (Jacksonian/Priabonian?) Stratigraphy in Graniteville and Hollow Creek Quadrangles, Aiken County, South Carolina". *Geological Society of America Abstracts with Programs, 18: 68.*

Nystrom, P. G., Jr., Willoughby, R. H., and Price, L. K., 1989, "The Cretaceous and Tertiary Stratigraphy of the Upper Coastal Plain of South Carolina". *Upper Cretaceous and Cenozoic Geology of the Southeastern Atlantic Coastal Plain.* 28th International Geological Congress Field Trip Guidebook T171, American Geophysical Union., Washington, D.C., pp. 23-42.

Nystrom, P. G., Jr., Willoughby, R. H., and Price, L. K., 1991, "Cretaceous and Tertiary Stratigraphy of the Upper Coastal Plain of South Carolina". *The Geology of the Carolinas,* University of Tennessee Press, Knoxville, TN, pp. 221-241.

Padgett, G. C., 1980, *Lithostratigraphy of the Black Mingo Formation in Sumter, Calhoun, and Richland Counties, South Carolina.* M.S. Thesis, Department of Geology, University of South Carolina, Columbia, SC.

Pooser, W. K., 1965, "Biostratigraphy of Cenozoic Ostracoda from South Carolina". *University of Kansas Paleontological Contributions, Arthropoda, 8: 80.*

Prowell, D. C., Edwards, L. E. and Frederiksen, N. O., 1985, *The Ellenton Formation in South Carolina – a Revised Age Designation from Cretaceous to Paleocene.* U.S. Geological Survey Bulletin 1605-A.

Reichert, S. O., 1967, *Summary Report on the Geology and Hydrology of the 100 and 200 Areas at Savannah River Plant for the Period 1961-1966.* DPST-67-475, E.I. DuPont de Nemours and Company, Savannah River Laboratory, Aiken, SC 29801.

Robertson, C. G., 1990, *A Textural, Petrographic, and Hydrogeological Study of the Congaree Formation at the Savannah River Site, South Carolina.* M.S. Thesis, University of North Carolina at Wilmington, Wilmington, NC

Robertson, C. G. and Thayer, P. A., 1992, "Petrology and Reservoir Characteristics of the Congaree Formation at the Savannah River Site, South Carolina". *Savannah River Region: Transition Between the Gulf and Atlantic Coastal Plains, Proceedings of the Second Bald Head Island Conference on Coastal Plains Geology*, University of North Carolina at Wilmington, pp. 54-55.

Siple, G. E., 1967, *Geology and Ground Water of the Savannah River Plant and Vicinity, South Carolina.* U.S. Geological Survey Water Supply Paper 1841.

Siple, G. E., and Pooser, W. K., 1975, *Proposal of the Name Orangeburg Group for Outcropping Beds of Eocene Age in Orangeburg County and Vicinity, South Carolina.* U.S. Geological Survey Bulletin 1395A.

Sloan, E., 1907, "Geology and Mineral Resources". *Handbook of South Carolina, Volume 2*, South Carolina State Department of Agriculture, Commerce, and Immigration, pp 77-145.

Sloan, E., 1908, *Catalogue of the Mineral Localities of South Carolina*, South Carolina Geological Survey, Series 5, Bulletin 2.

Sloss, L. L., Dapples, E. C., and Krumbein, W. C., 1960, *Lithofacies Maps — An Atlas of the United States and Southern Canada.* p 108, John Wiley & Sons, Inc., New York.

Steele, K. B., 1985, *Lithostratigraphic Correlation of Cretaceous and Younger Strata of the Atlantic Coastal Plain Province within Aiken, Allendale, and Barnwell Counties, South Carolina.* M.S. Thesis, Department of Geology, University of South Carolina, Columbia, SC.

Thayer, P. A., Smits, A. D., Harris, M. K., Amidon, M. B., and Lewis, C. L., 1993, *Hydrostratigaphic Maps of the General Separations Area (GSA), Savannah River Site (SRS), Aiken, South Carolina, Phase II (U),* WSRC-RP-94-40, Westinghouse Savannah River Company, Aiken, SC 29808.

U. S. Army Corps of Engineers, 1952, *Foundation Grouting Operations Savannah River Plant,* U.S. Army Corps of Engineers, Charleston District.

Van Nieuwenhuise, D. S., and Colquhoun, D. J., 1982 "The Paleocene-Lower Eocene Black Mingo Group of the East Central Coastal Plain of South Carolina". *South Carolina Geology, 26:27-67.*

WSRC, 1990, "ESSOP-2-15: Microscopic Examination of Sediment Cores". *Environmental Sciences Section Operating Procedures.* Manual WSRC-L-14.1, Westinghouse Savannah River Company, Aiken, SC 29808.

Willoughby, R. H., 1983, *Geologic Map of the Graniteville Quadrangle*. South Carolina Geological Survey Open-File Report 31, 1:24,000.

Willoughby, R. H., 1985, *Geologic Map of the Coastal Plain in Johnston and Edgefield Quadrangle*. South Carolina Geological Survey Open-File Report 46, 1:24,000.

Willoughby, R. H., 1986, "Stratigraphy of the Northwestern Edge of the Coastal Plain in Aiken and Lexington Counties, South Carolina". *Geological Society of America Abstracts with Programs, 18: 272-273.*

(This page intentionally left blank)

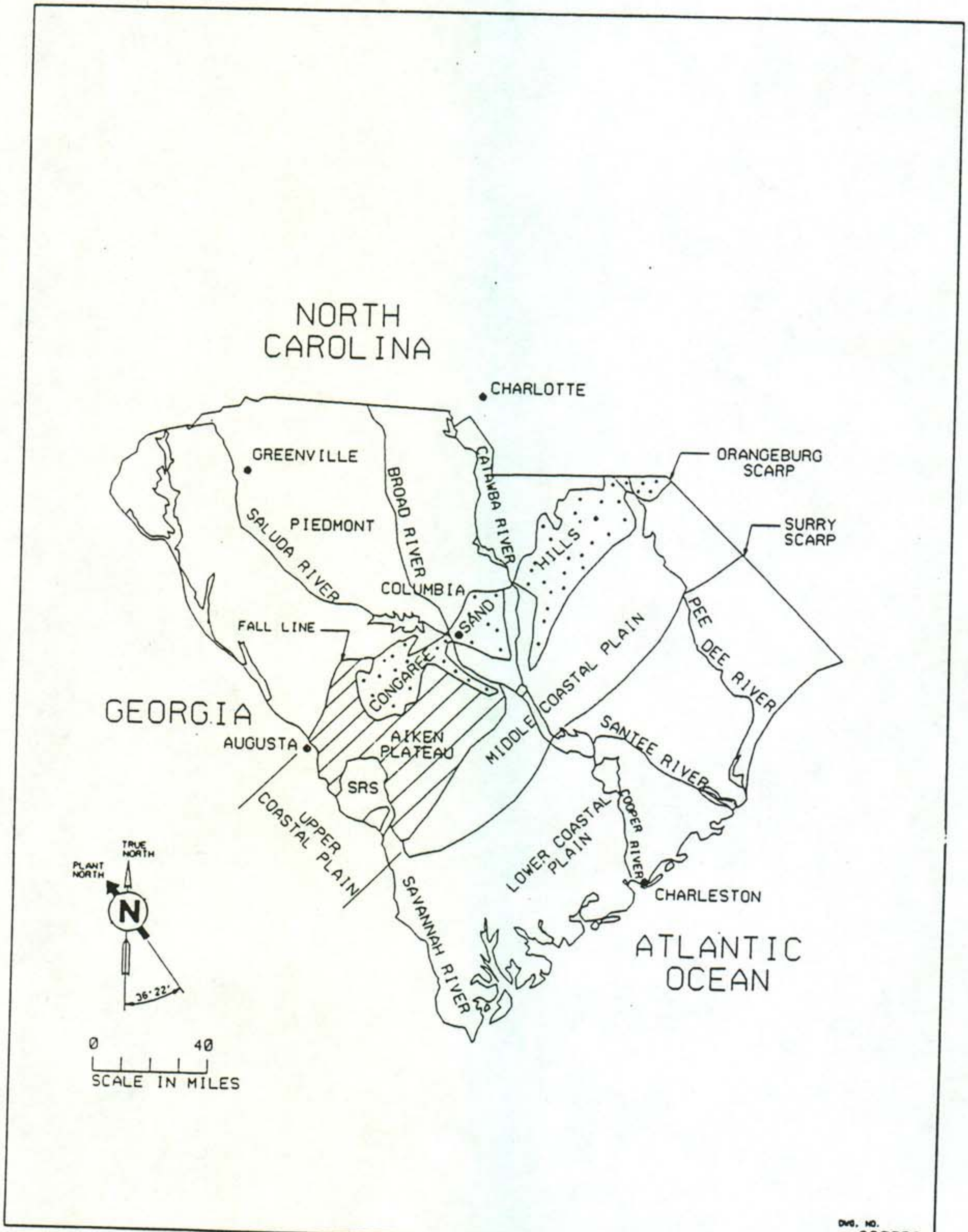

Figure 1. Location of the Savannah River Site and Physiography of the Surrounding Region

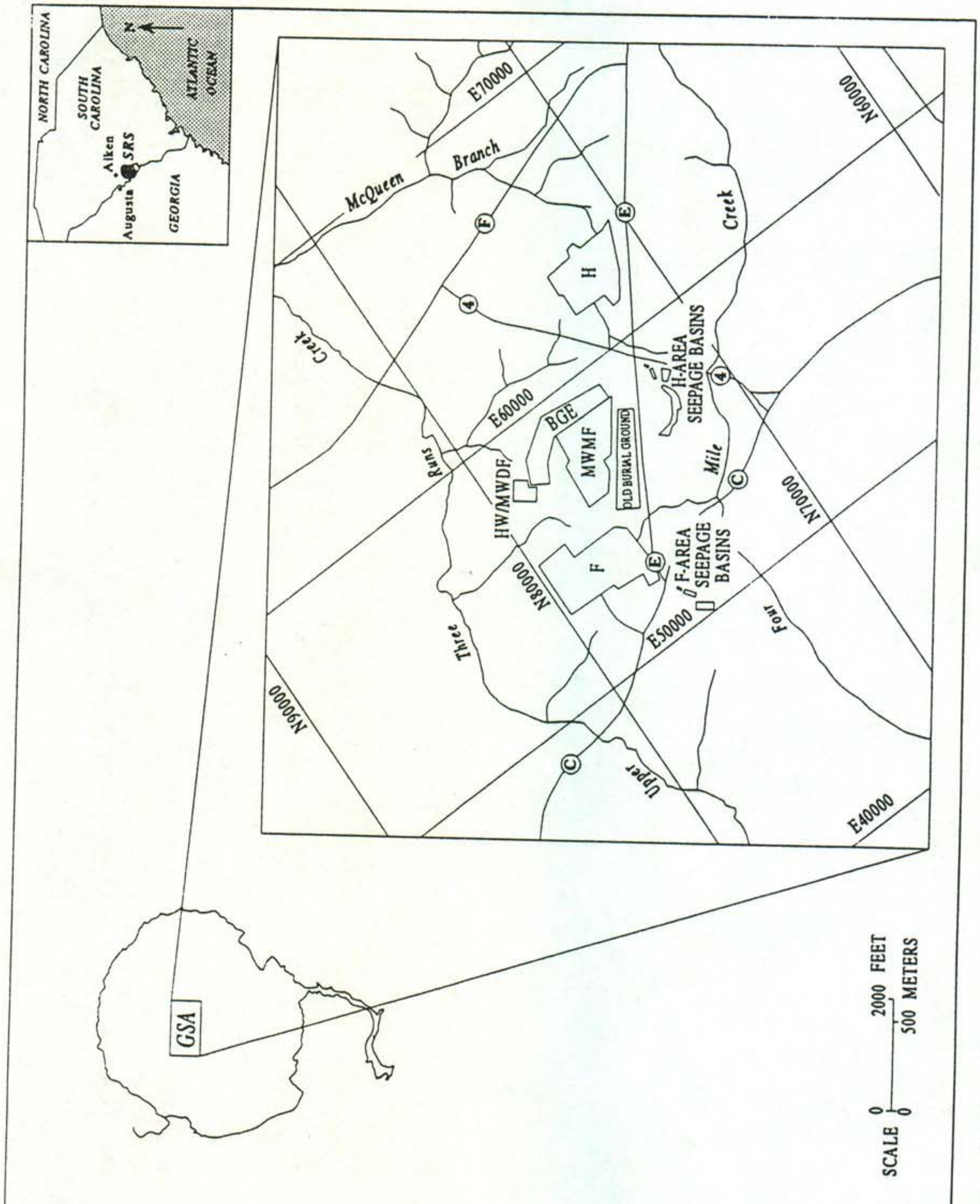

Figure 2. Location of the General Separations Area, Savannah River Site, South Carolina

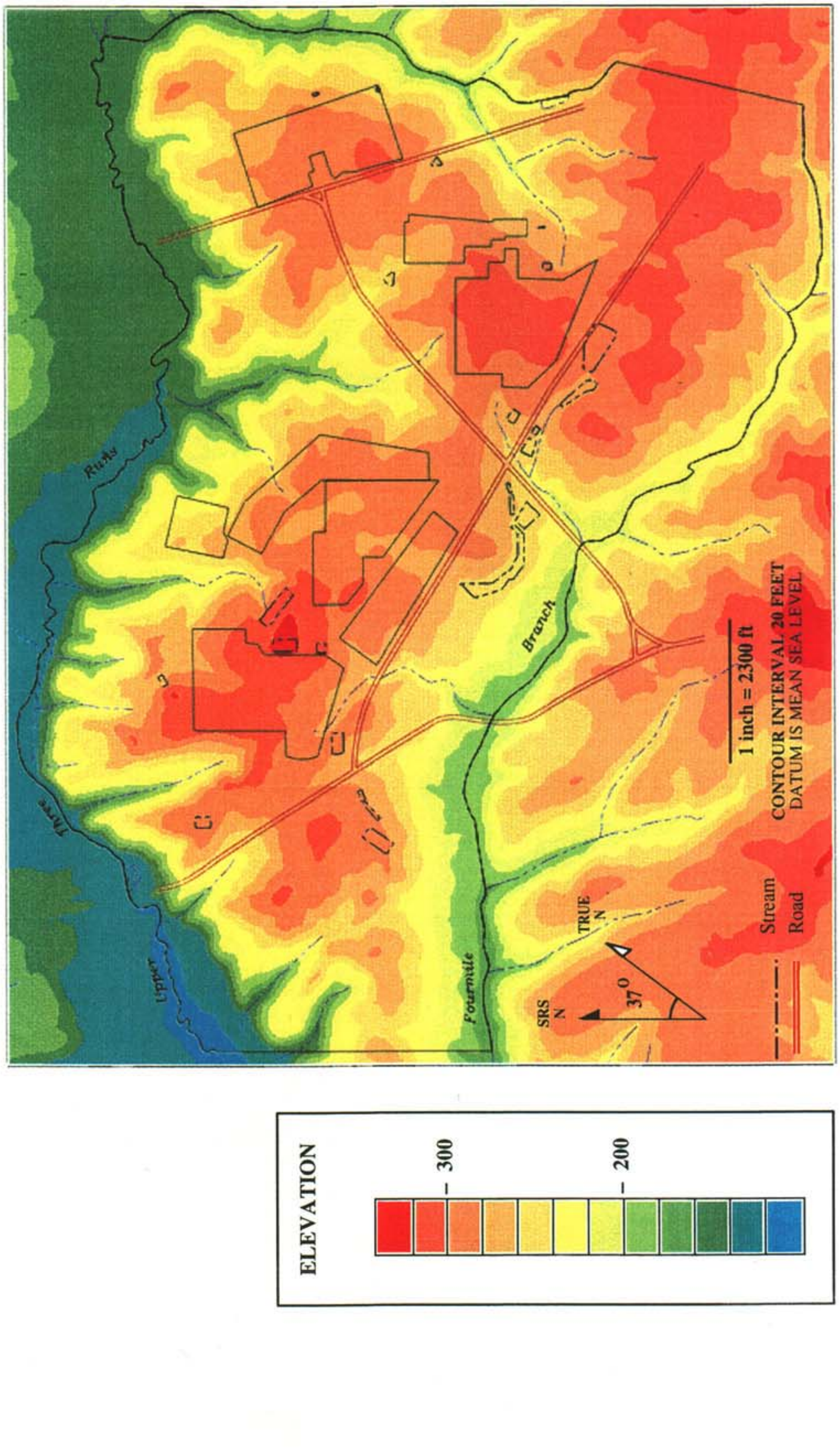

Figure 3. Topography and Drainage Features, General Separations Area, SRS

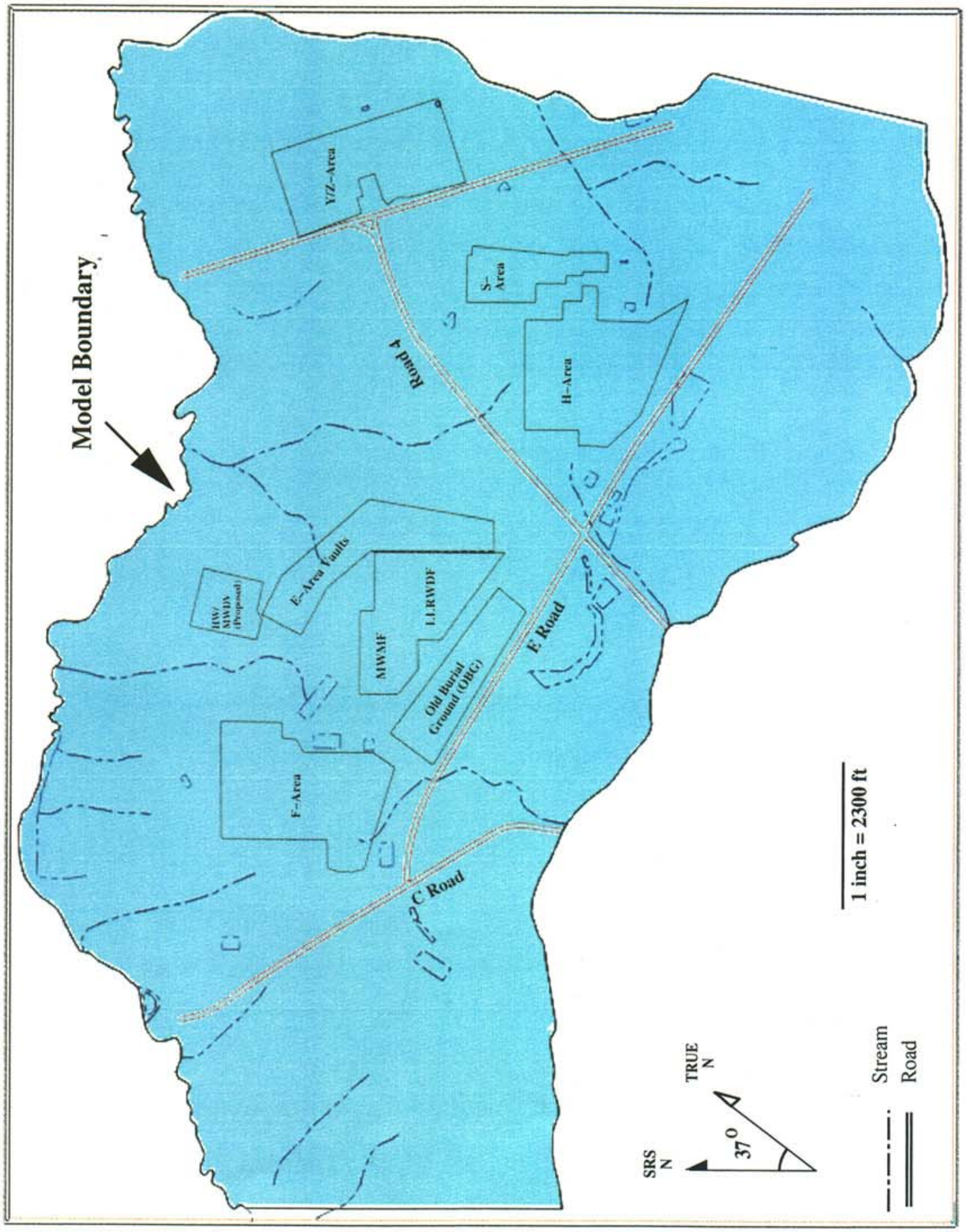

Figure 4. Model Boundaries

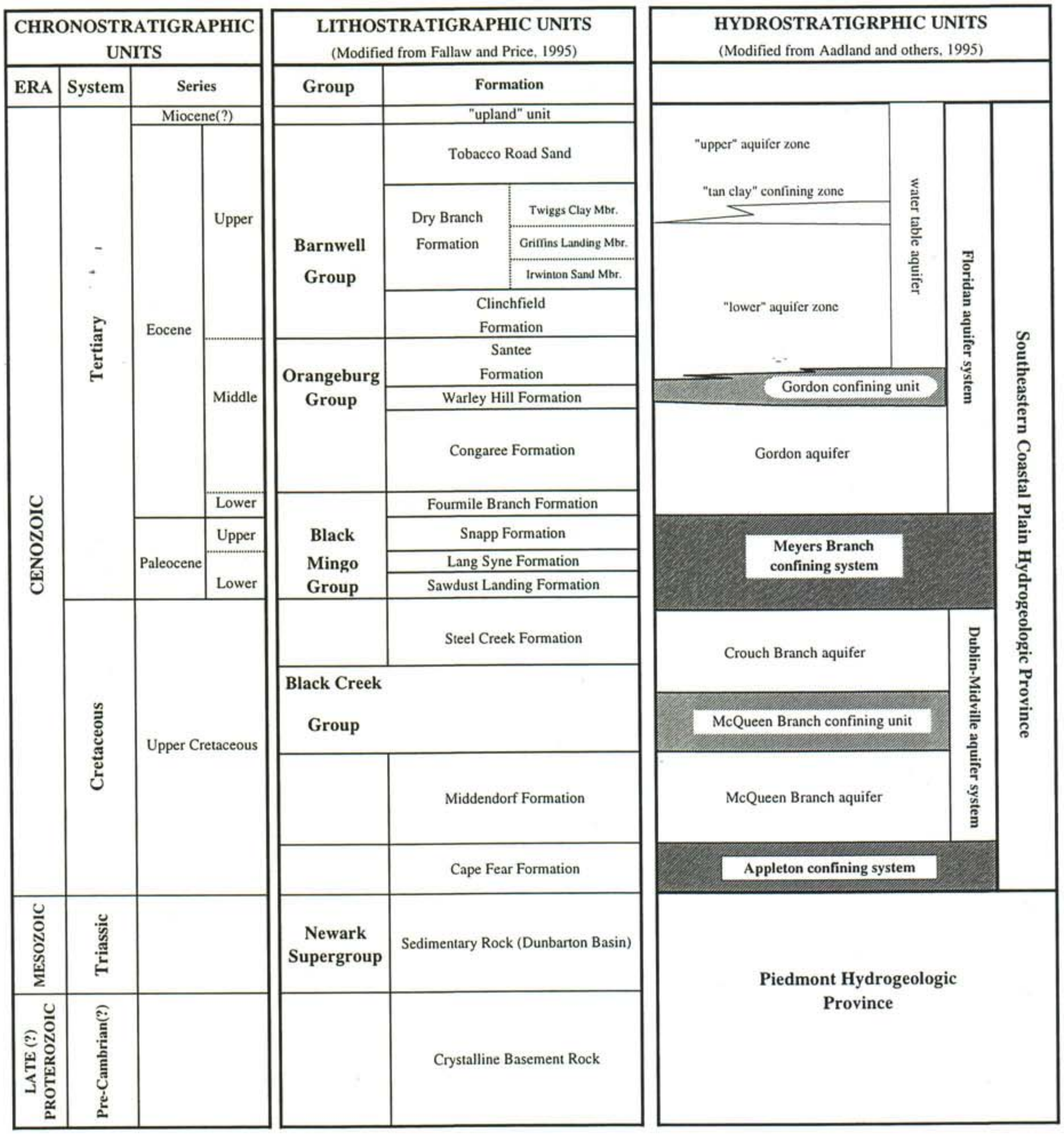

Figure 5. Comparison of Lithostratigraphic and Hydrostratigraphic Units at SRS

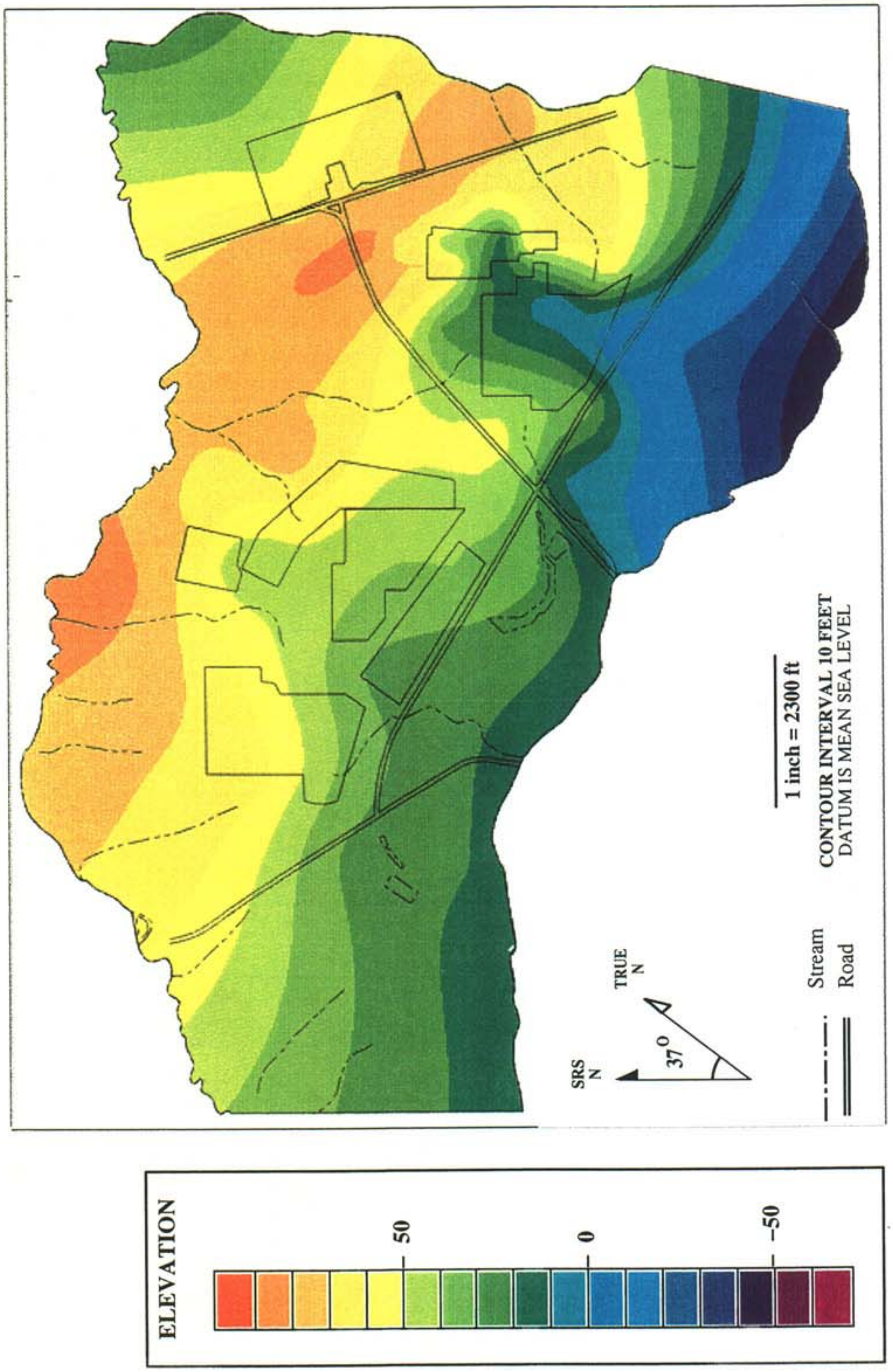

Figure 6. Structure–Contour Map of the Top of the Lang Syne Formation

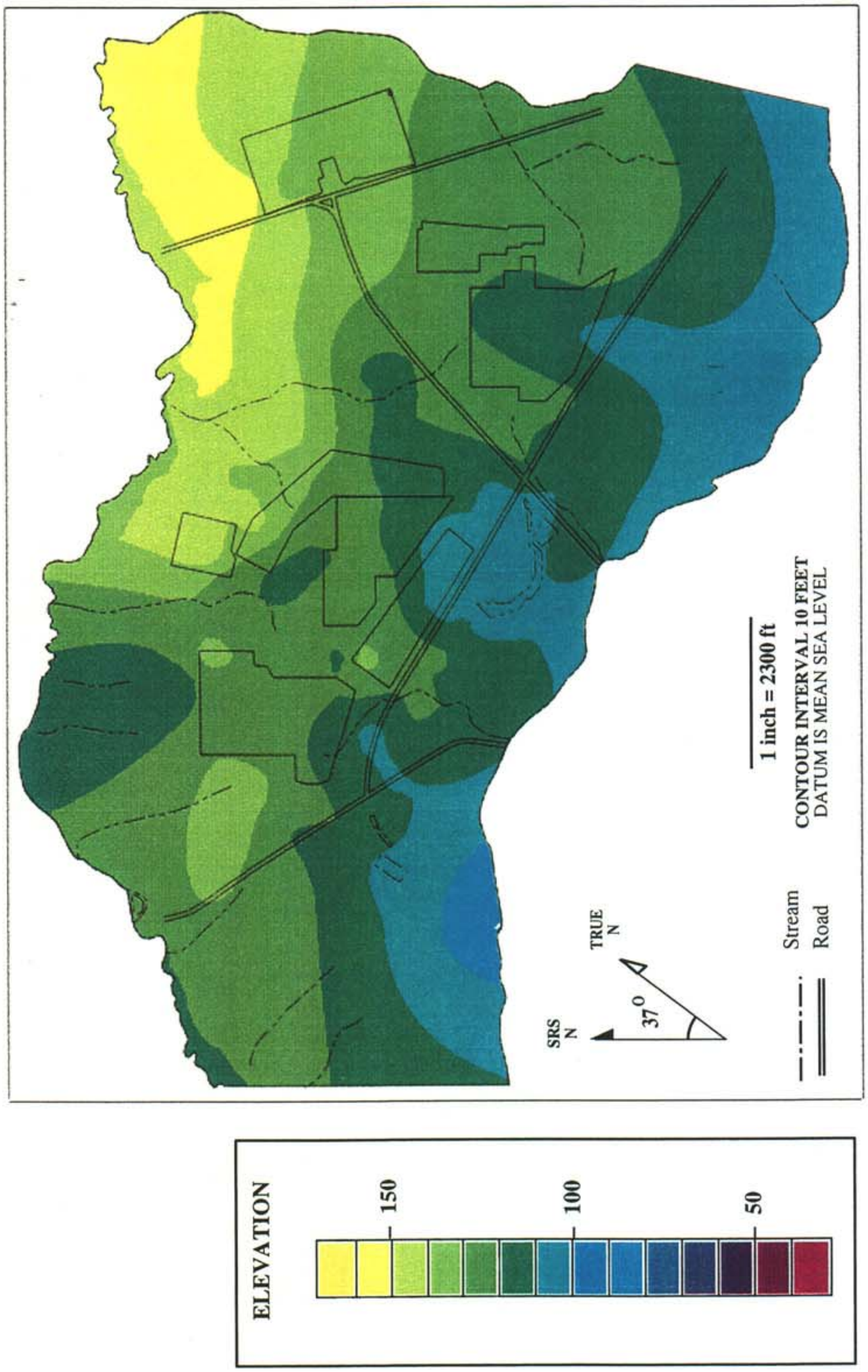

Figure 7. Structure–Contour Map of the Top of the Congaree Formation

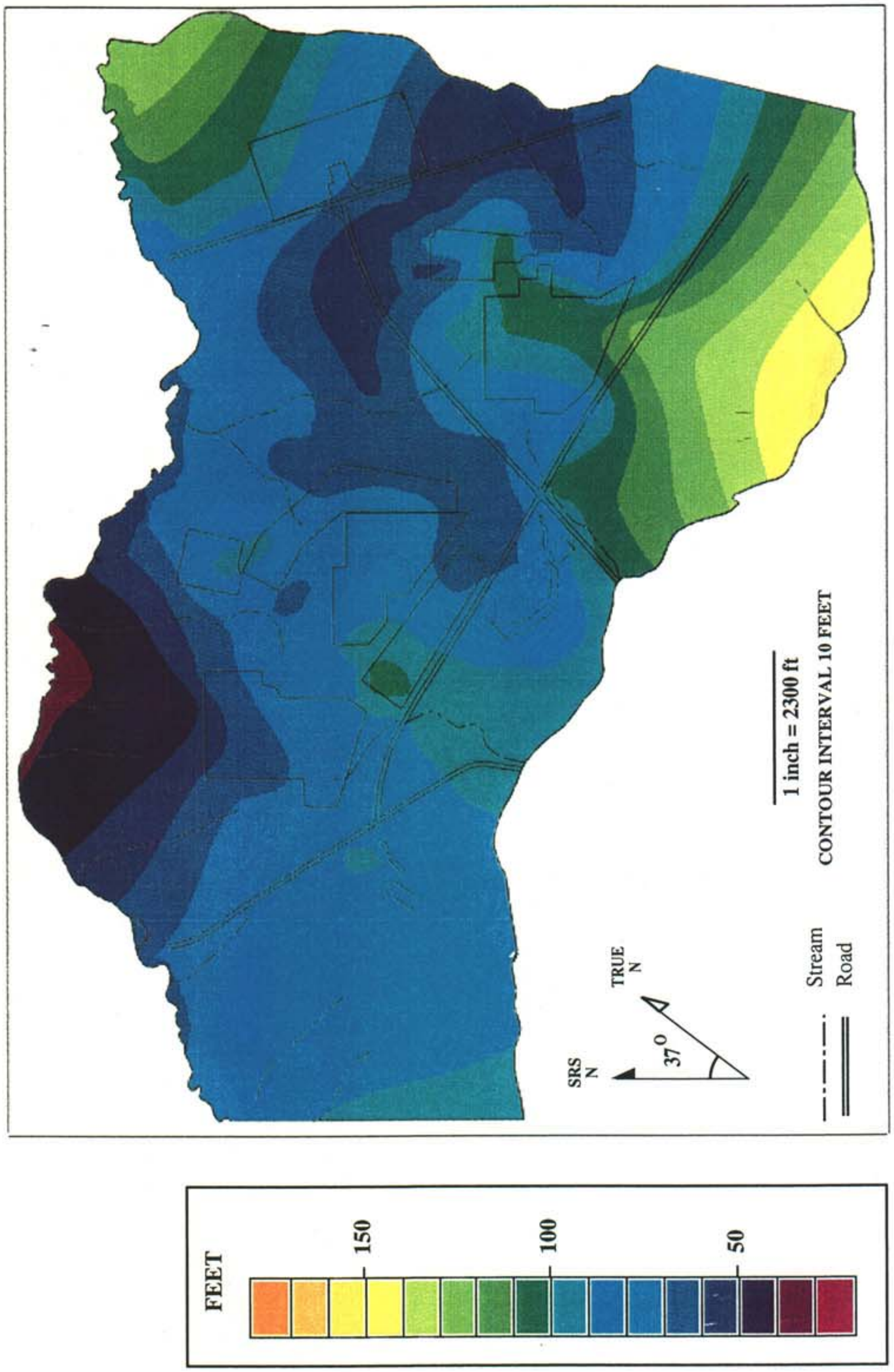

Figure 8. Isopach Map of the Congaree Formation

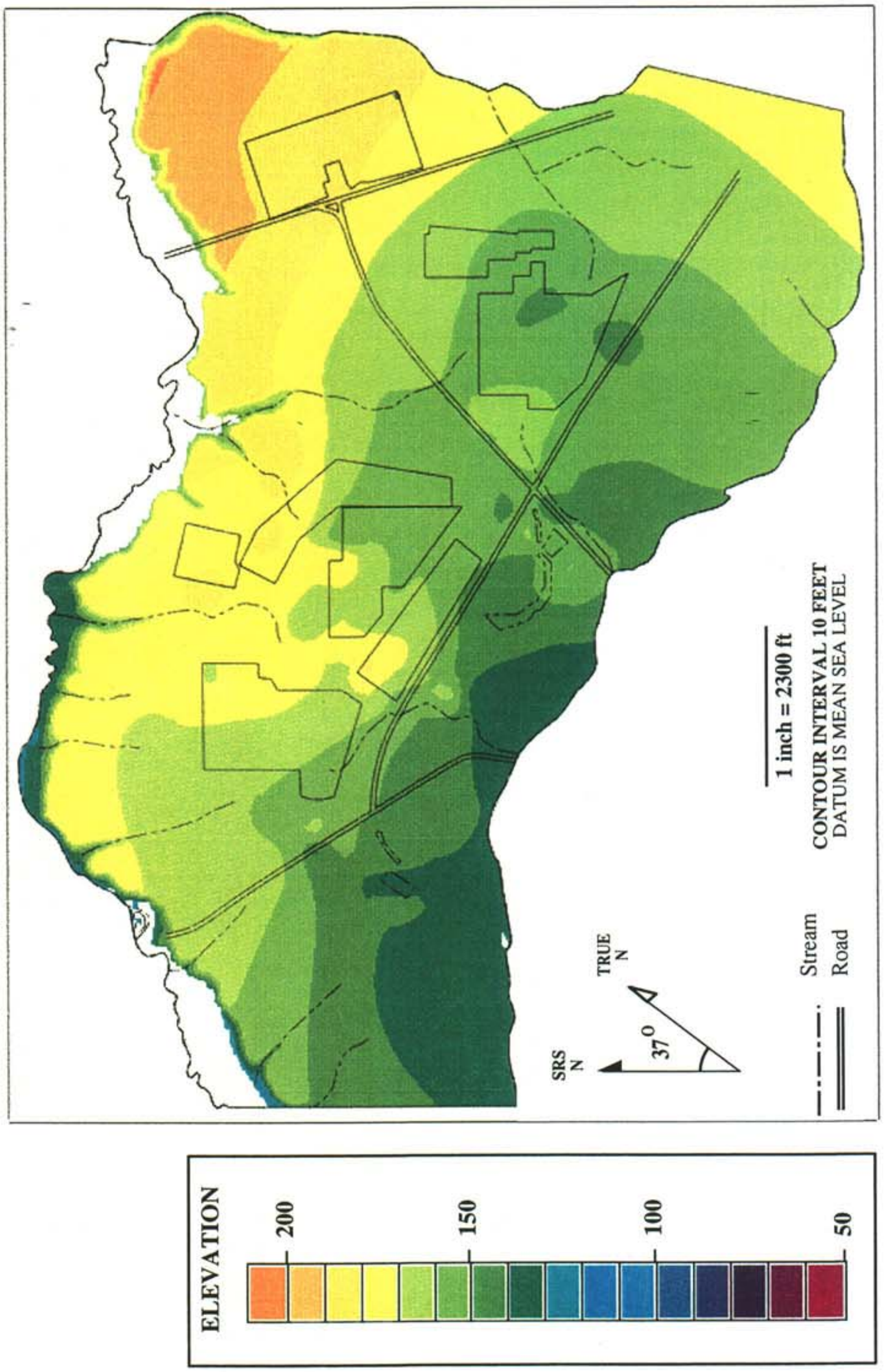

Figure 9. Structure–Contour Map of the Top of the Santee Formation

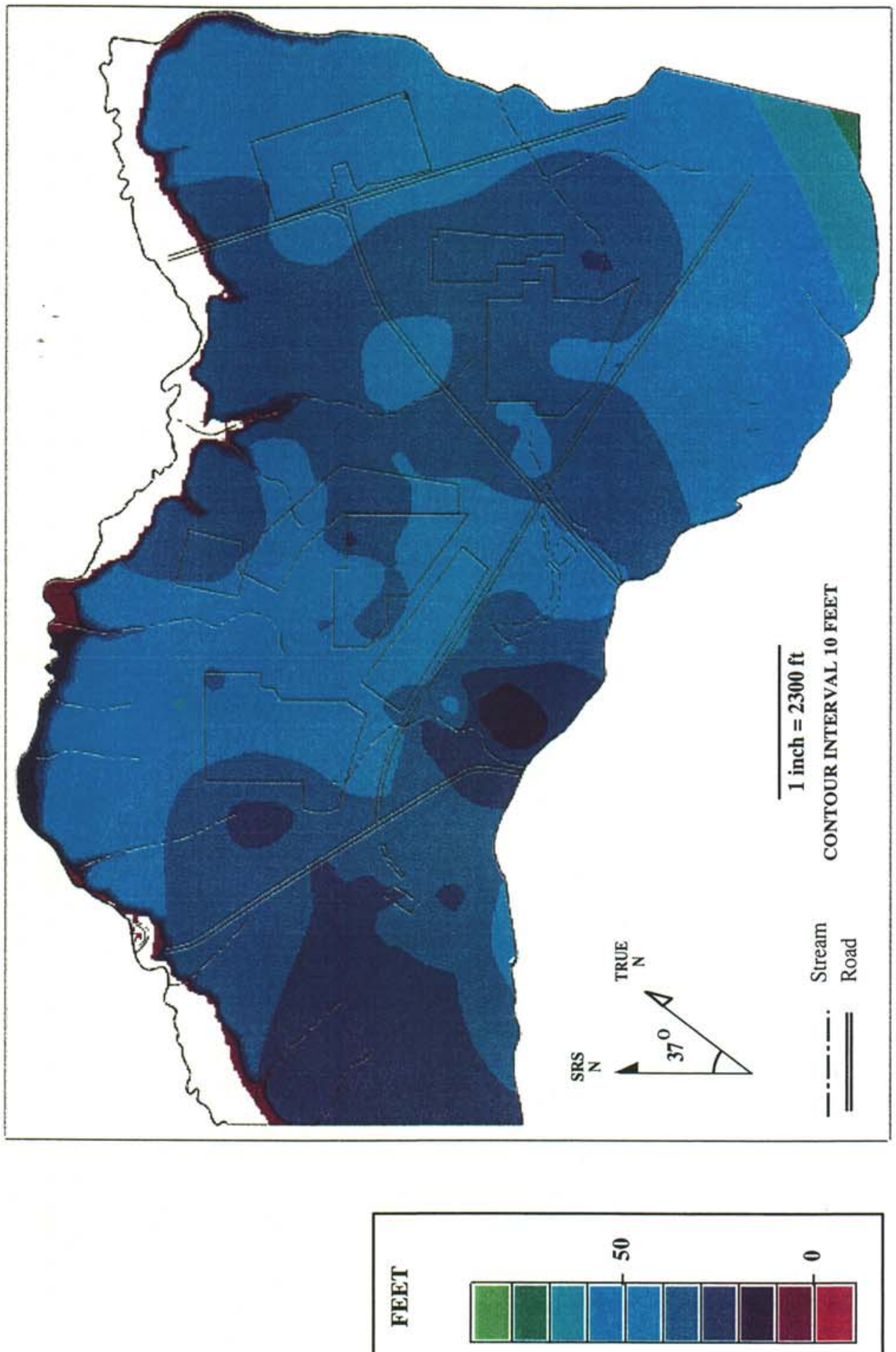

Figure 10. Isopach Map of the Santee Formation

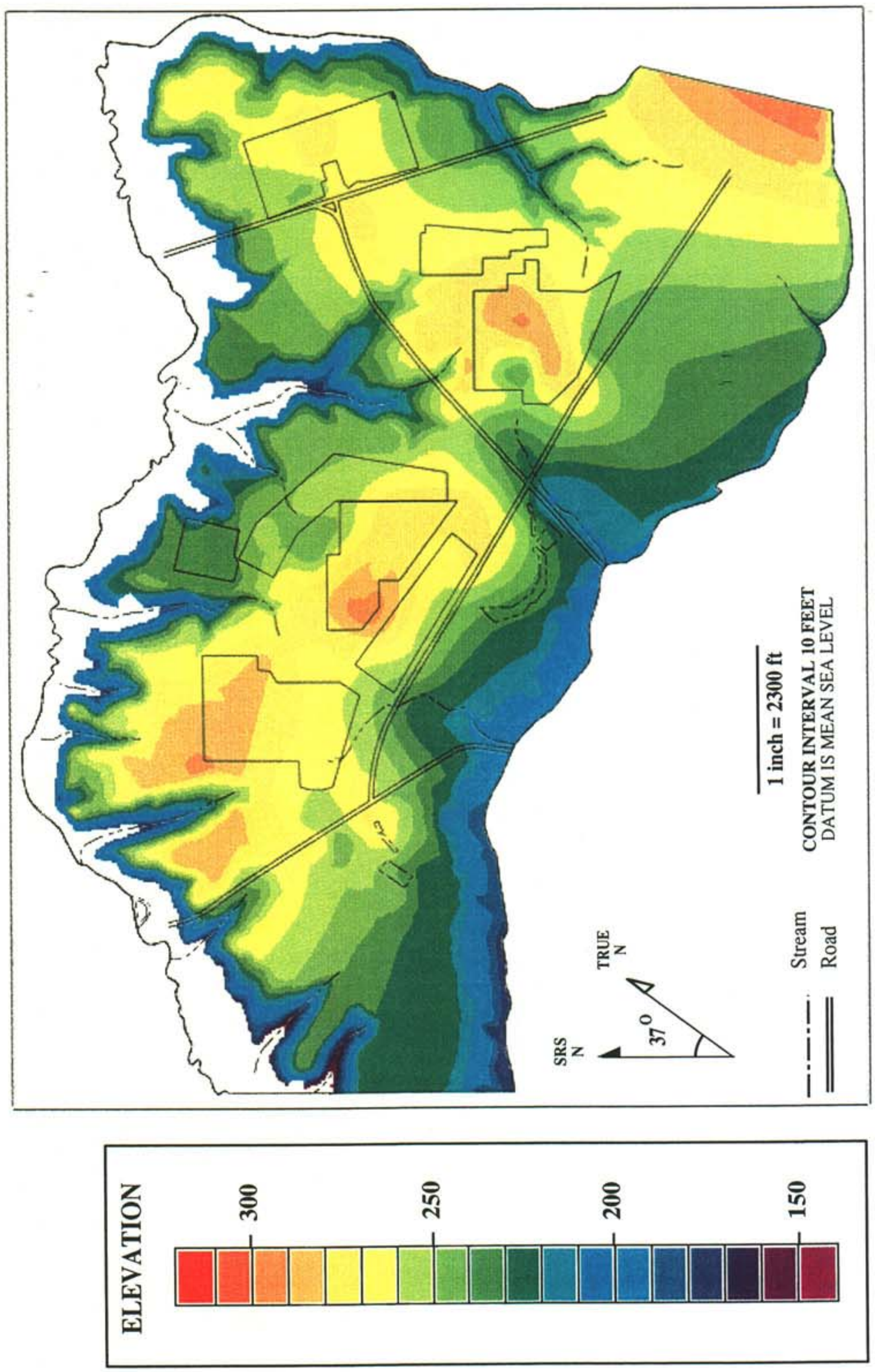

Figure 11. Structure–Contour Map of the Top of the Barnwell Group

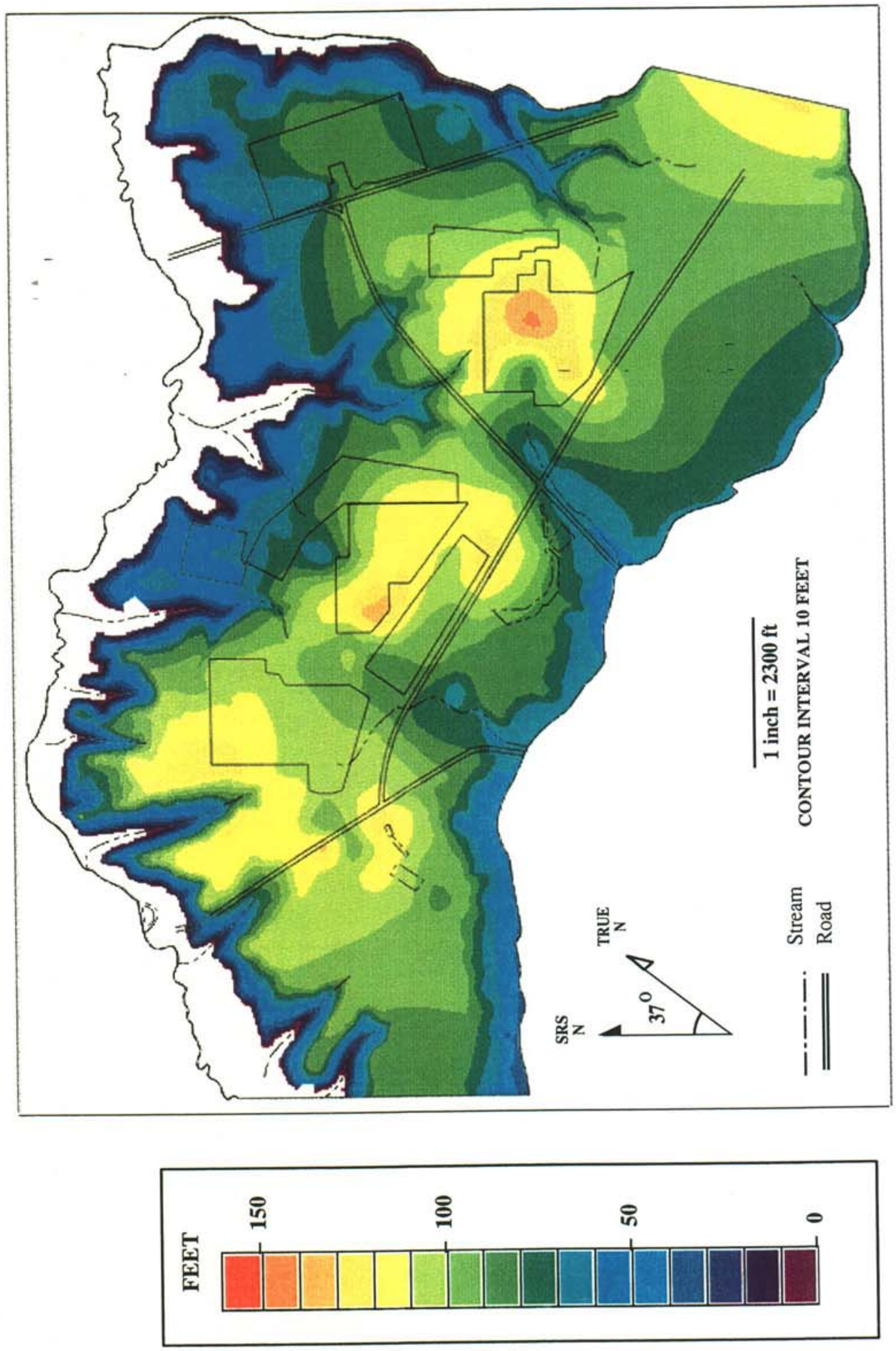

Figure 12. Isopach Map of the Barnwell Group

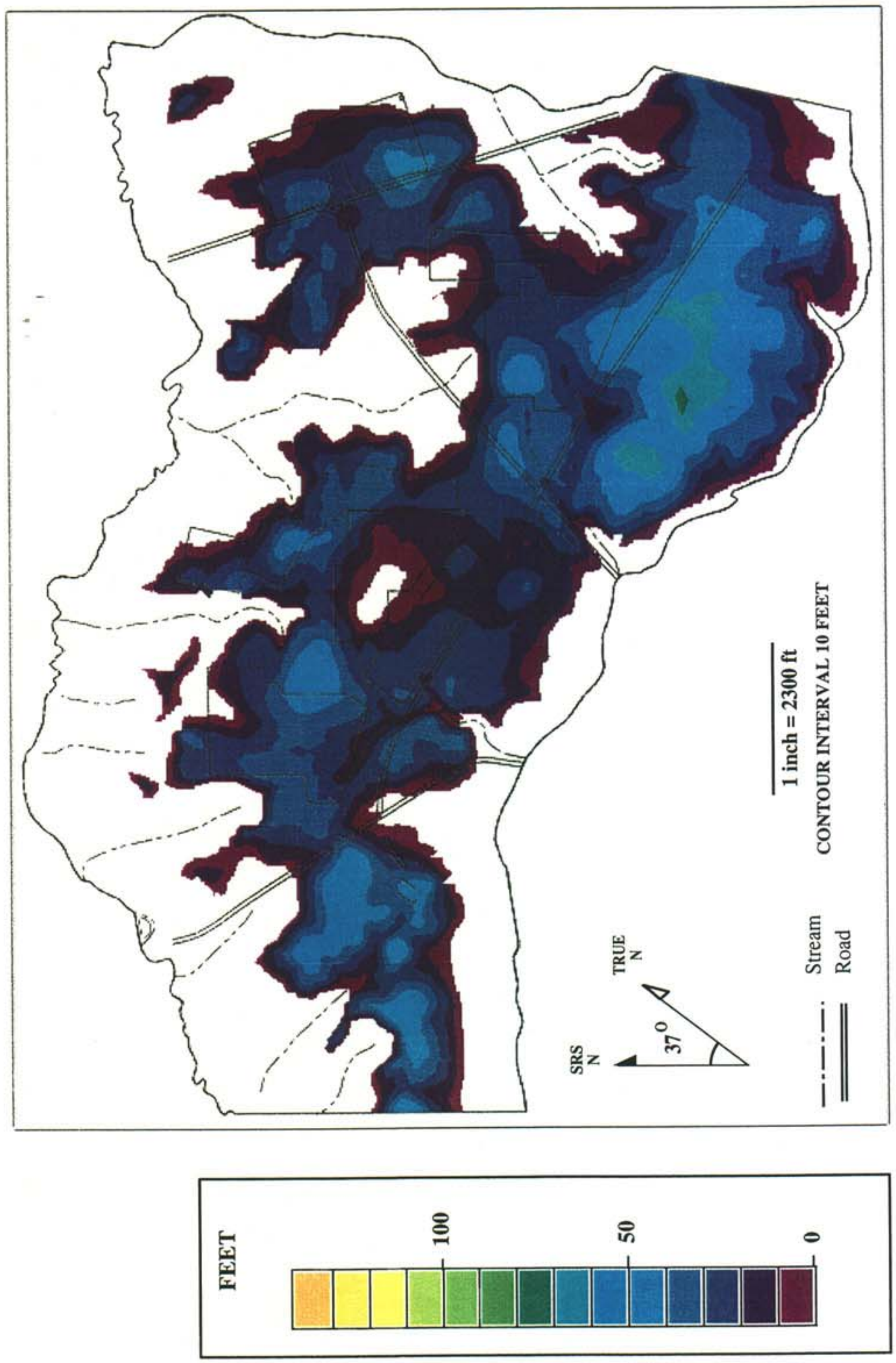

Figure 13. Isopach Map of the "Upland" Unit

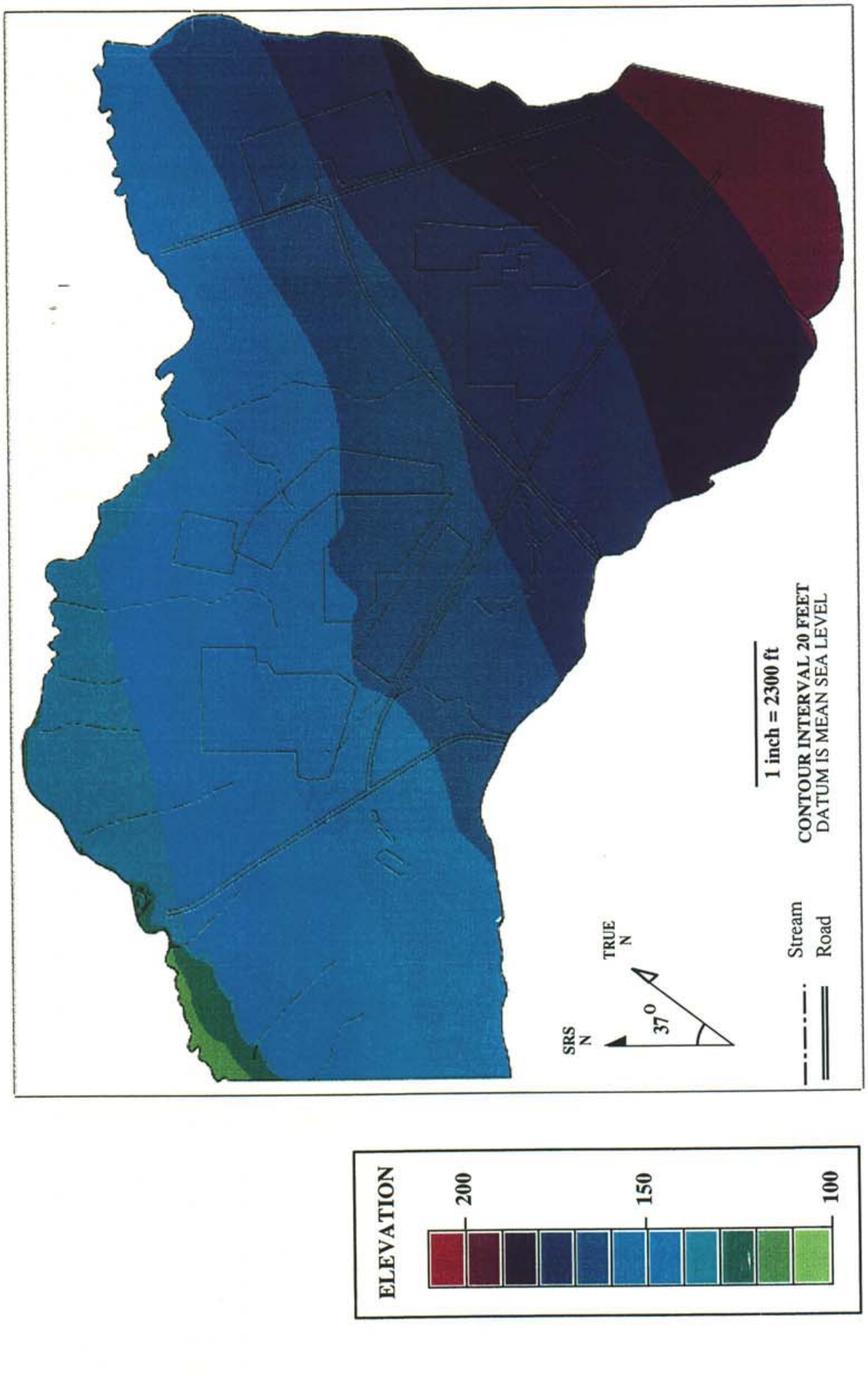

Figure 14. Potentiometric Surface of the Gordon Aquifer

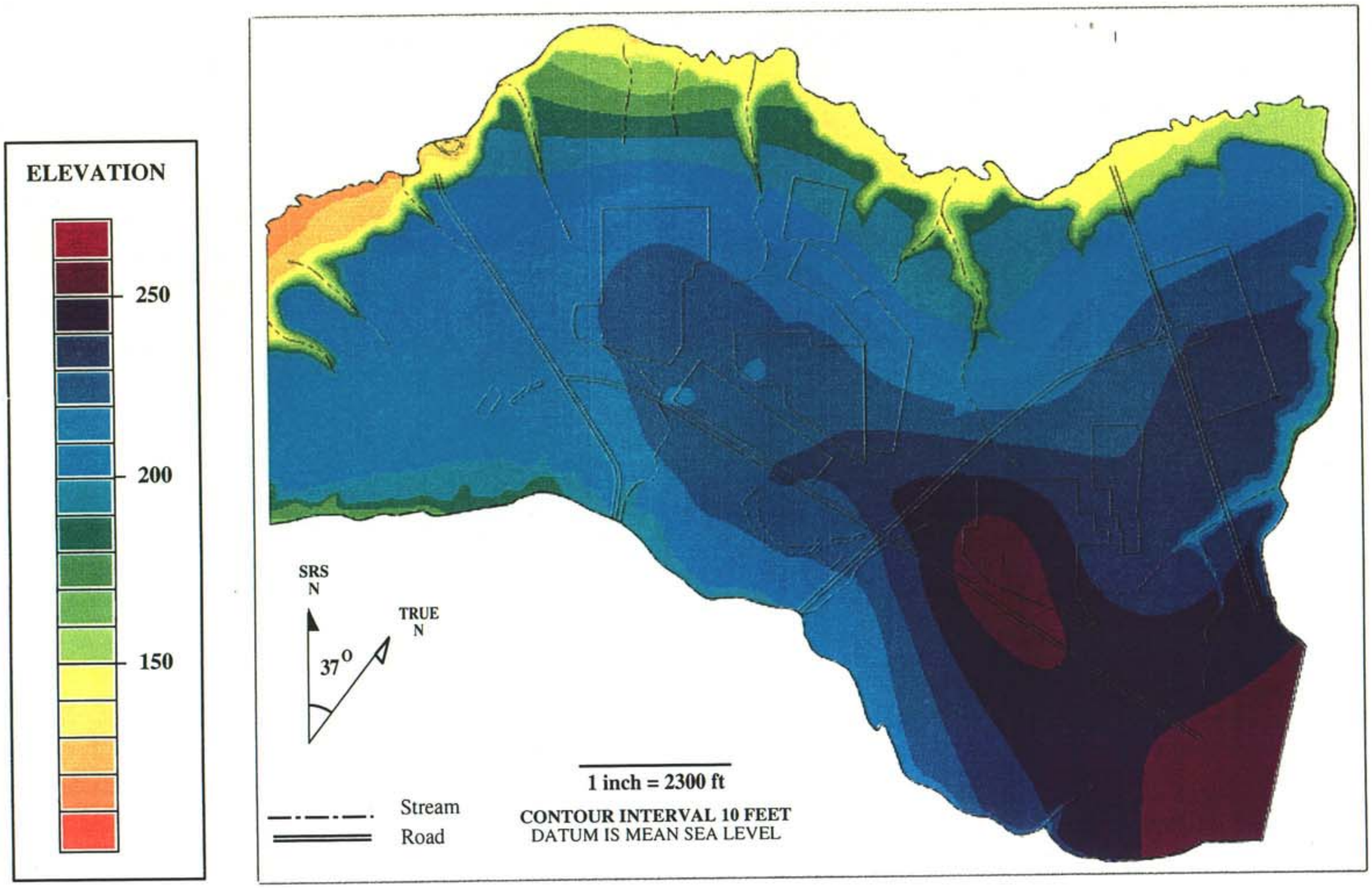

Figure 15. Potentiometric Surface of the "Lower" Aquifer Zone of the Water Table Aquifer

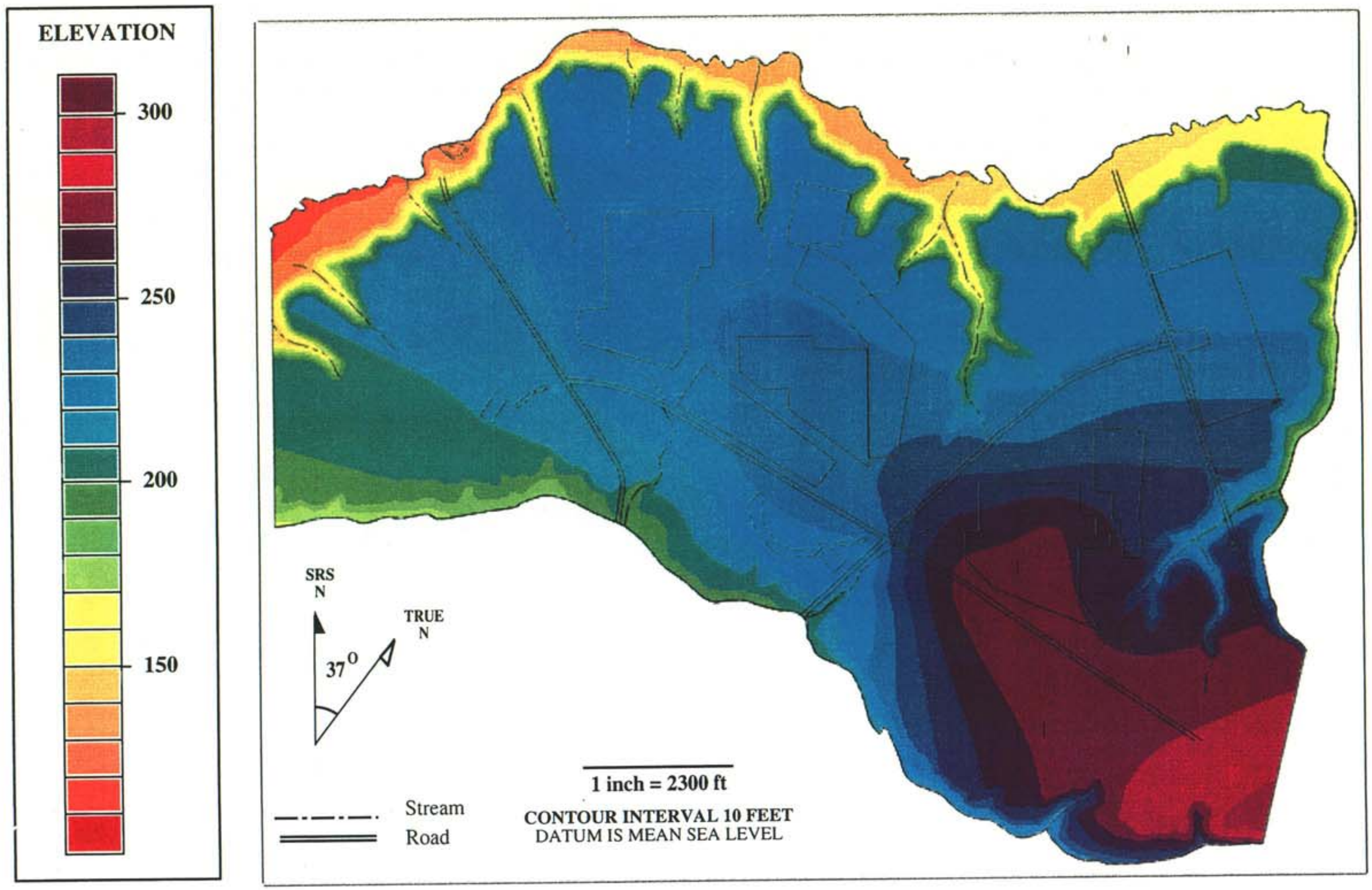

Figure 16. Water–Table Surface within the "Upper" Aquifer Zone of the Water Table Aquifer

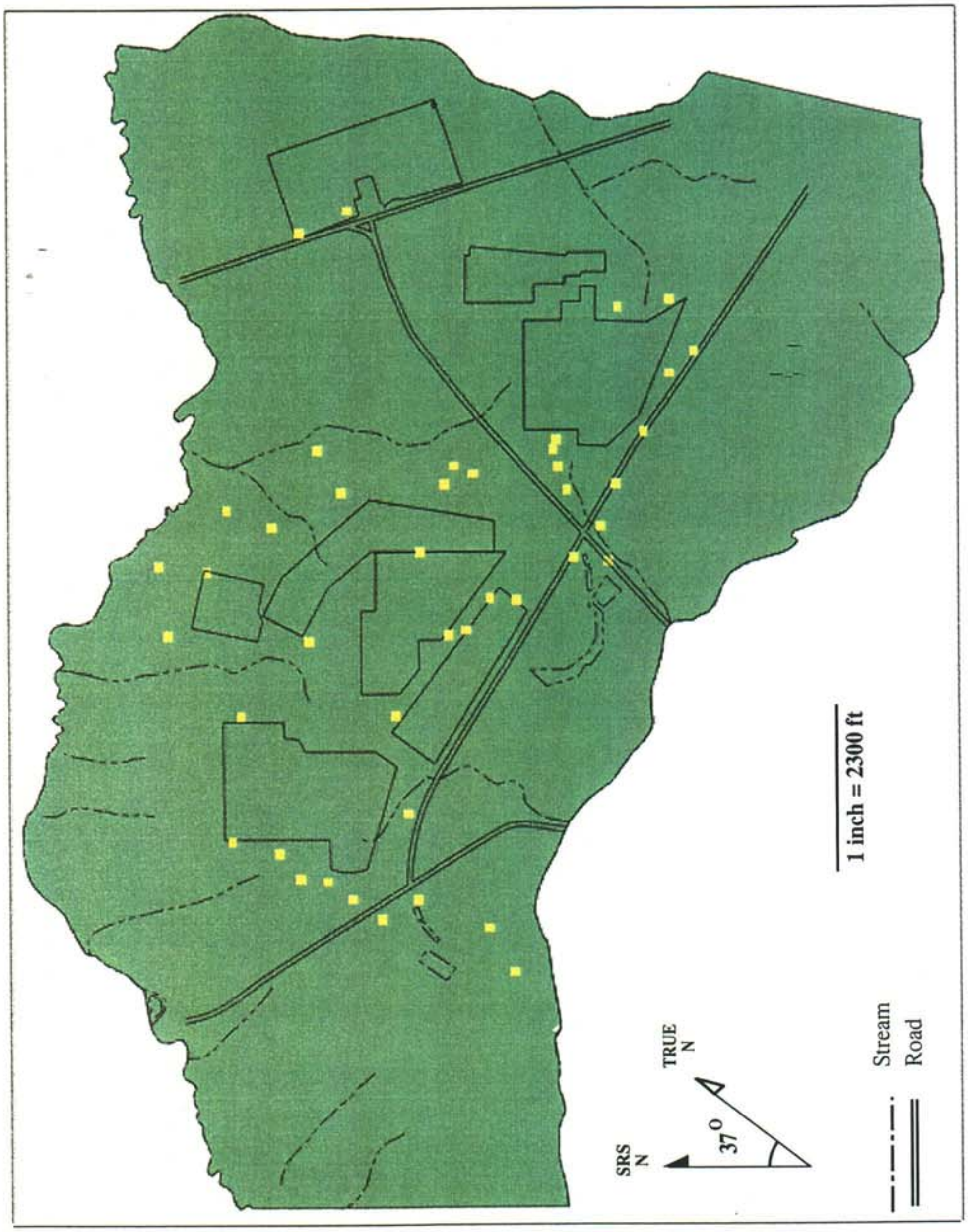

Figure 17. Data Points Used to Grid the Meyers Branch Confining System

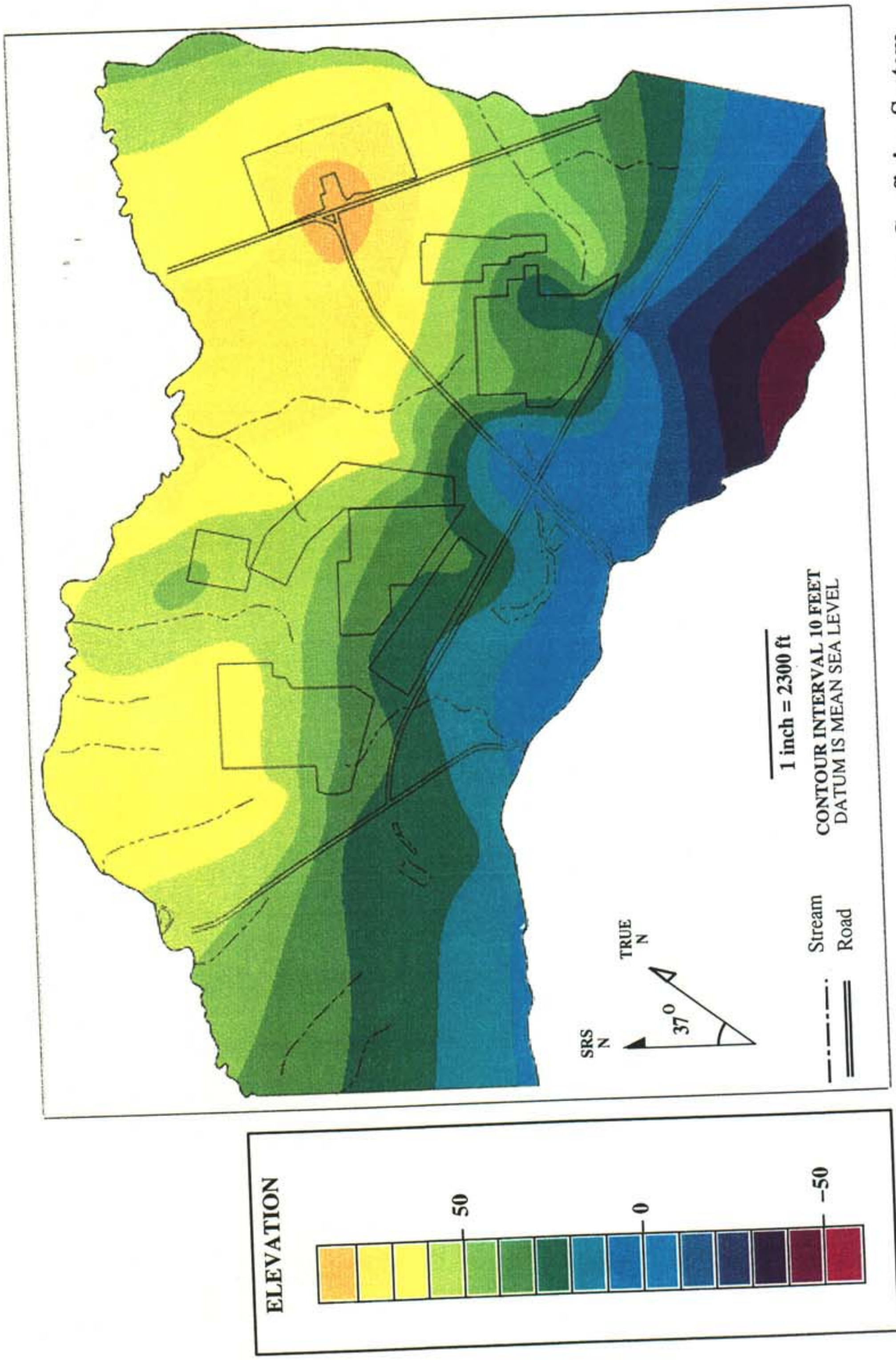

Figure 18. Altitude–Contour Map of the Top of the Meyers Branch Confining System

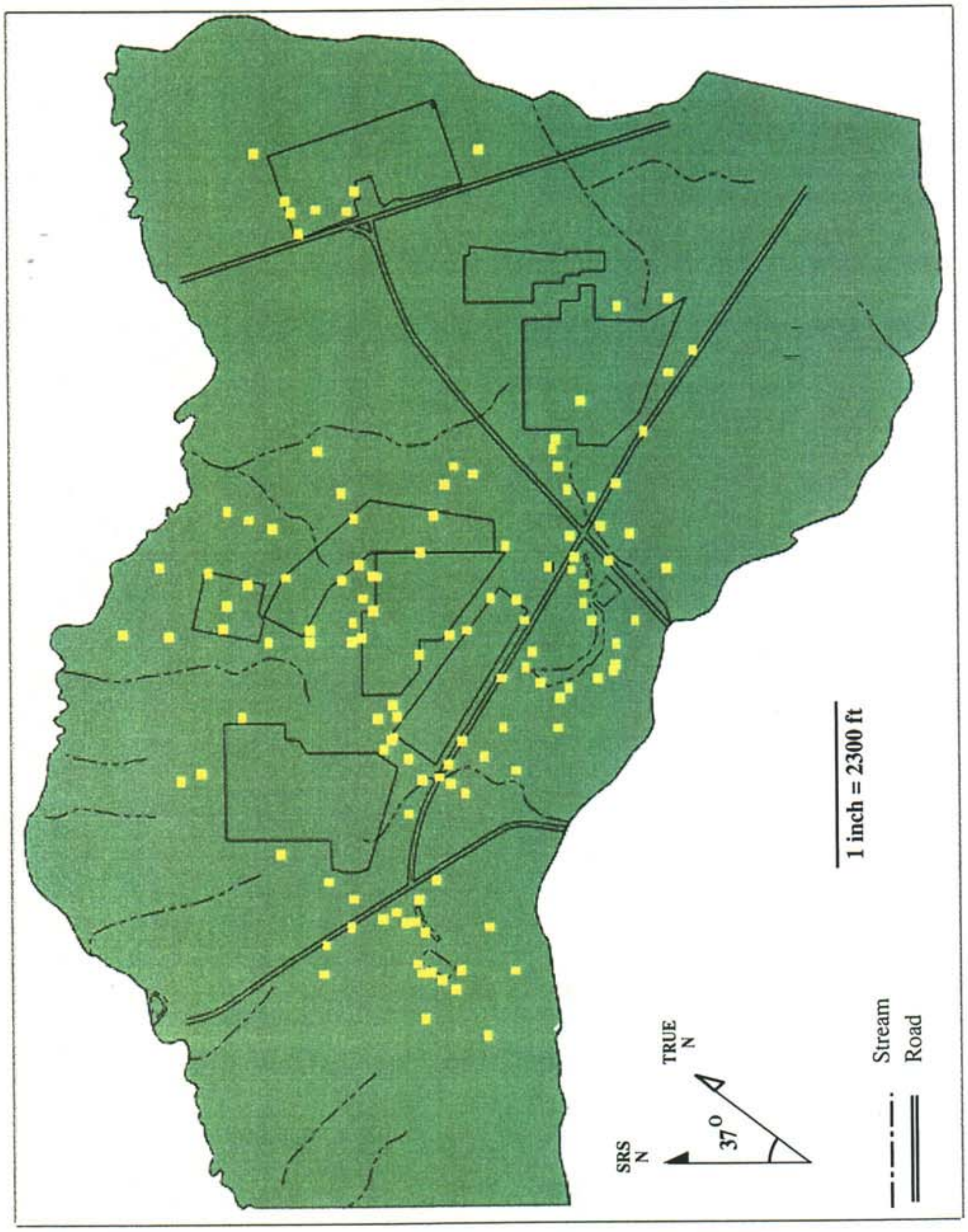

Figure 19. Data Points Used to Grid the Gordon Aquifer

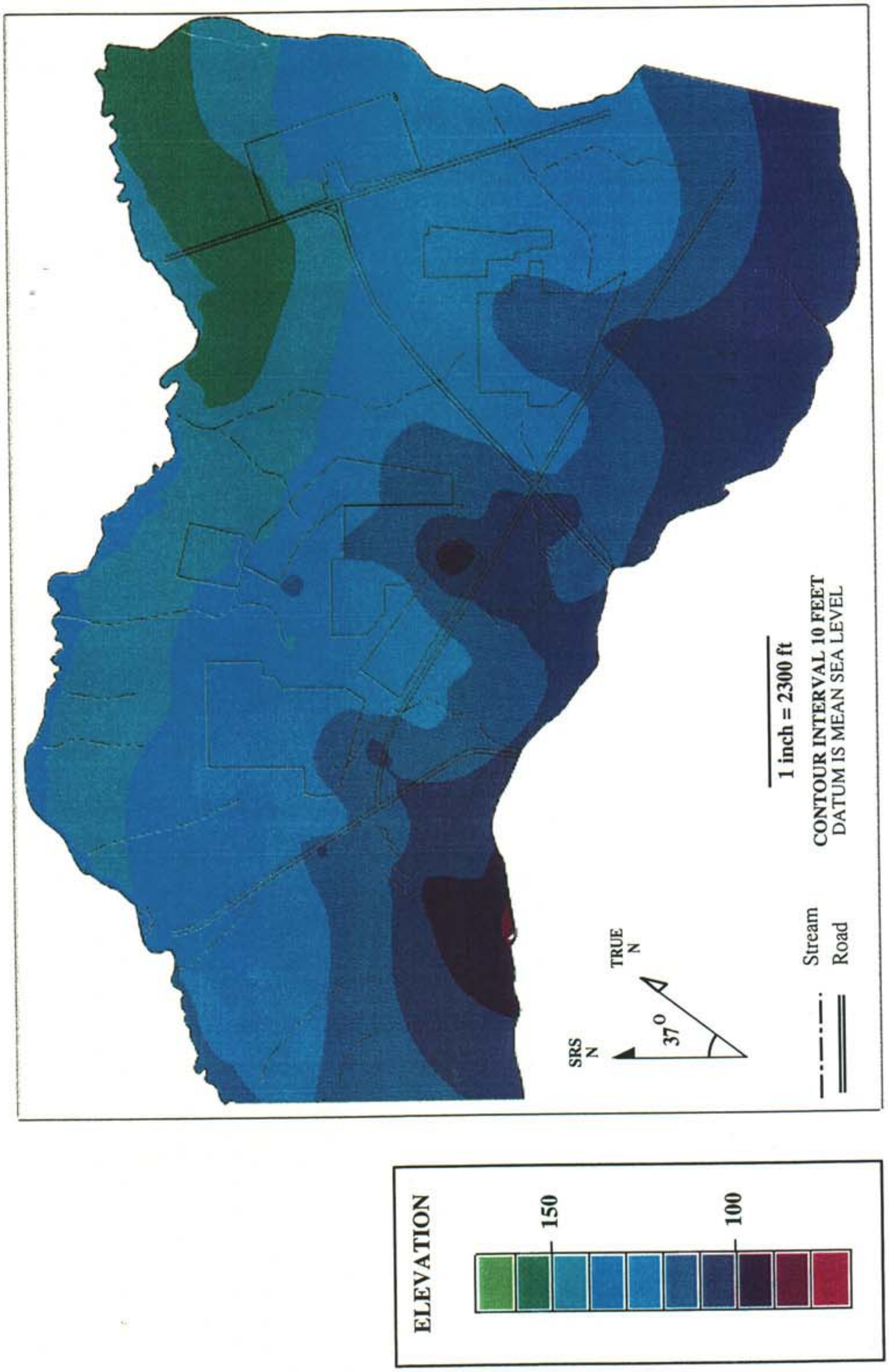

Figure 20. Structure–Contour Map of the Top of the Gordon Aquifer

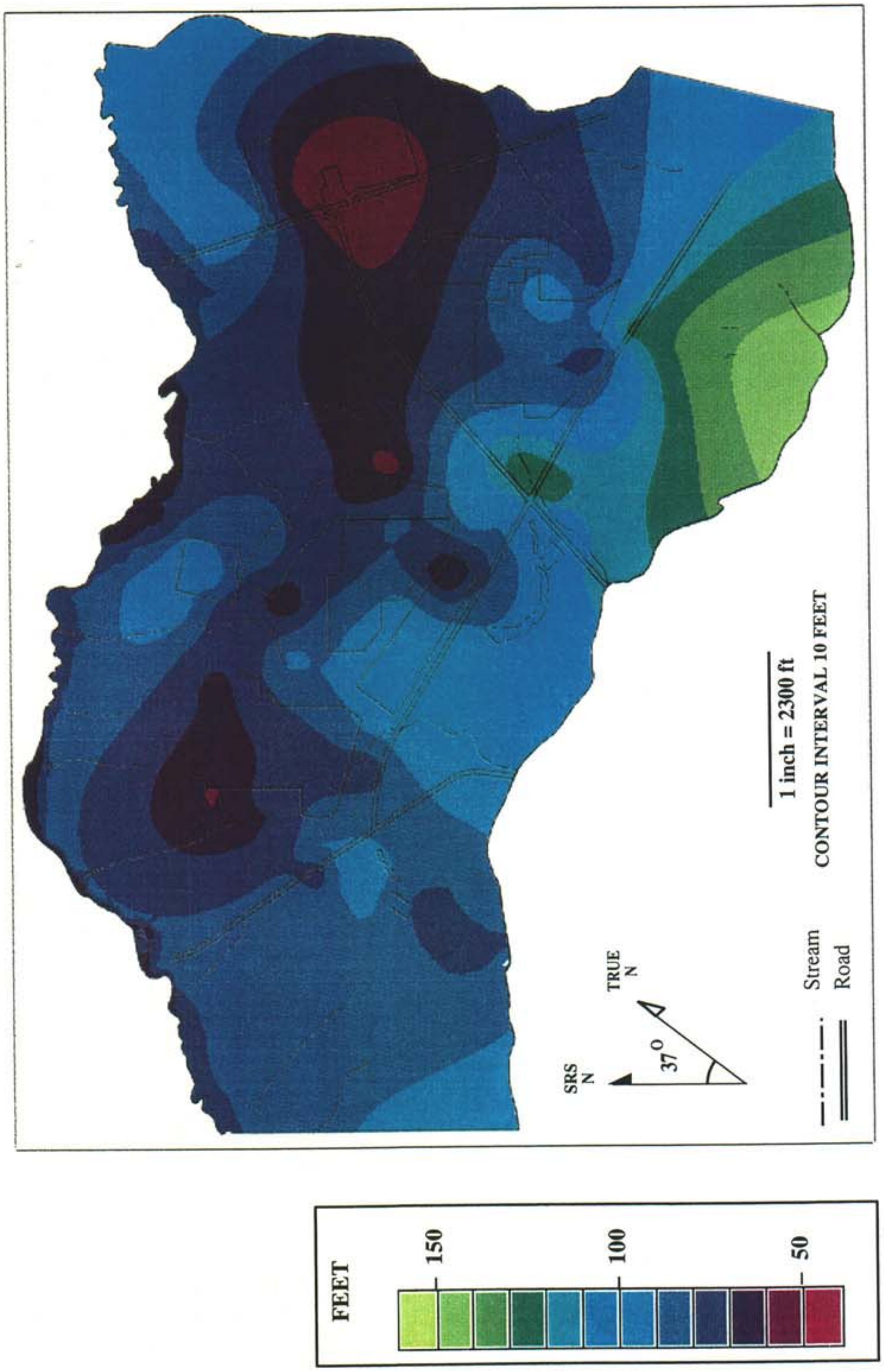

Figure 21. Isopach Map of the Gordon Aquifer

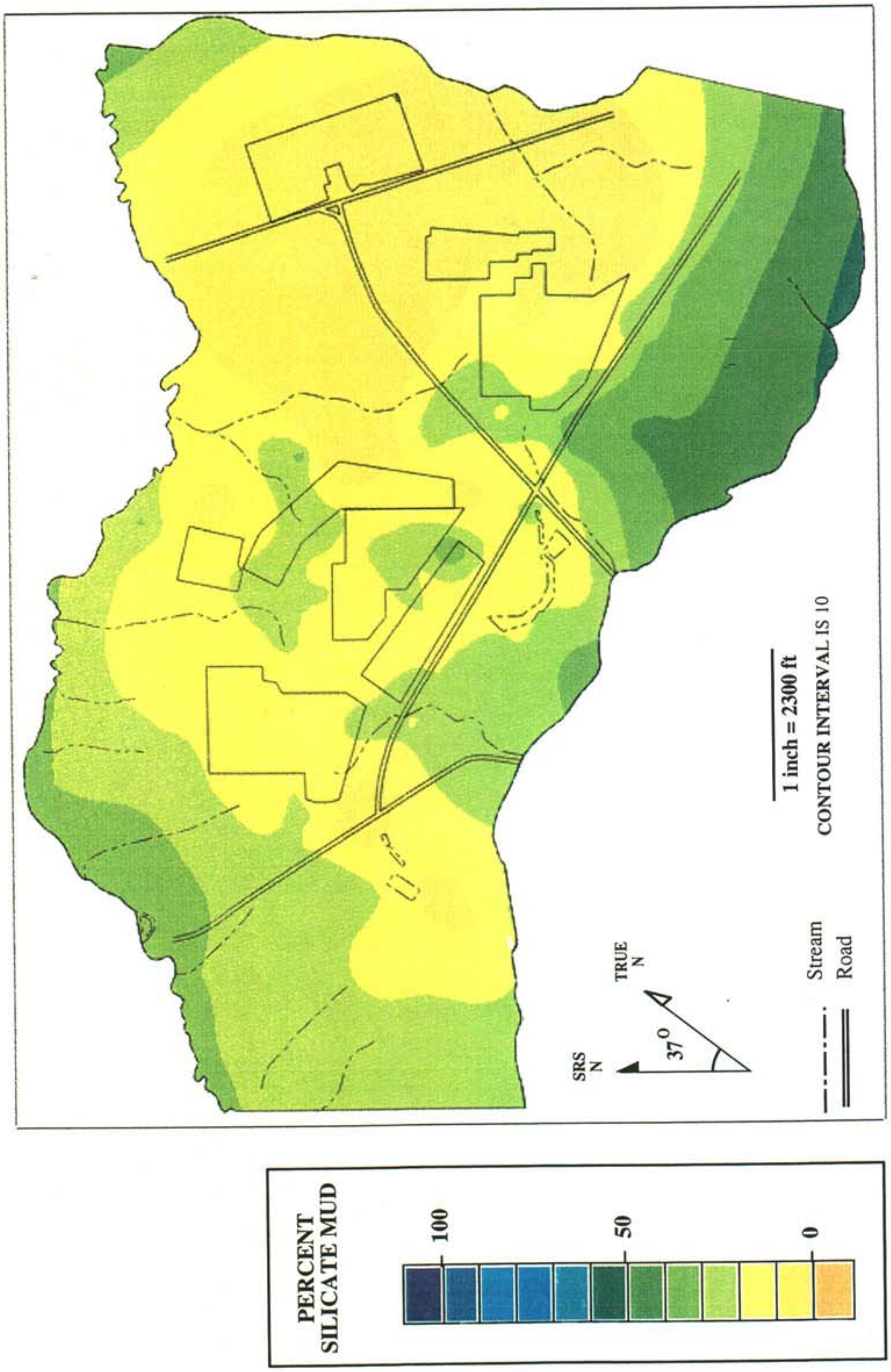

Figure 22. Map of Average Percent Silicate Mud in the Gordon Aquifer

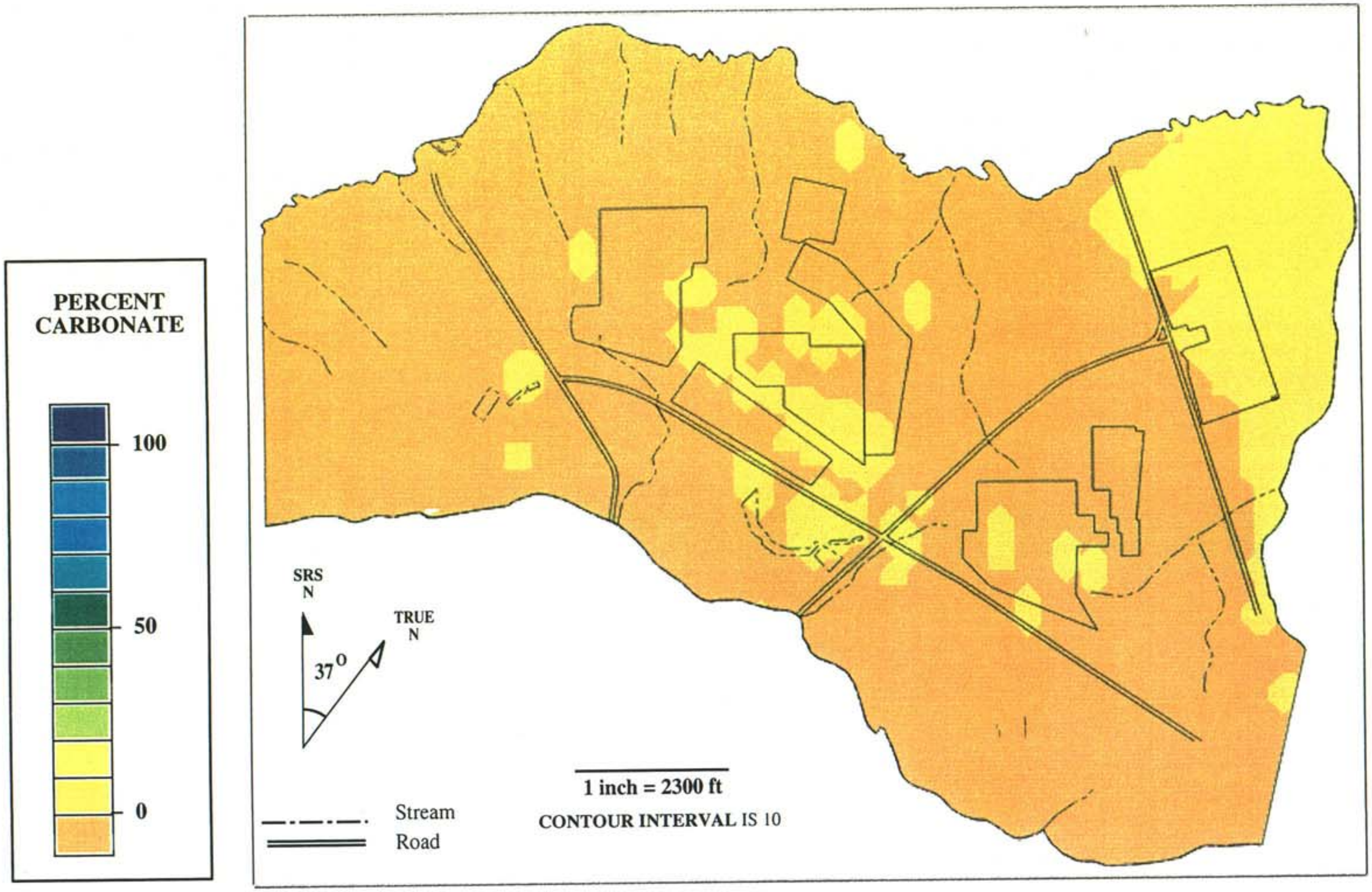

Figure 23. Map of Average Percent Carbonate in the Gordon Aquifer

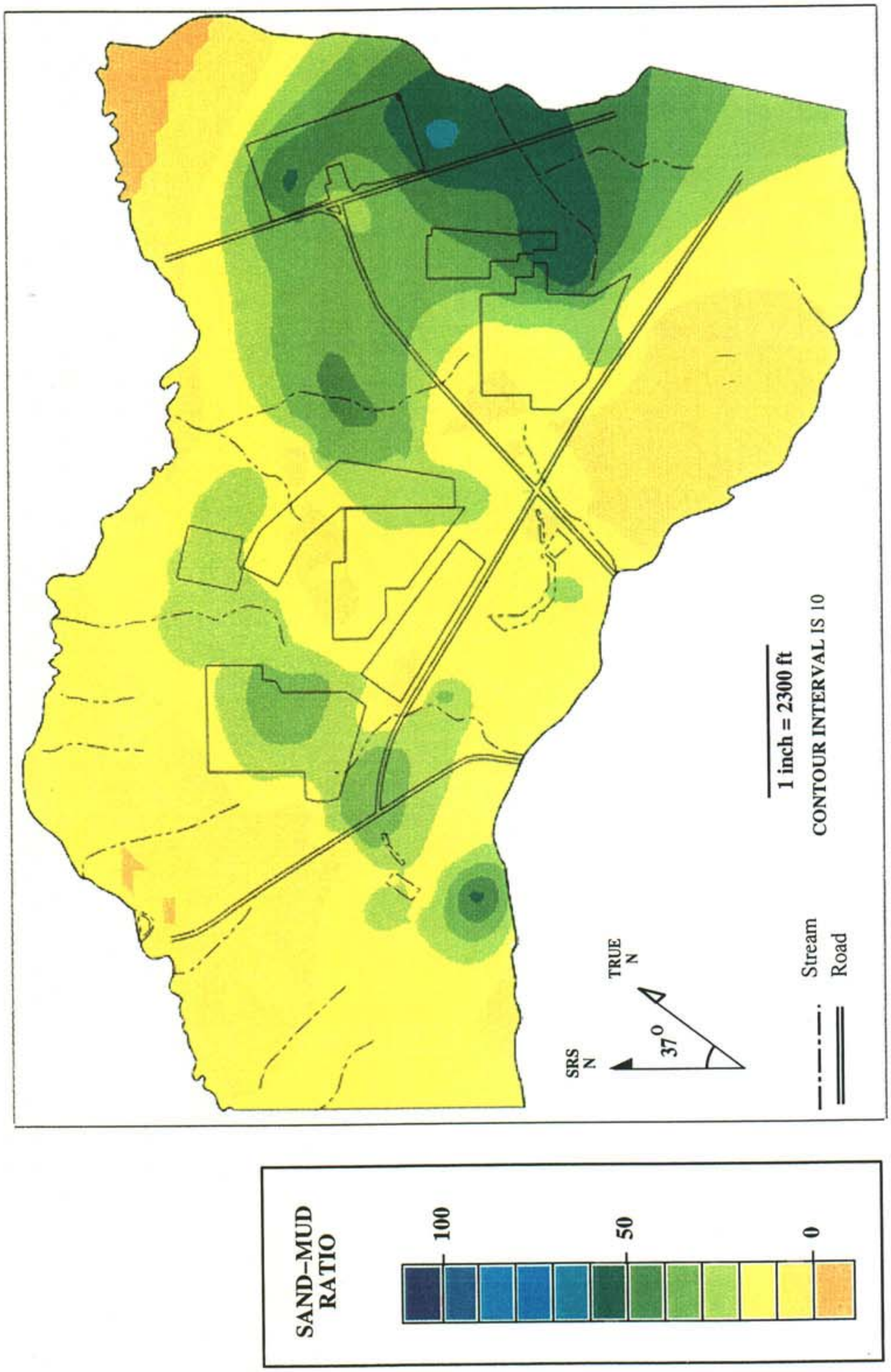

Figure 24. Map of Average Sand–Mud Ratios in the Gordon Aquifer

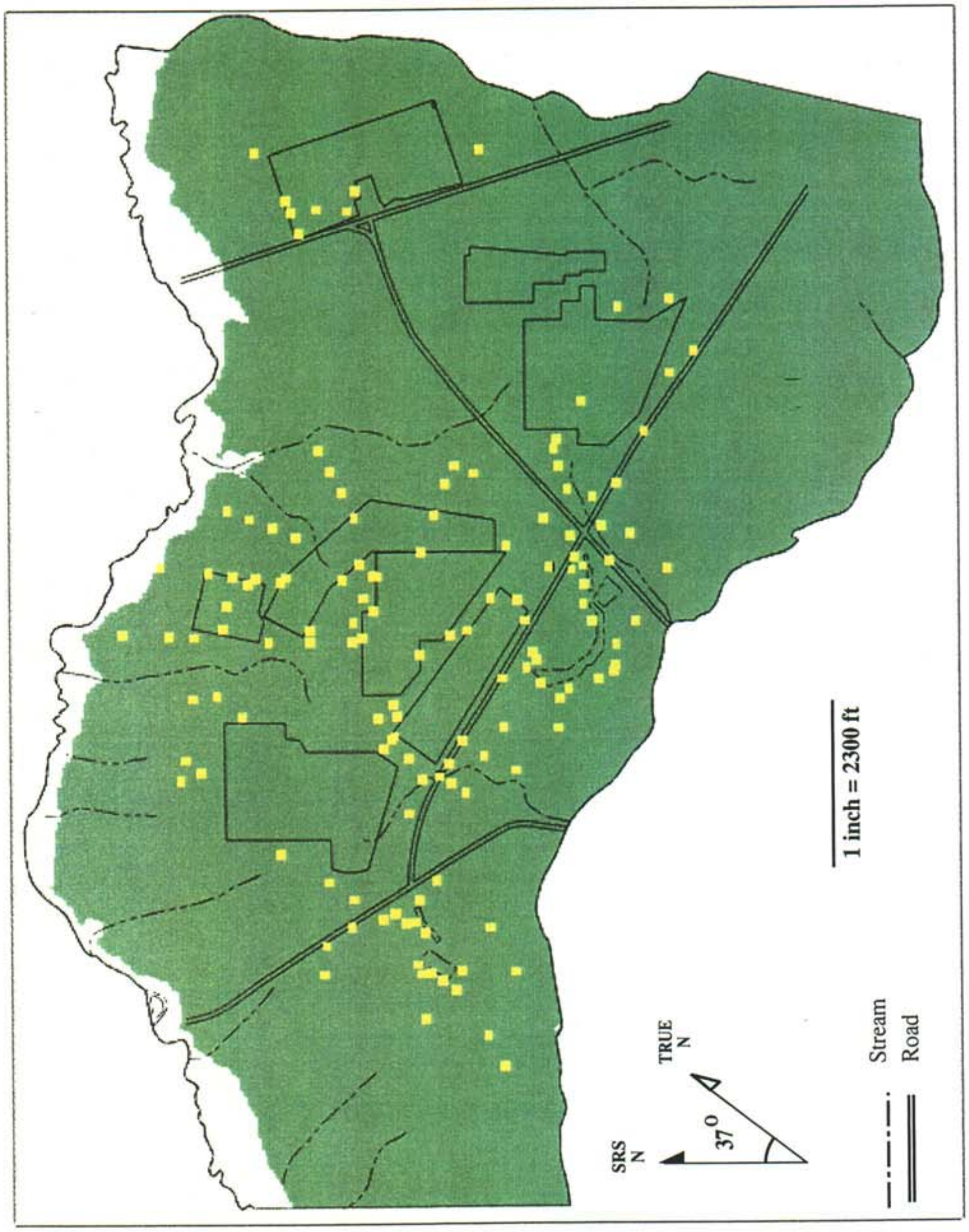

Figure 25. Data Points Used to Grid the Gordon Confining Unit

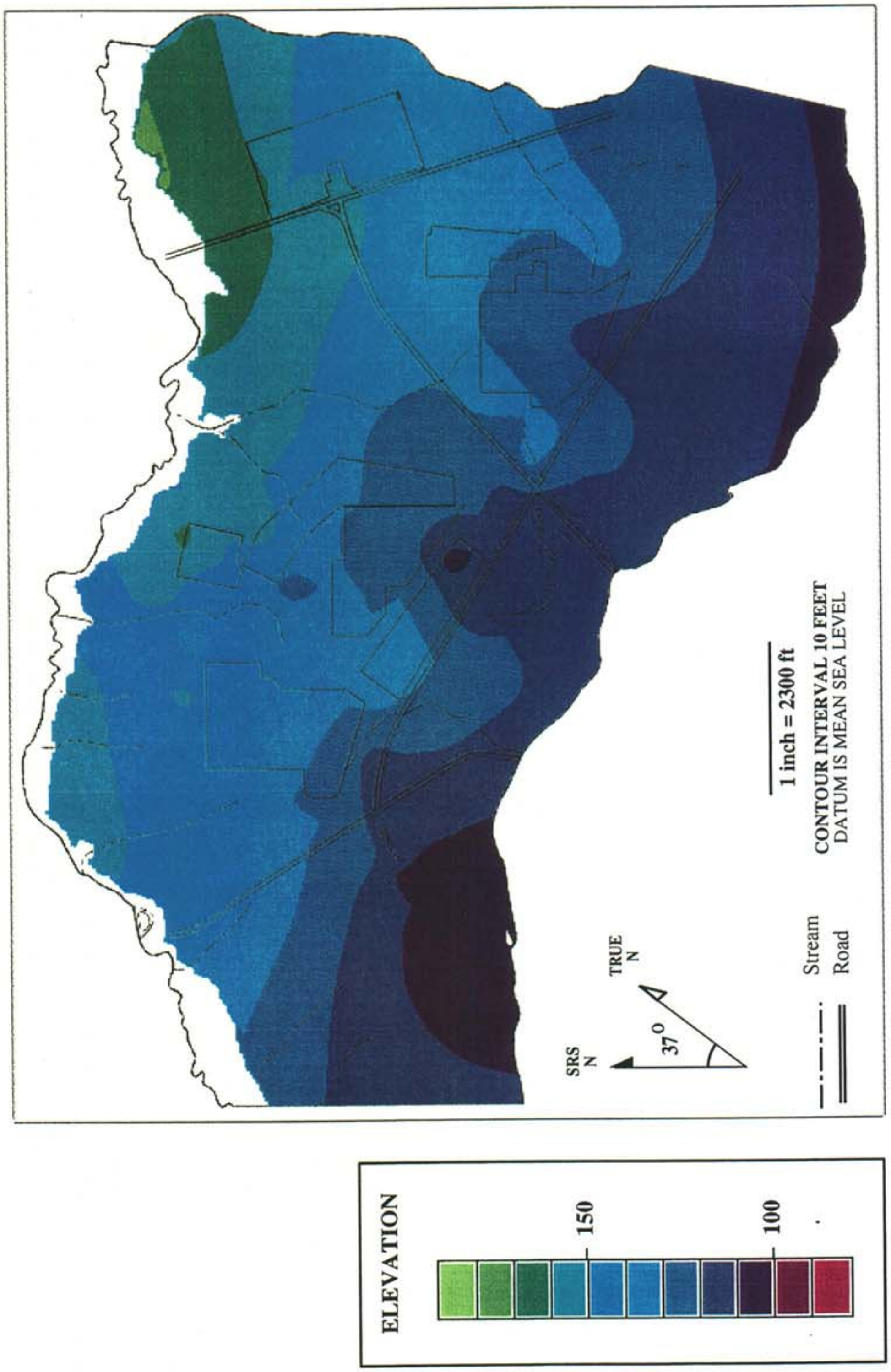

Figure 26. Altitude–Contour Map of the Top of the Gordon Confining Unit

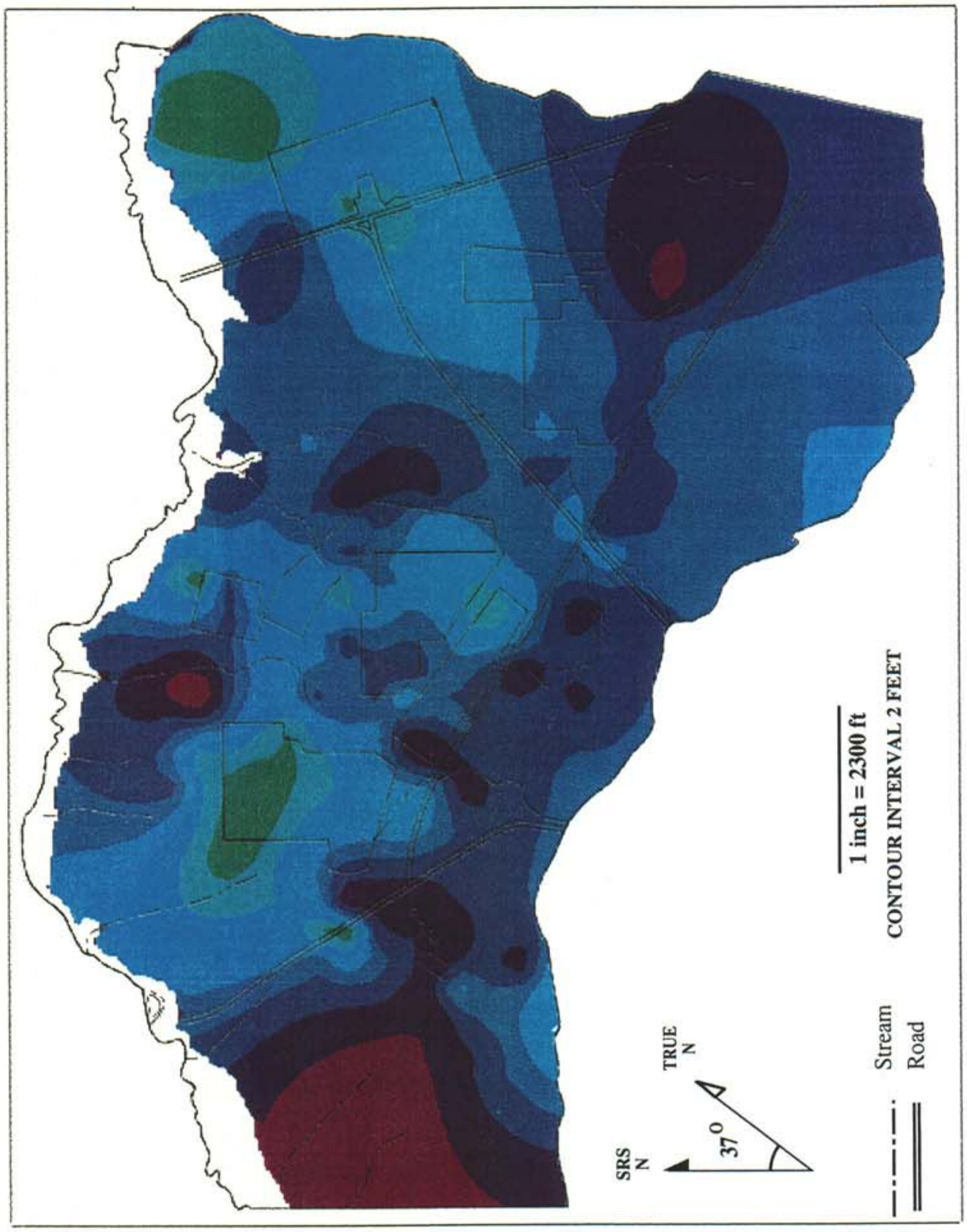

Figure 27. Isopach Map of the Gordon Confining Unit

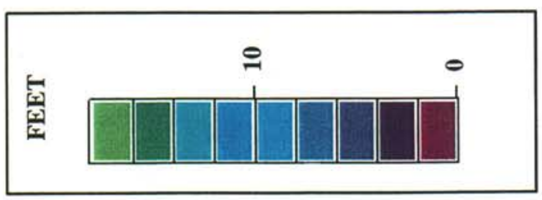

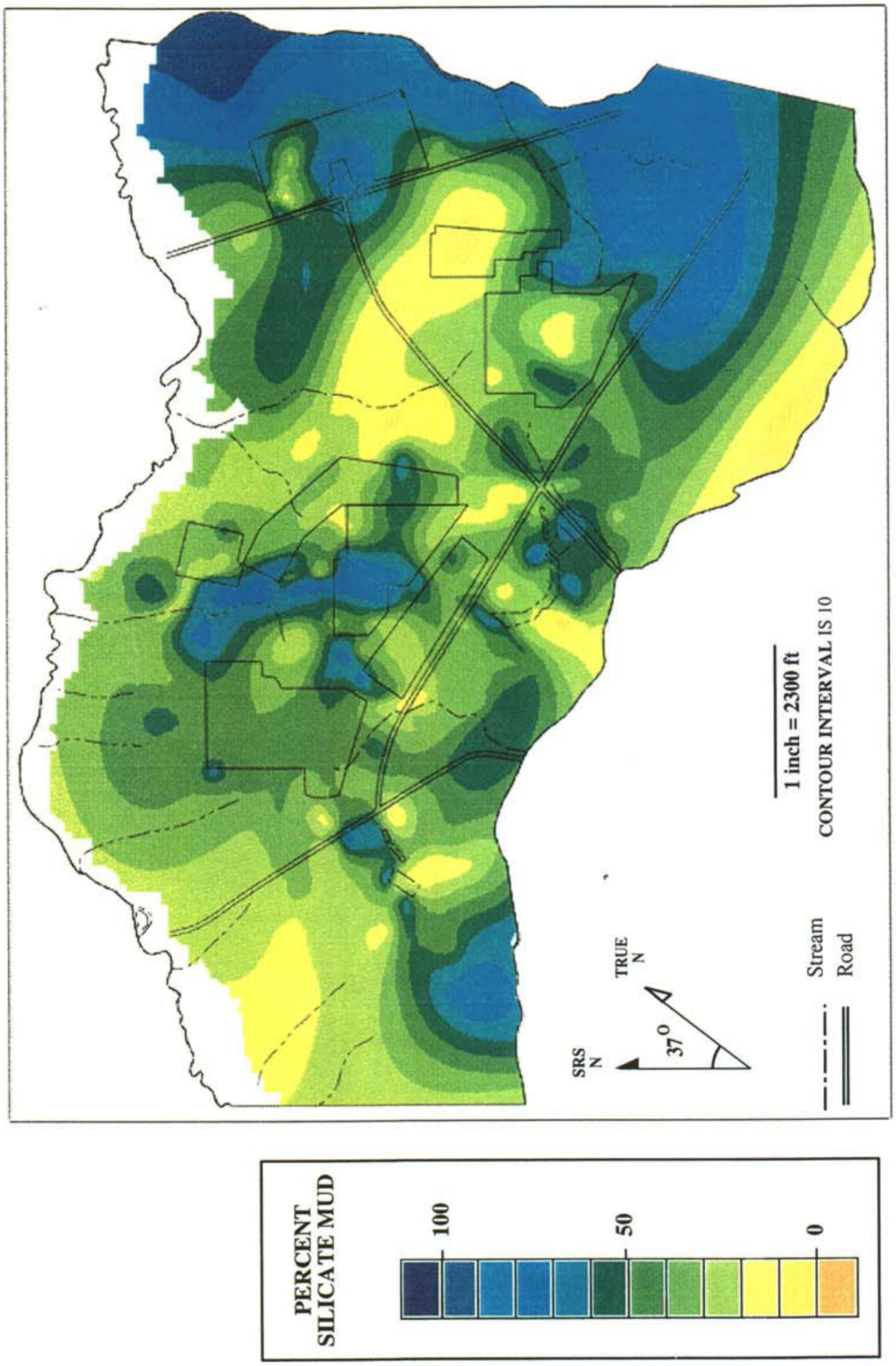

Figure 28. Map of Average Percent Silicate Mud in the Gordon Confining Unit

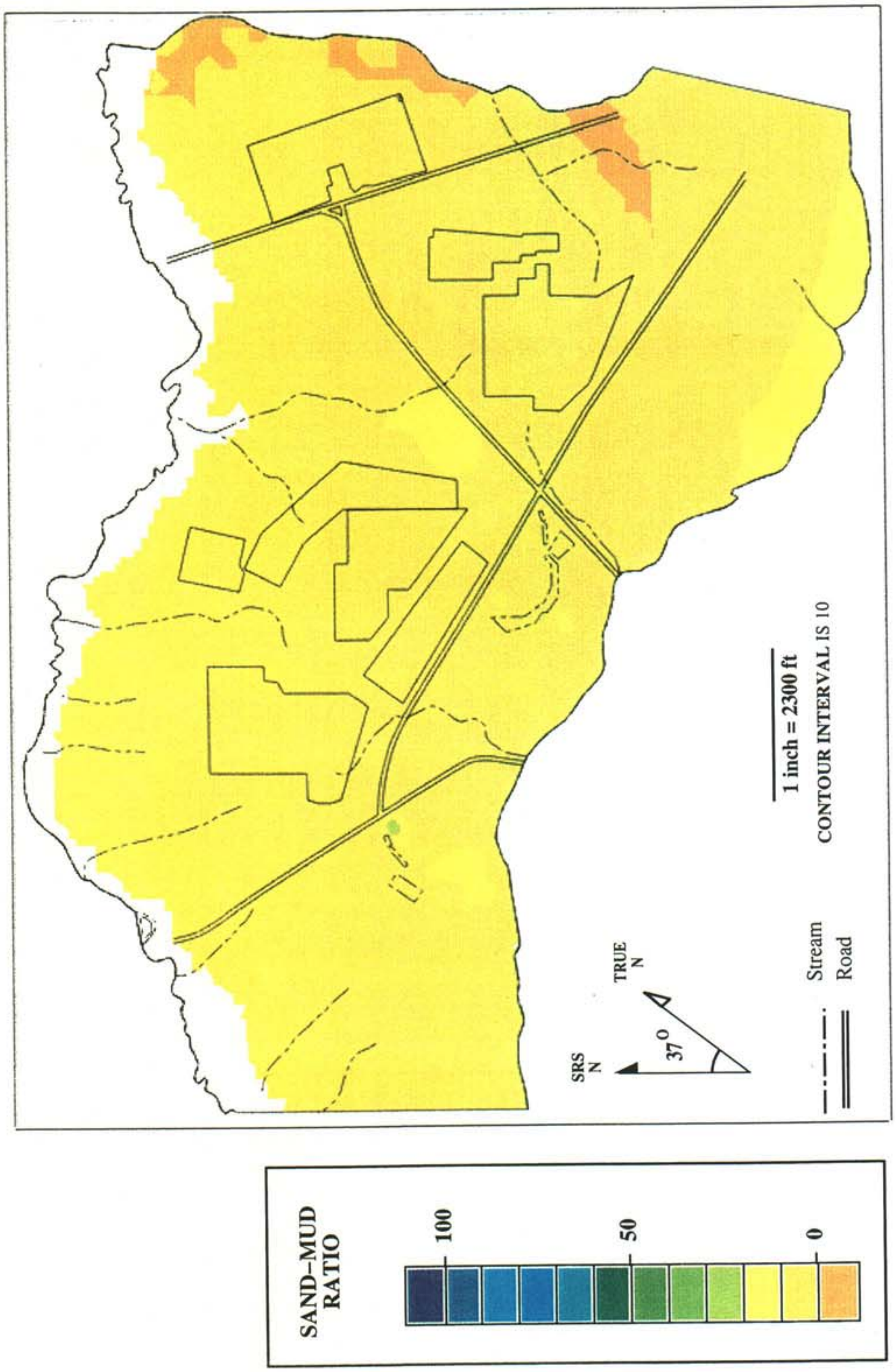

Figure 30. Map of Average Sand–Mud Ratios in the Gordon Confining Unit

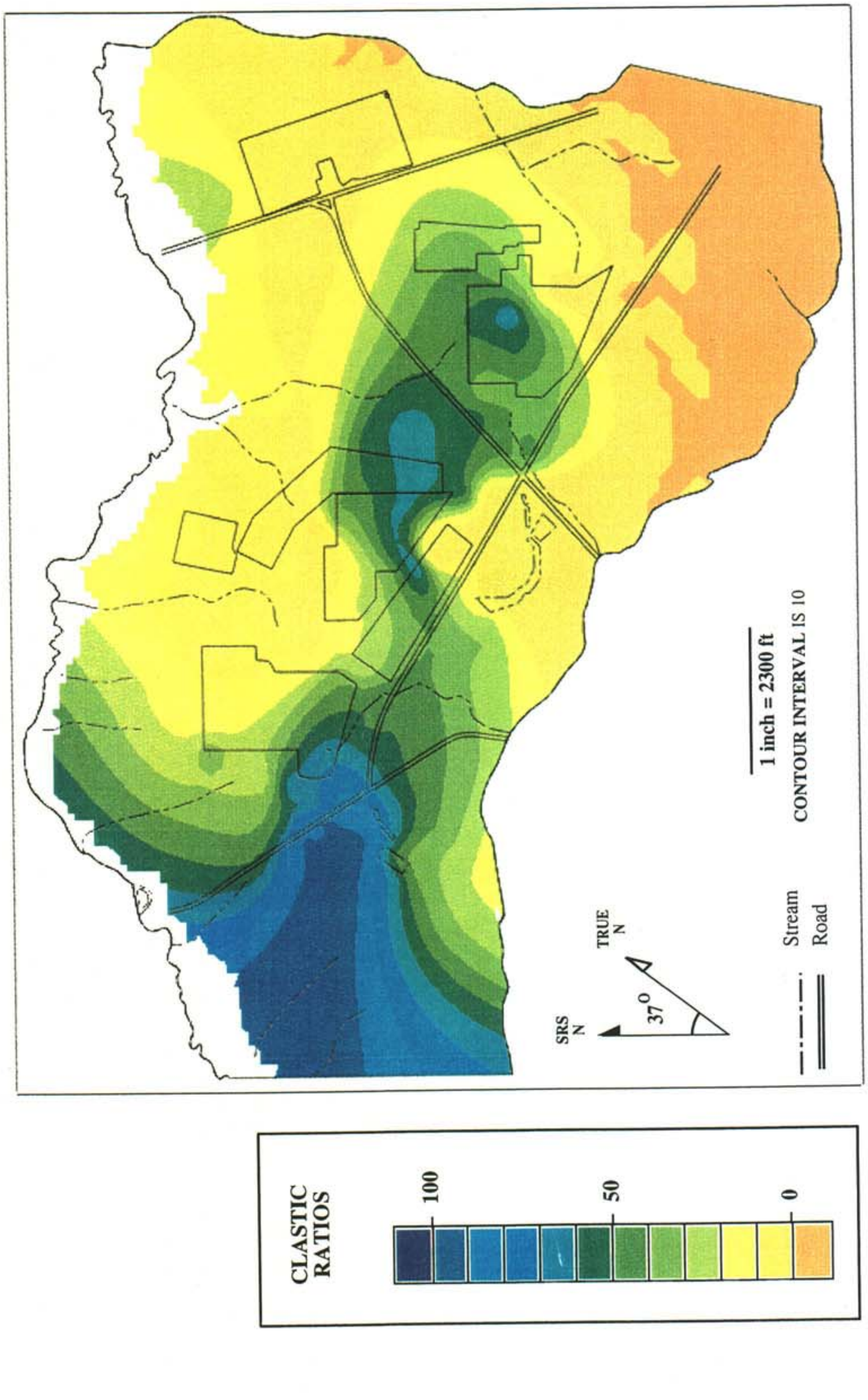

Figure 31. Map of Average Clastic–Ratios in the Gordon Confining Unit

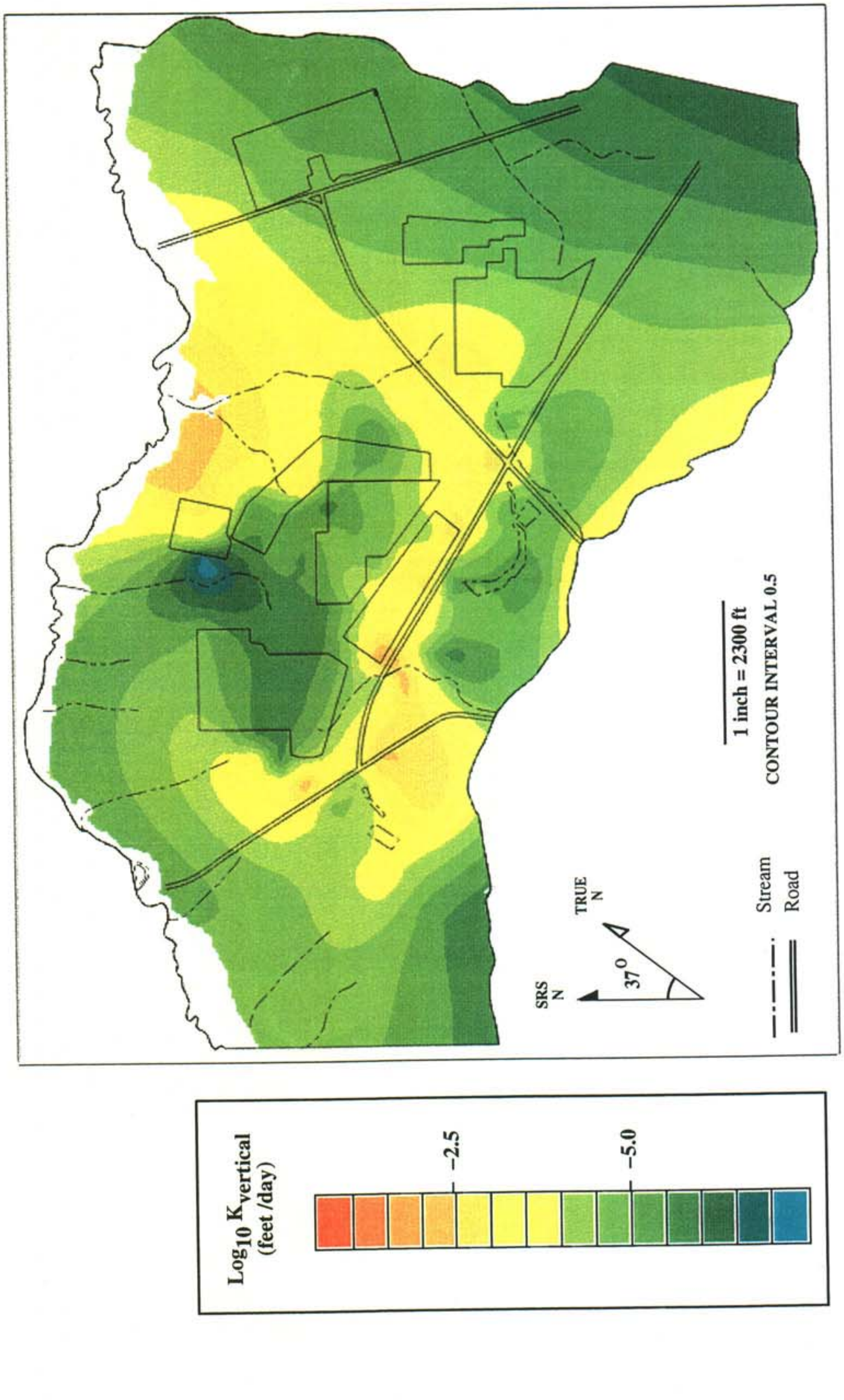

Figure 32. Map of Vertical Conductivity Distribution in the Gordon Confining Unit

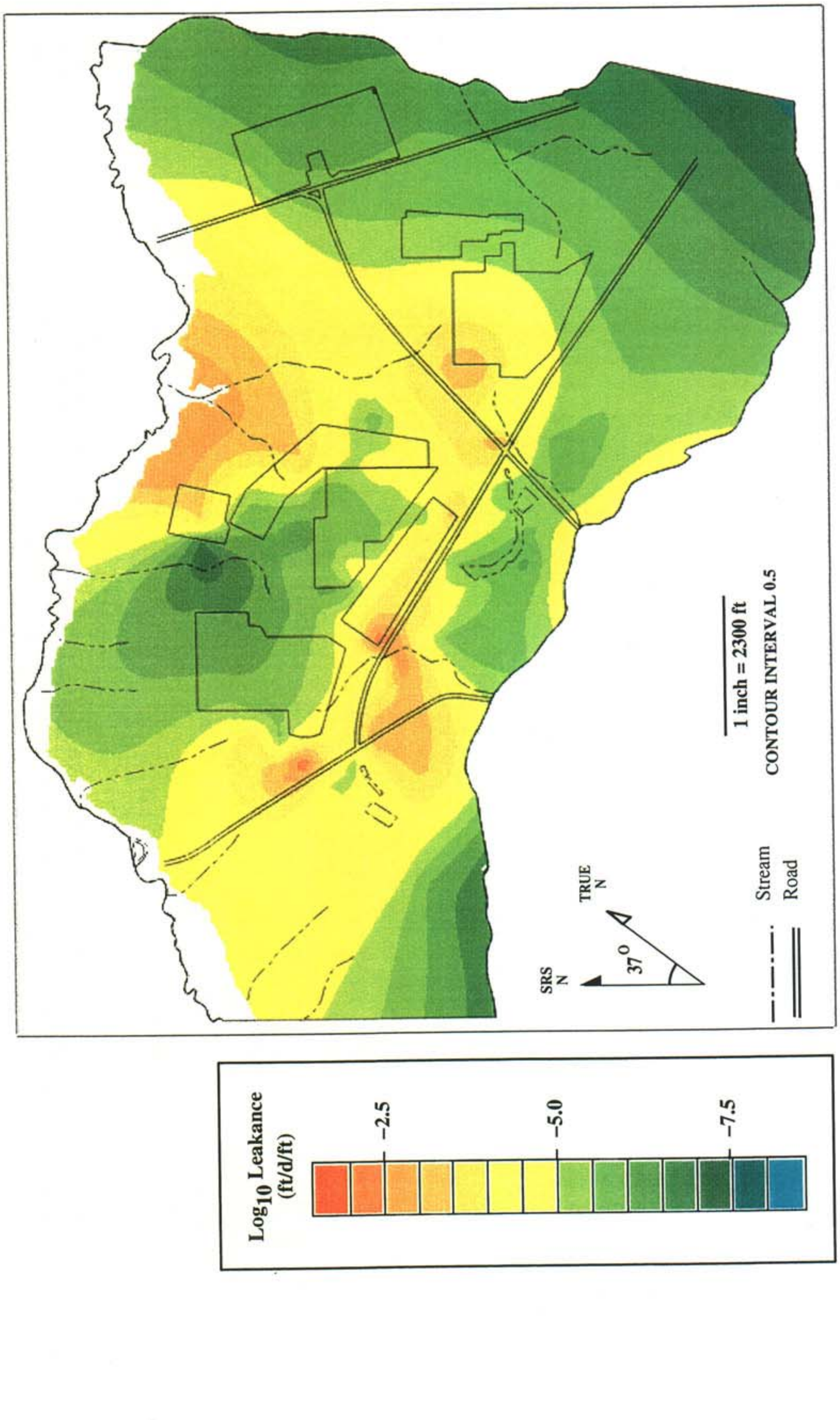

Figure 33. Map of Leakance Distribution in the Gordon Confining Unit

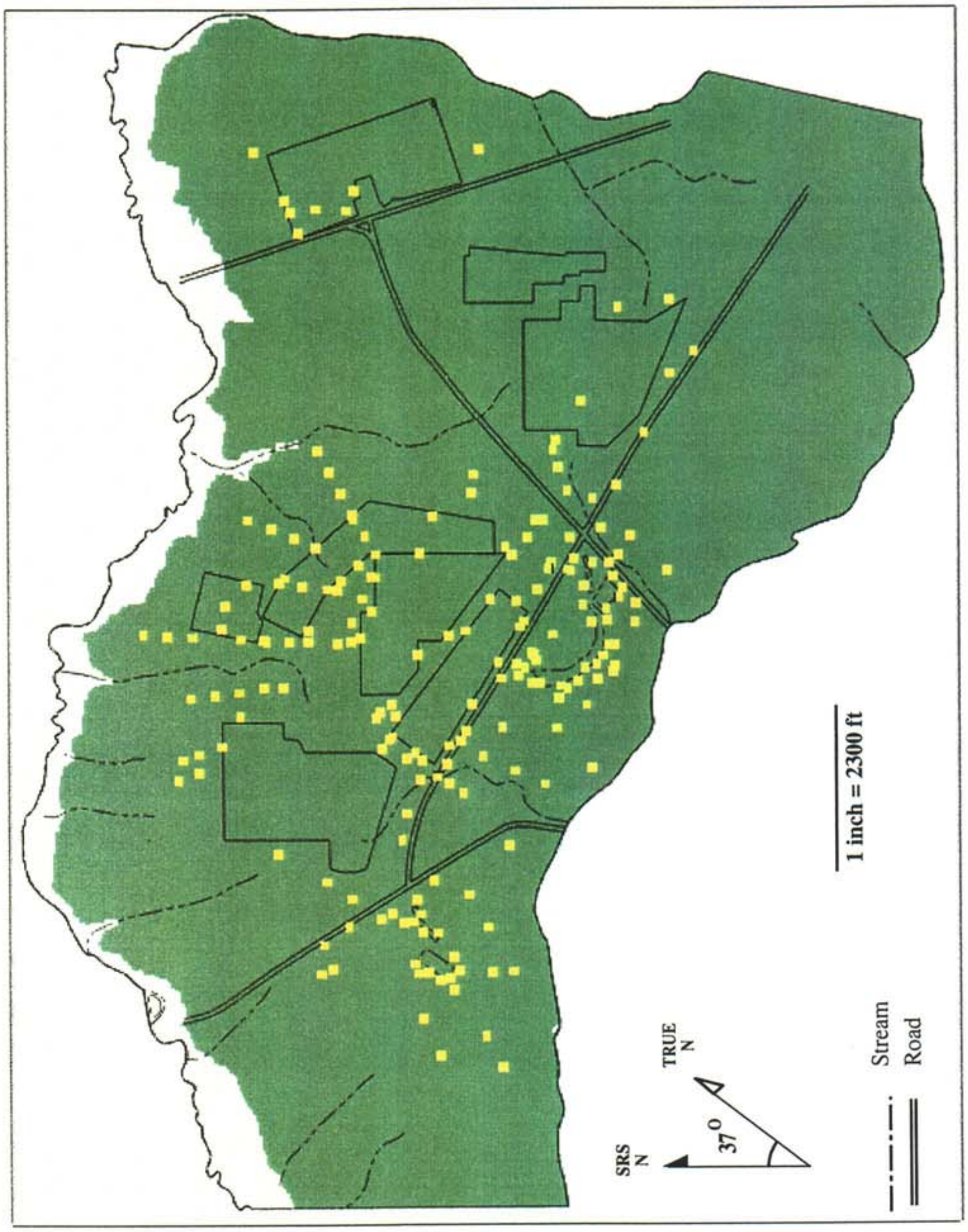

Figure 34. Data Points Used to Grid the "Lower" Aquifer Zone

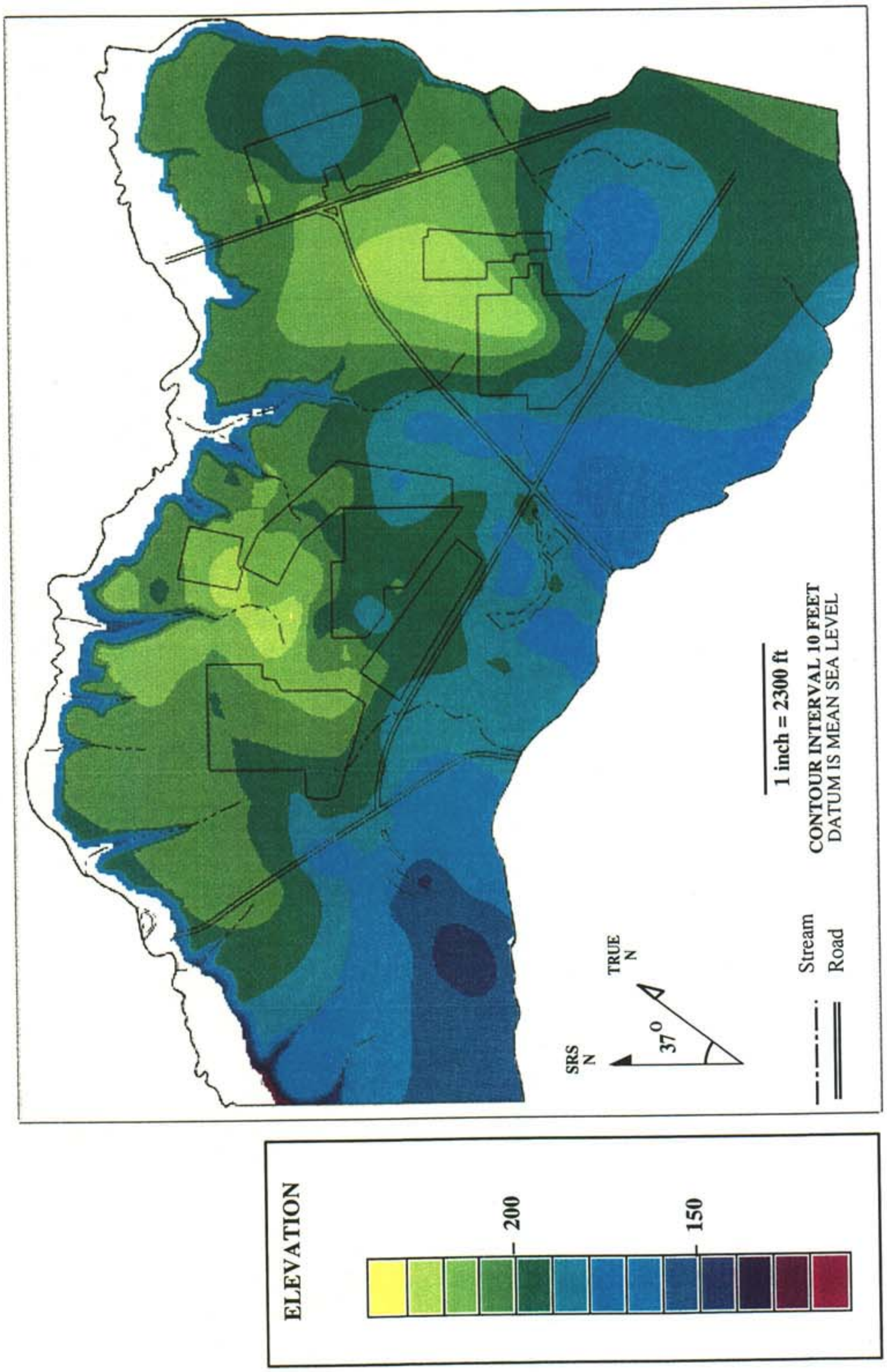

Figure 35. Structure–Contour Map of the Top of the "Lower" Aquifer Zone

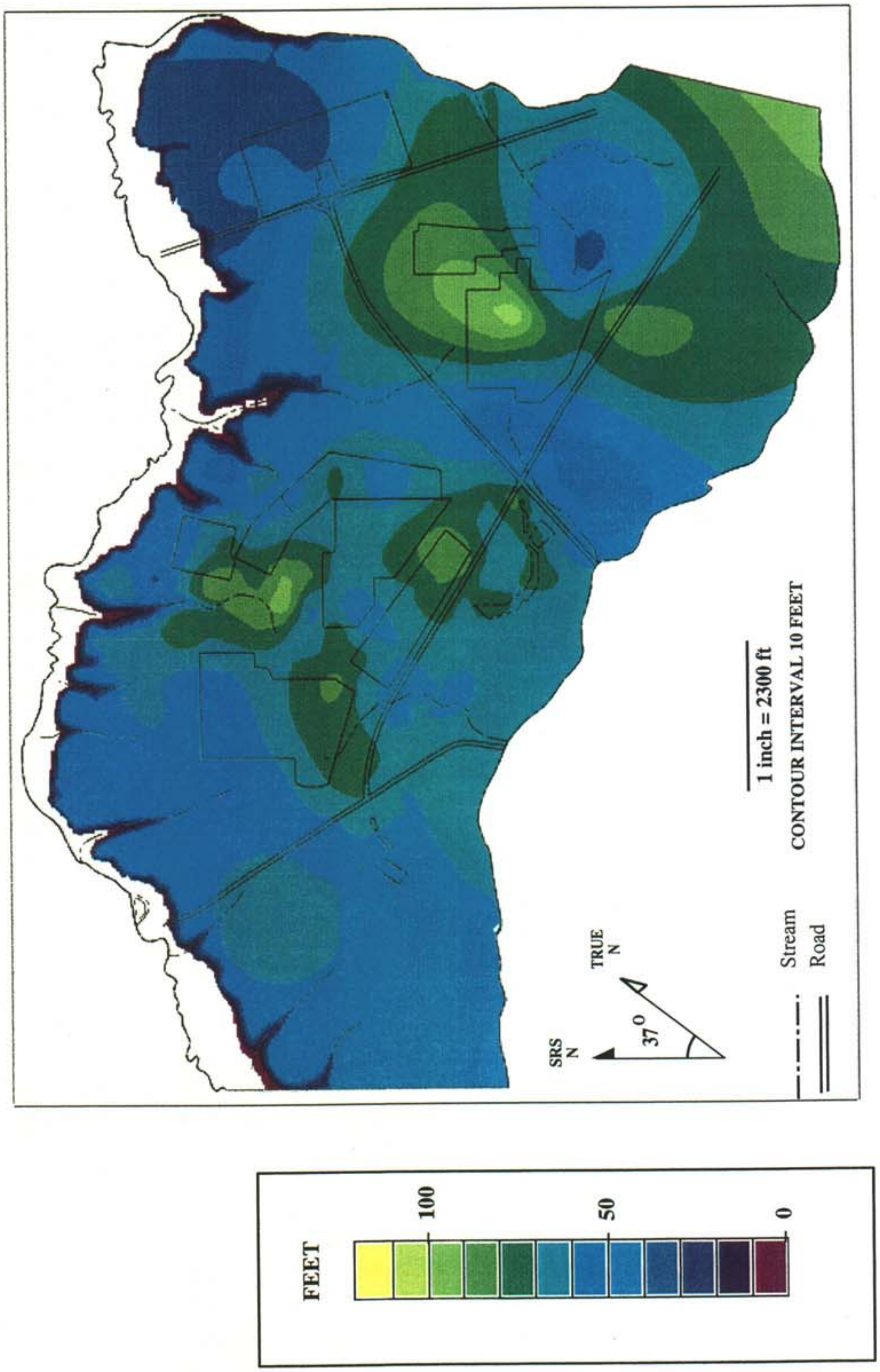

Figure 36. Isopach Map of the "Lower" Aquifer Zone

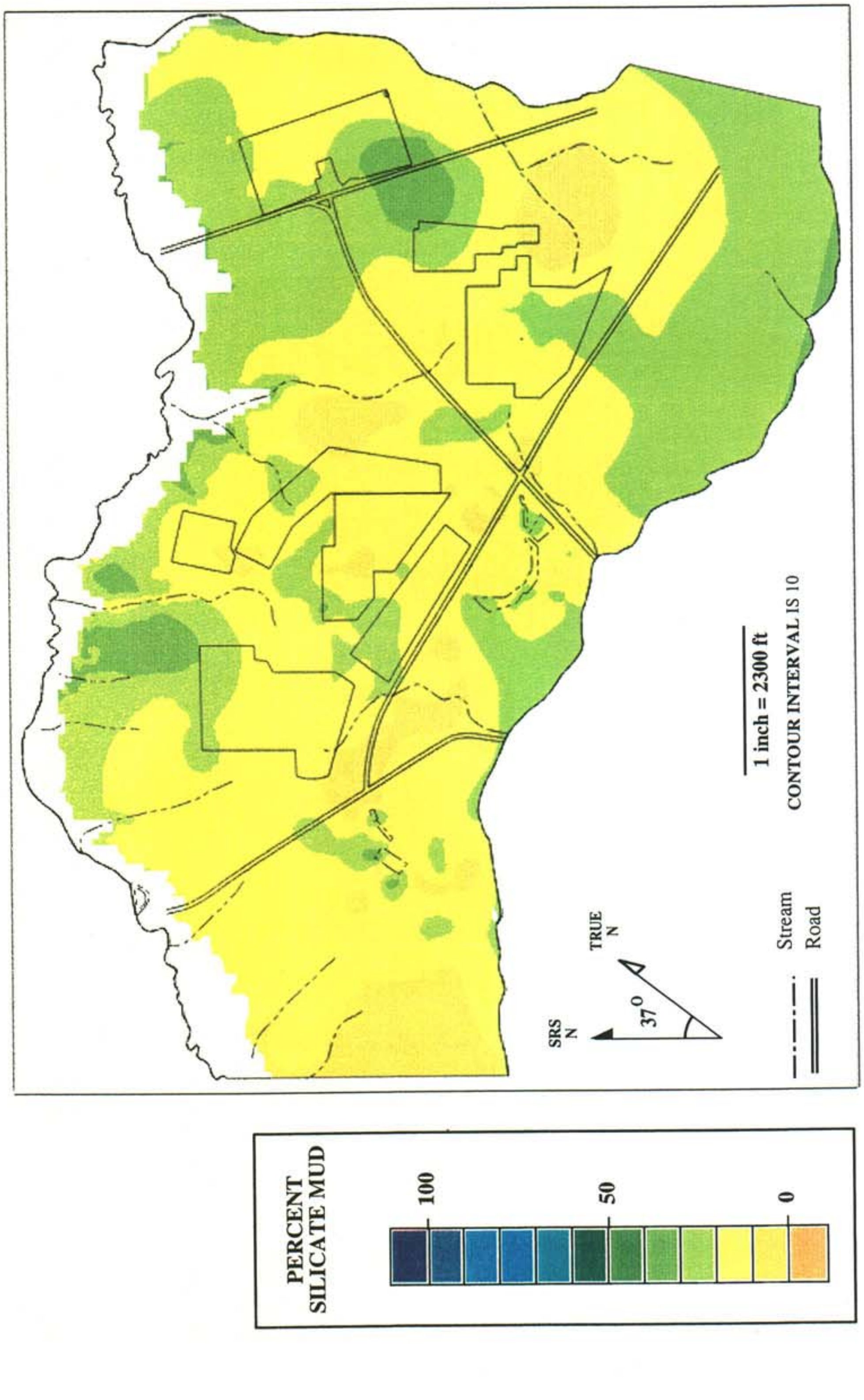

Figure 37. Map of Average Percent Silicate Mud in the "Lower" Aquifer Zone

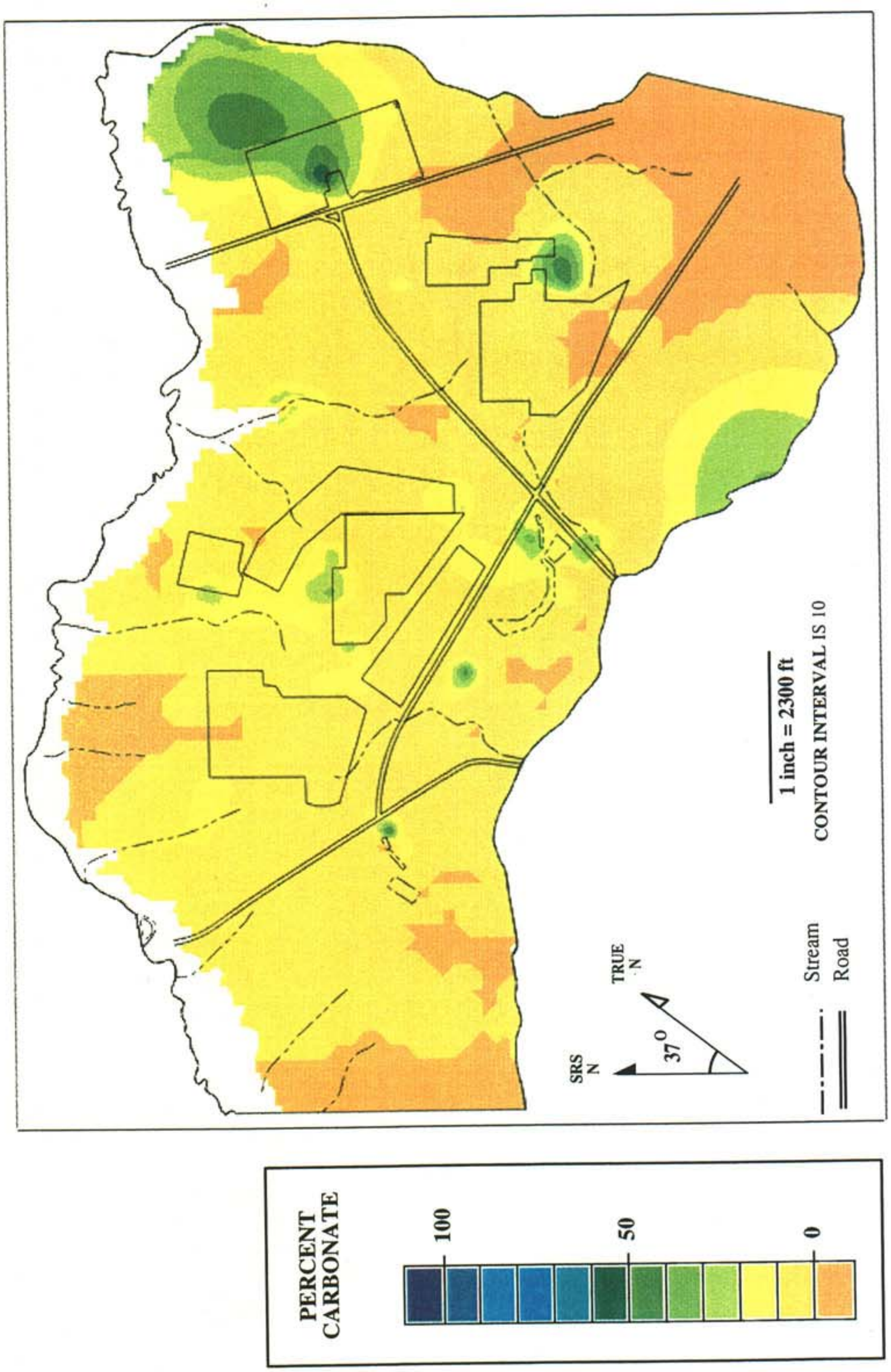

Figure 38. Map of Average Percent Carbonate in the "Lower" Aquifer Zone

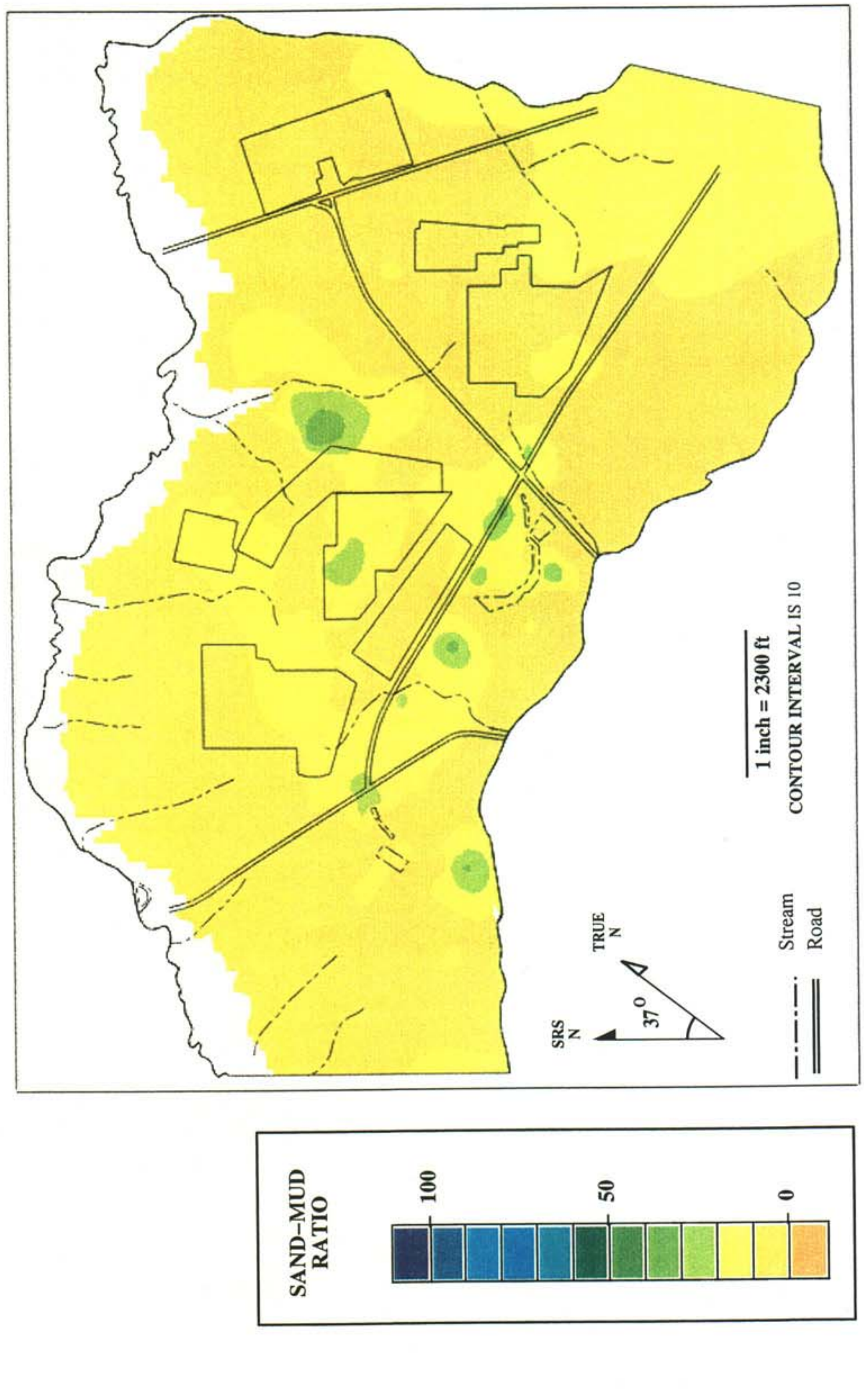

Figure 39. Map of Average Sand–Mud Ratios in the "Lower" Aquifer Zone

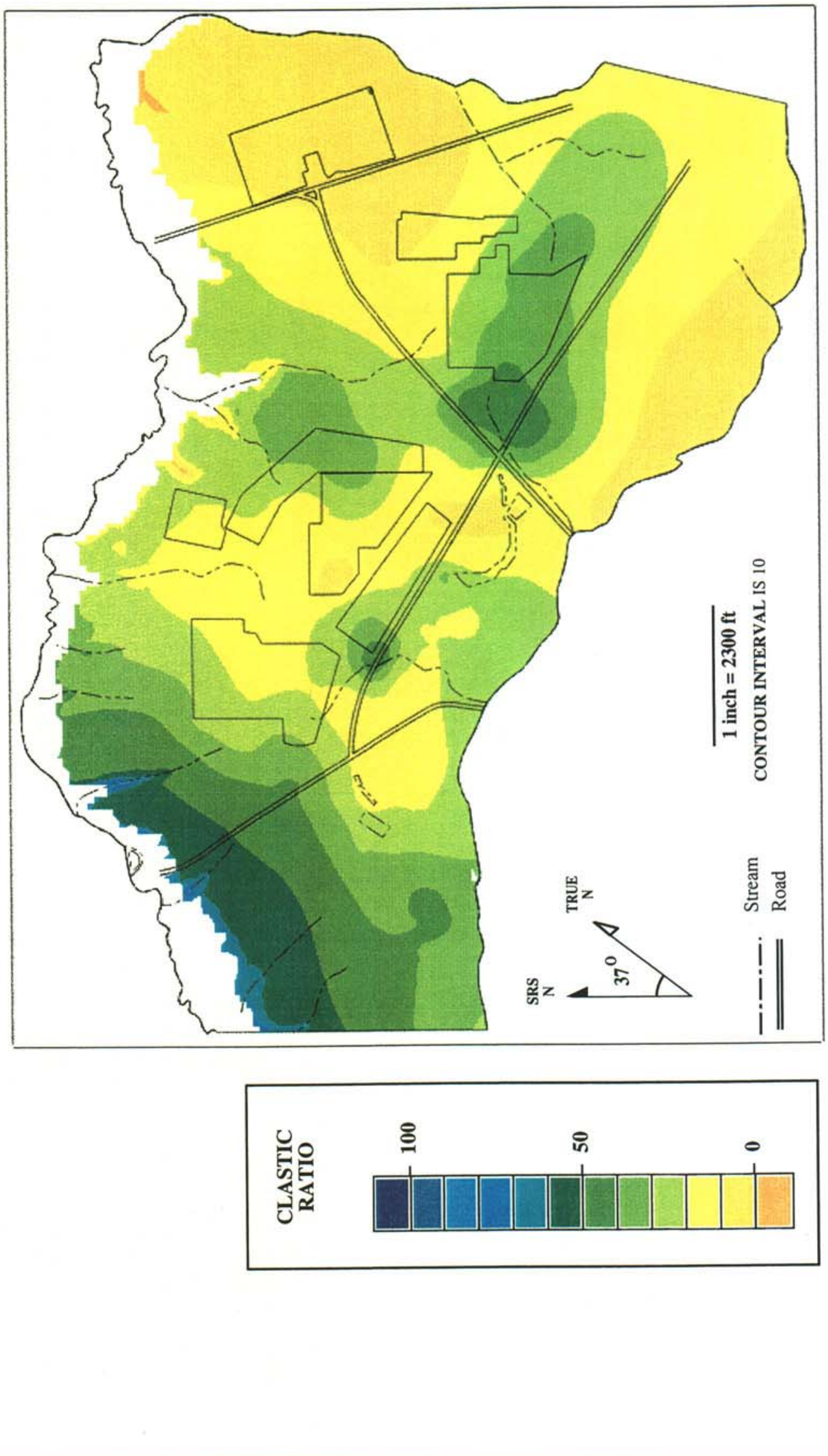

Figure 40. Map of Average Clastic–Ratios in the "Lower" Aquifer Zone, GSA

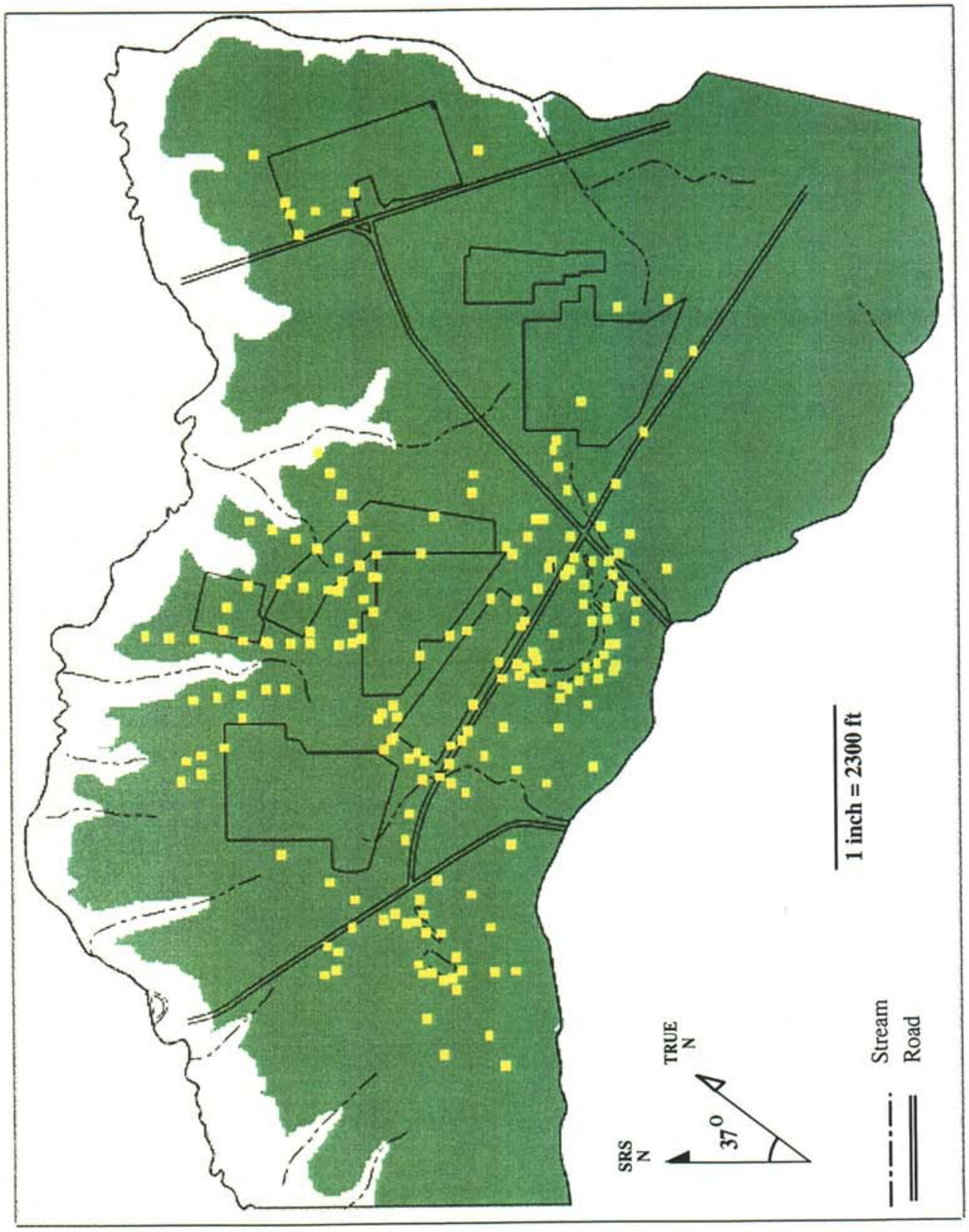

Figure 41. Data Points Used to Grid the "Tan Clay" Confining Zone

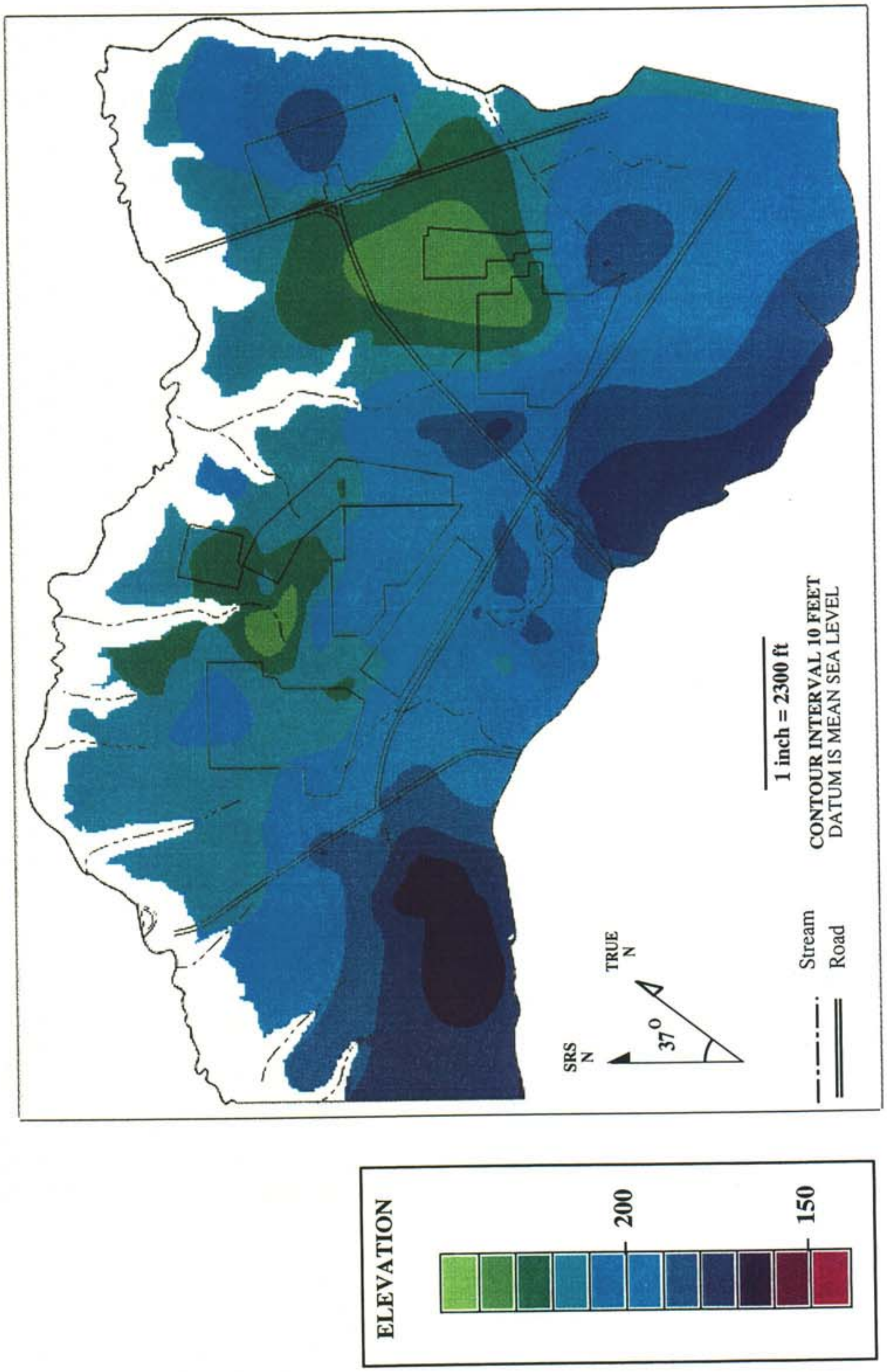

Figure 42. Structure–Contour Map of the Top of the "Tan Clay" Confining Zone

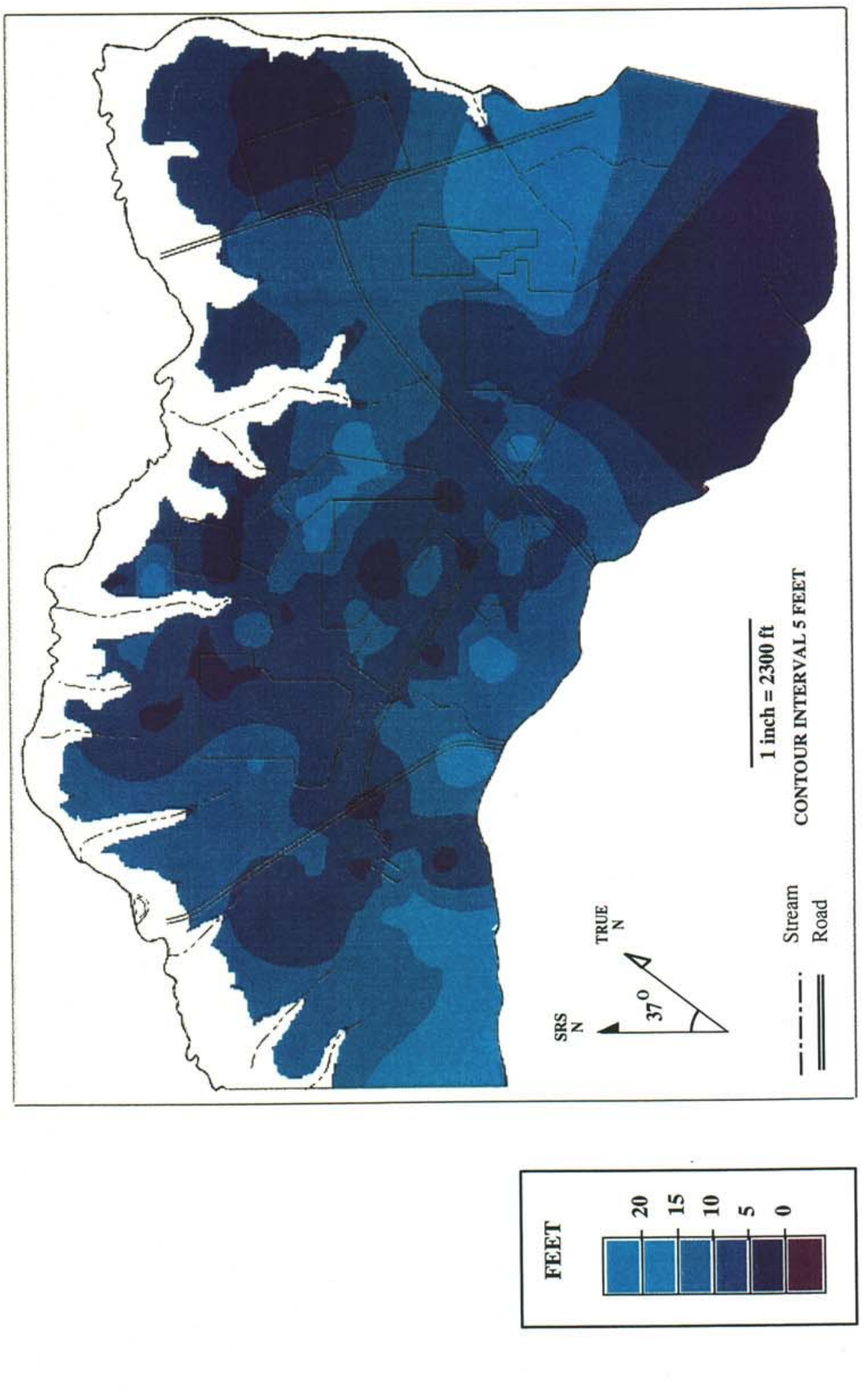

Figure 43. Isopach Map of the "Tan Clay" Confining Zone

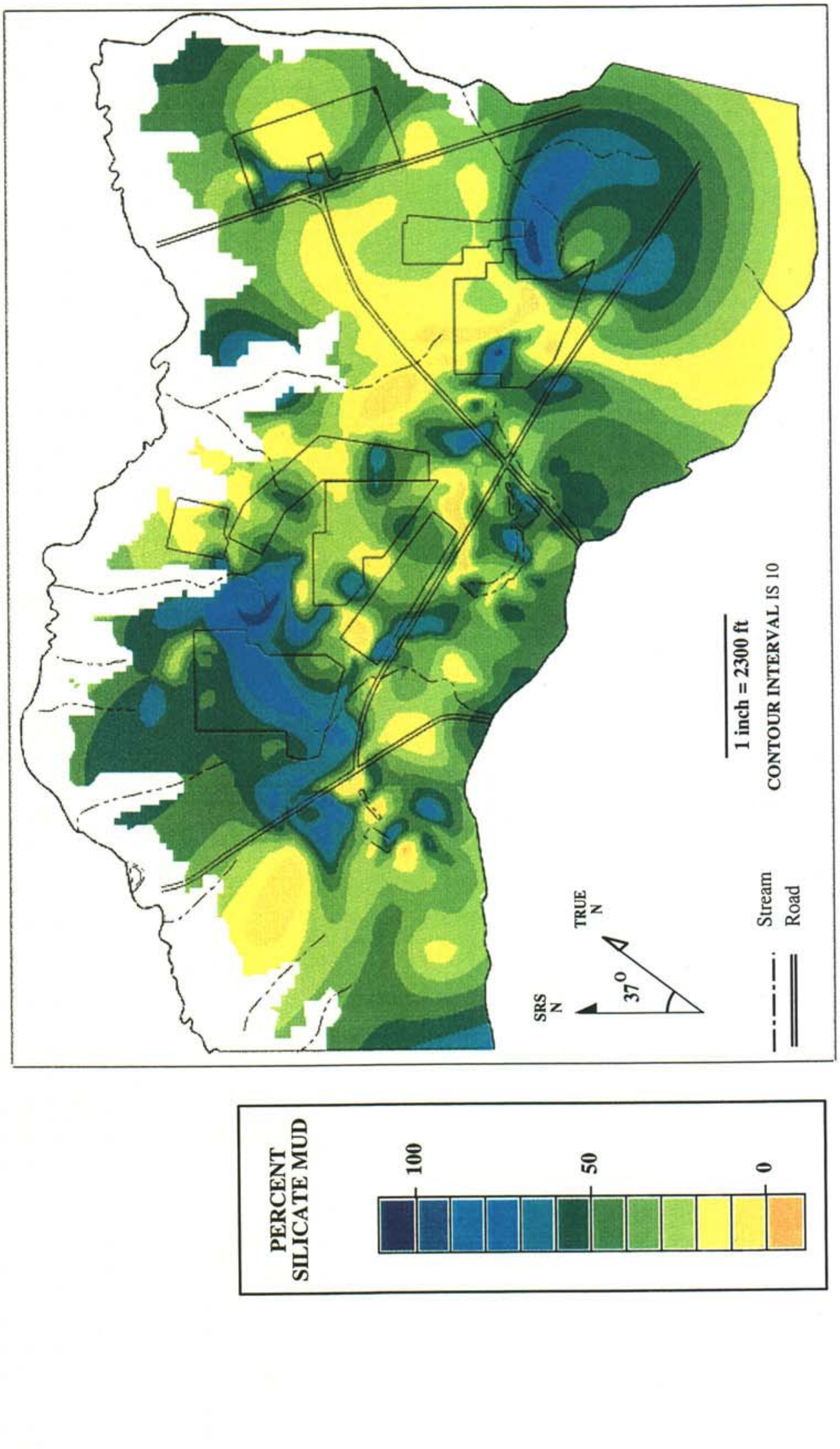

Figure 44. Map of Average Percent Silicate Mud in the "Tan Clay" Confining Zone

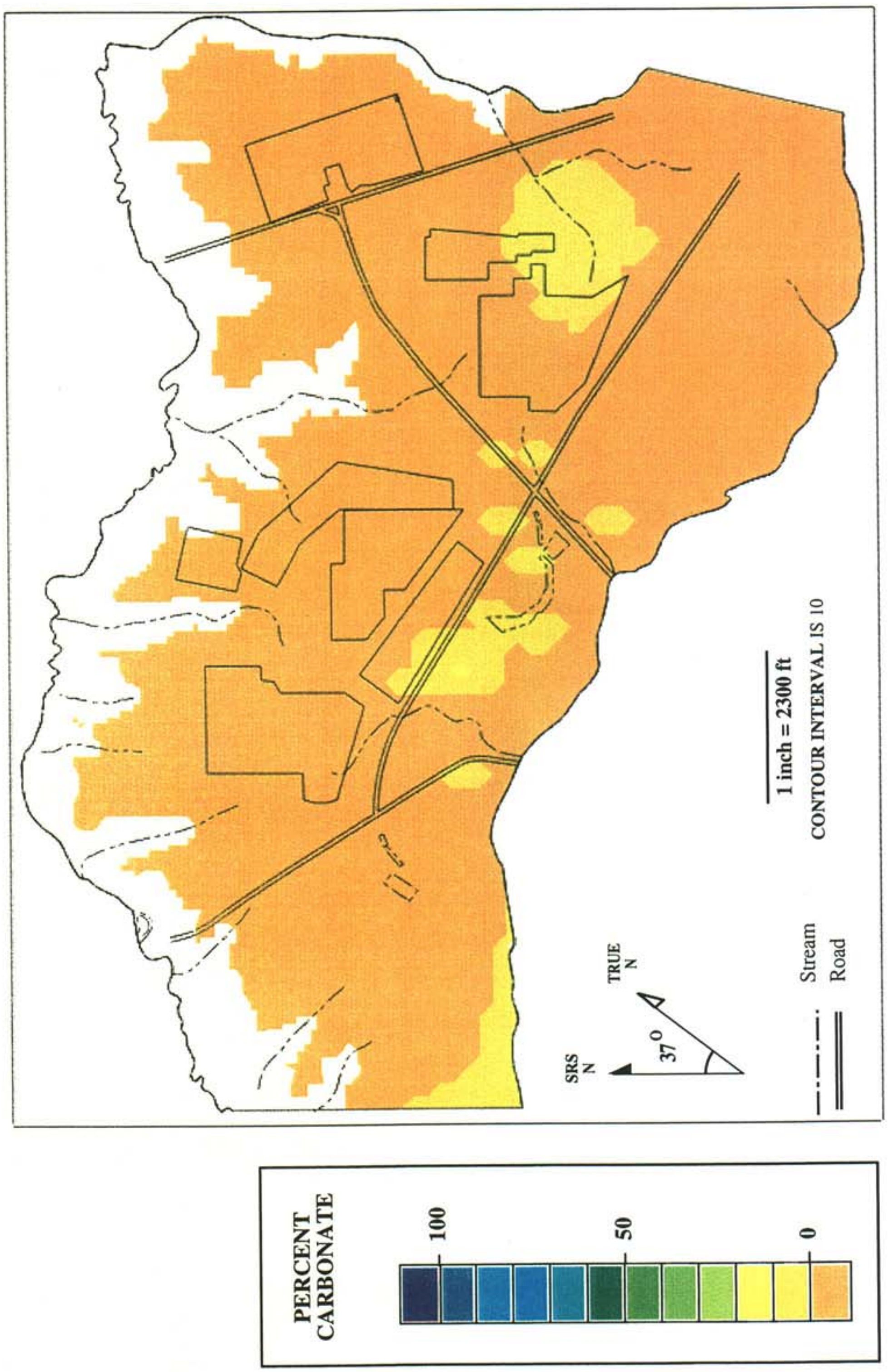

Figure 45. Map of Average Percent Carbonate in the "Tan Clay" Confining Zone

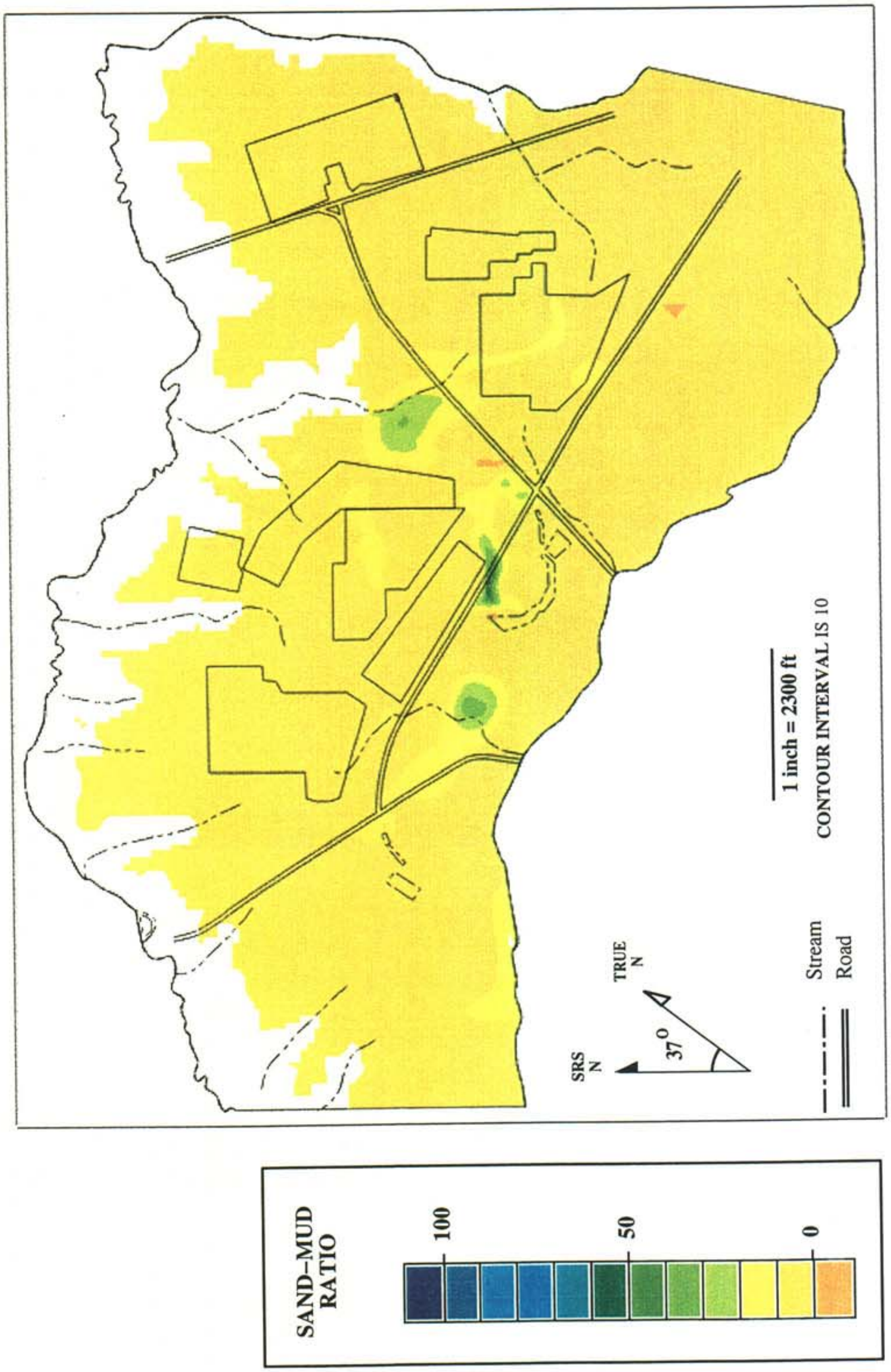

Figure 46. Map of Average Sand–Mud Ratios in the "Tan Clay" Confining Zone

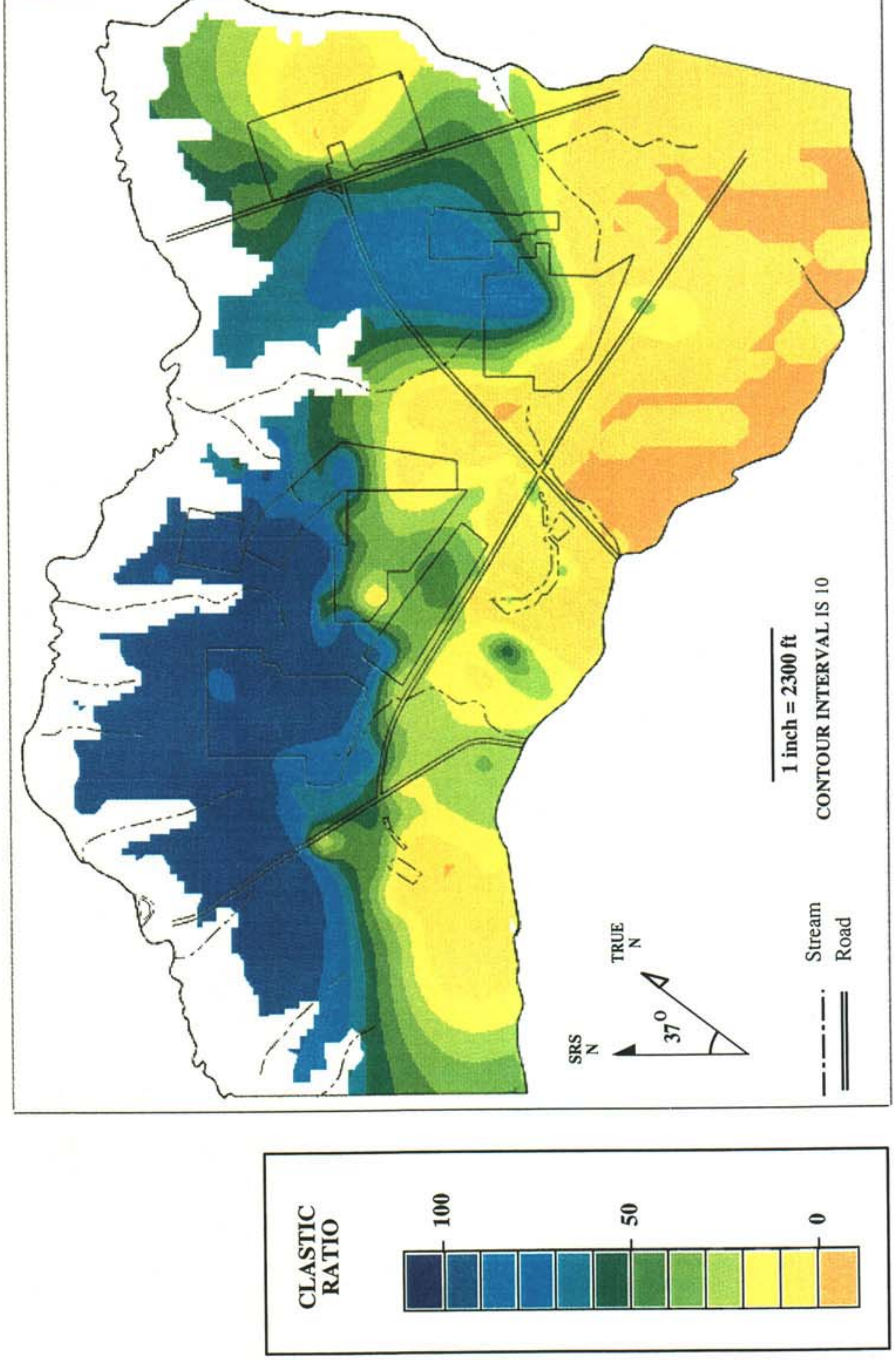

Figure 47. Map of Average Clastic Ratios in the "Tan Clay" Confining Zone

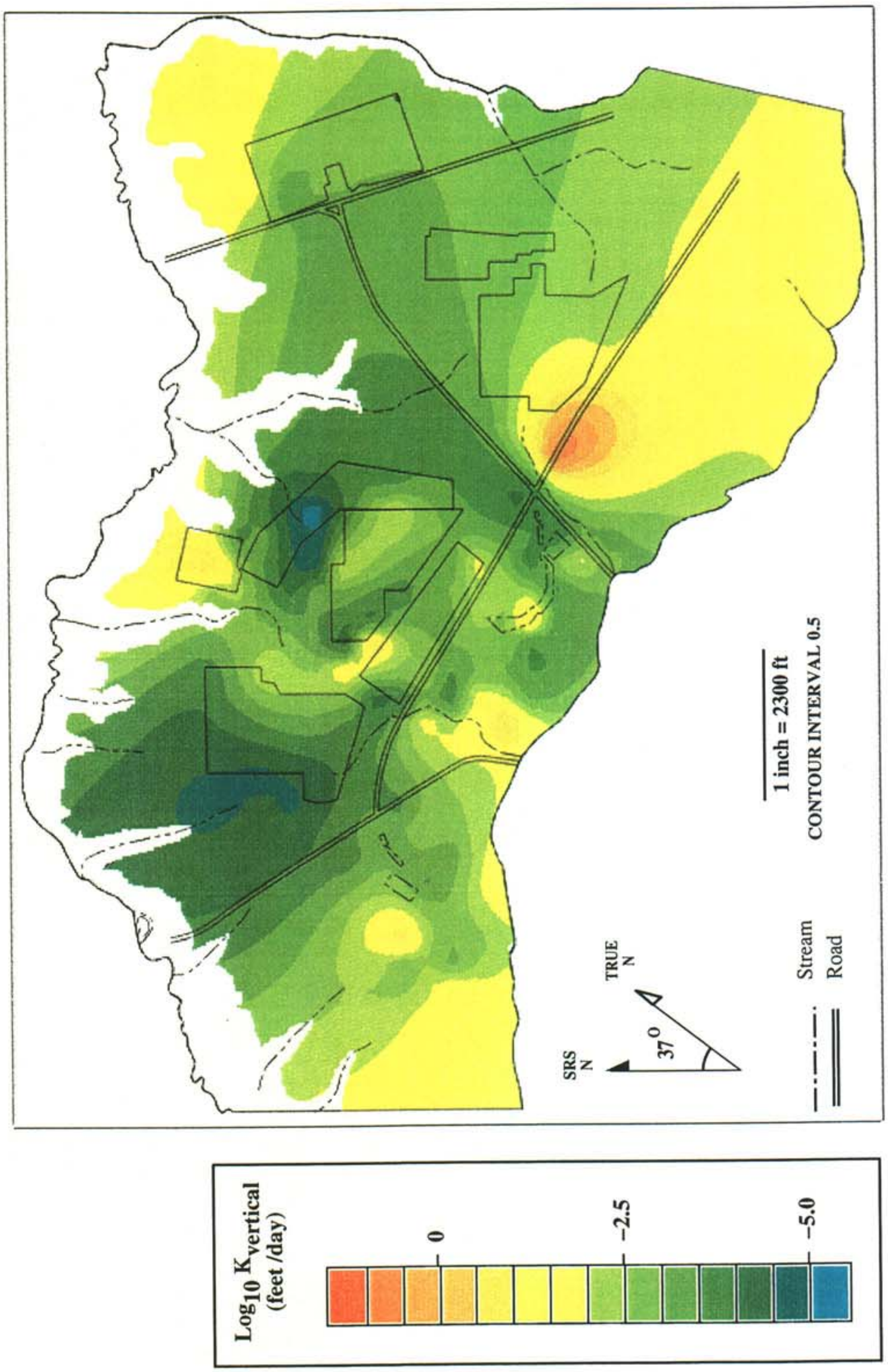

Figure 48. Map of Vertical Conductivity Distribution in the "Tan Clay" Confining Zone

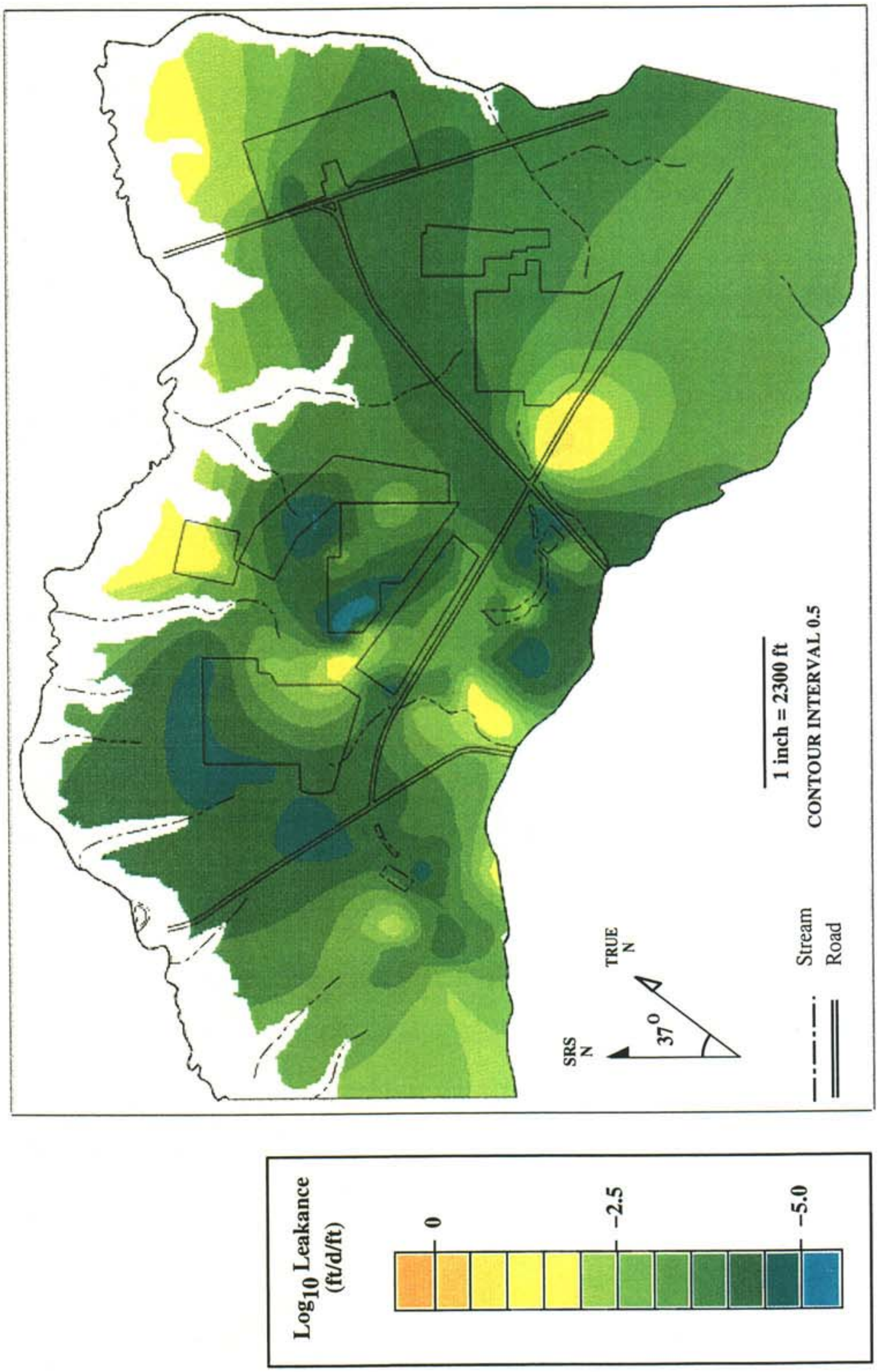

Figure 49. Map of Leakance Distribution in the "Tan Clay" Confining Zone

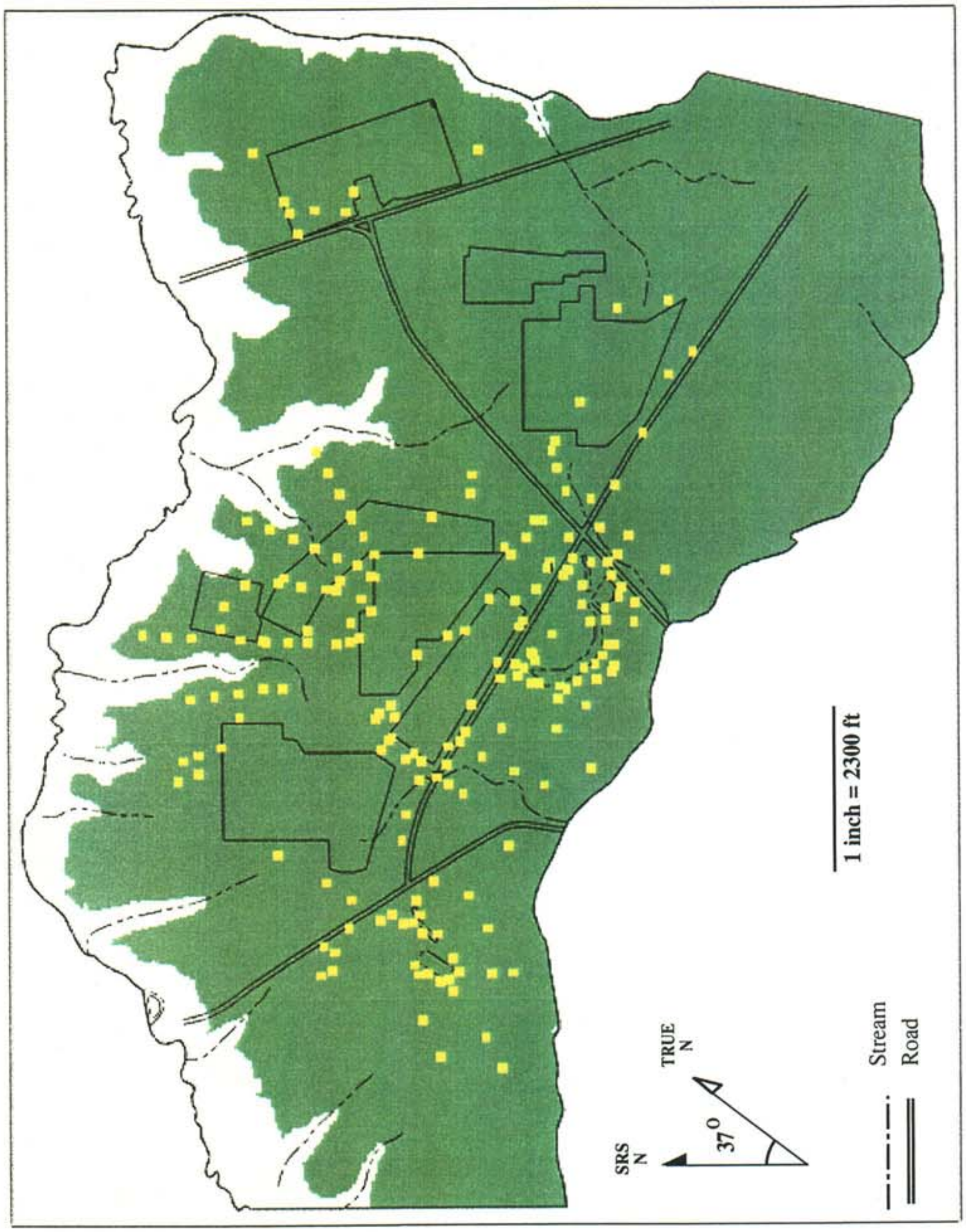

Figure 50. Data Points Used to Grid the "Upper" Aquifer Zone

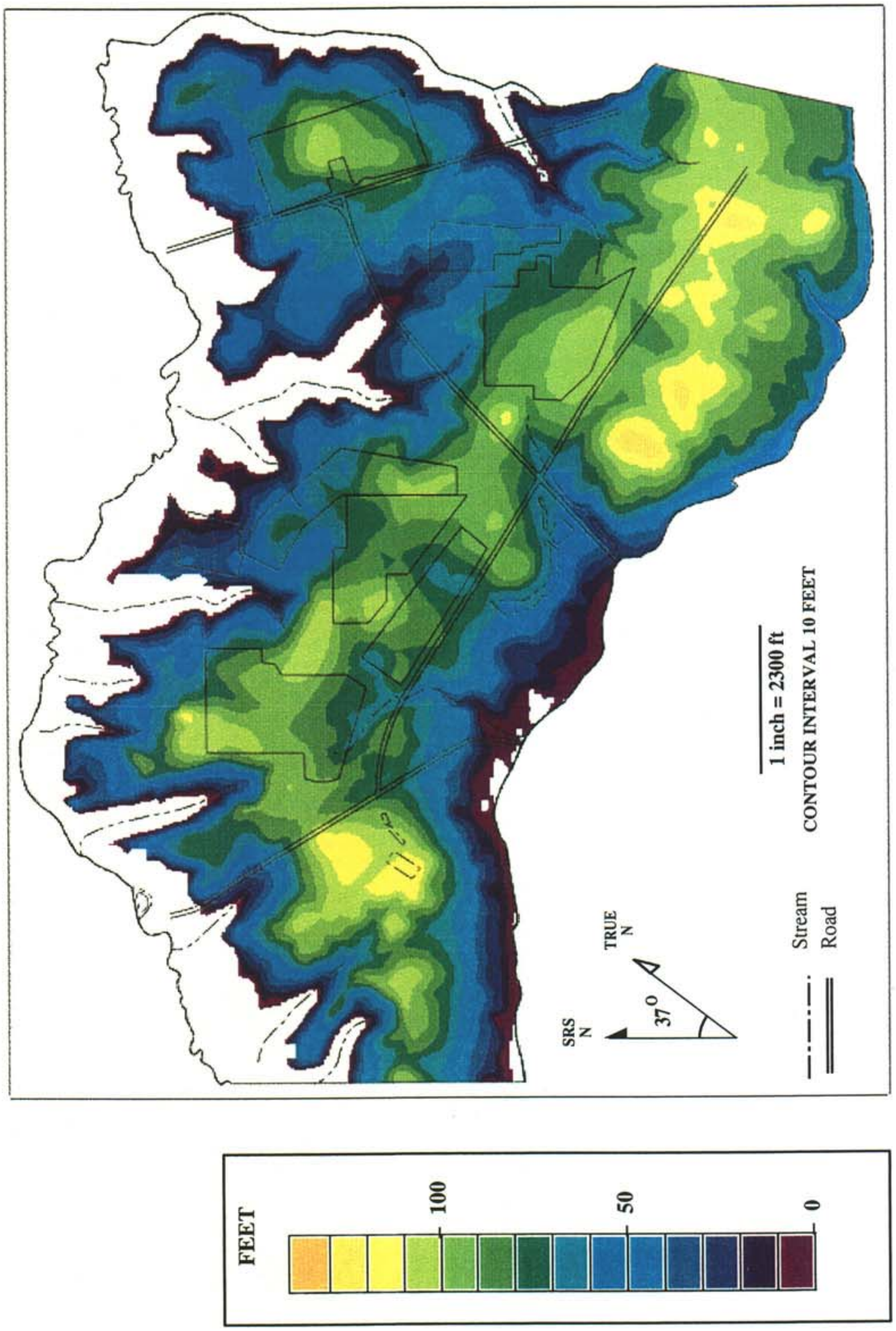

Figure 51. Isopach Map of the "Upper" Aquifer Zone

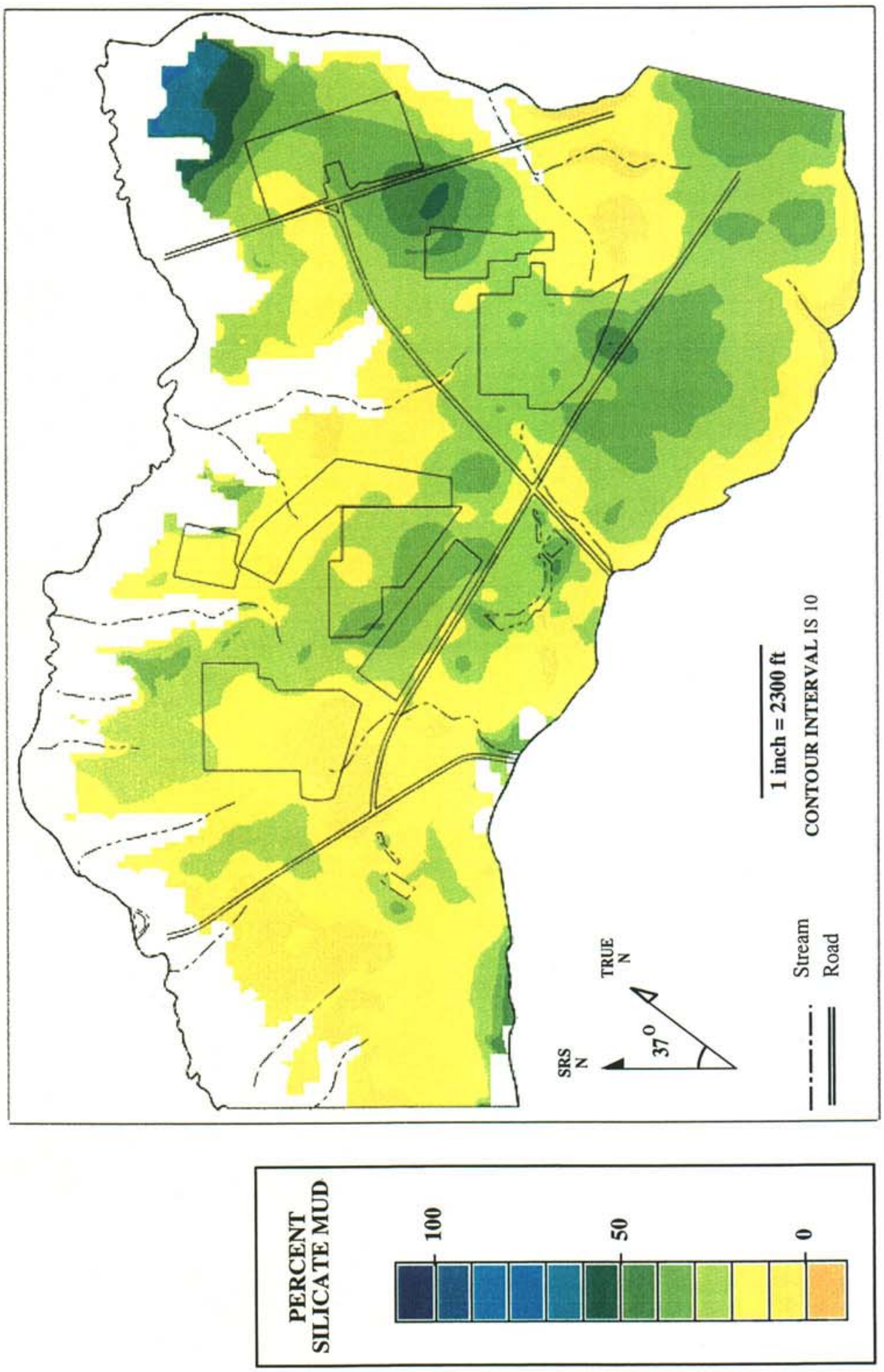

Figure 52. Map of Average Percent Silicate Mud in the "Upper" Aquifer Zone

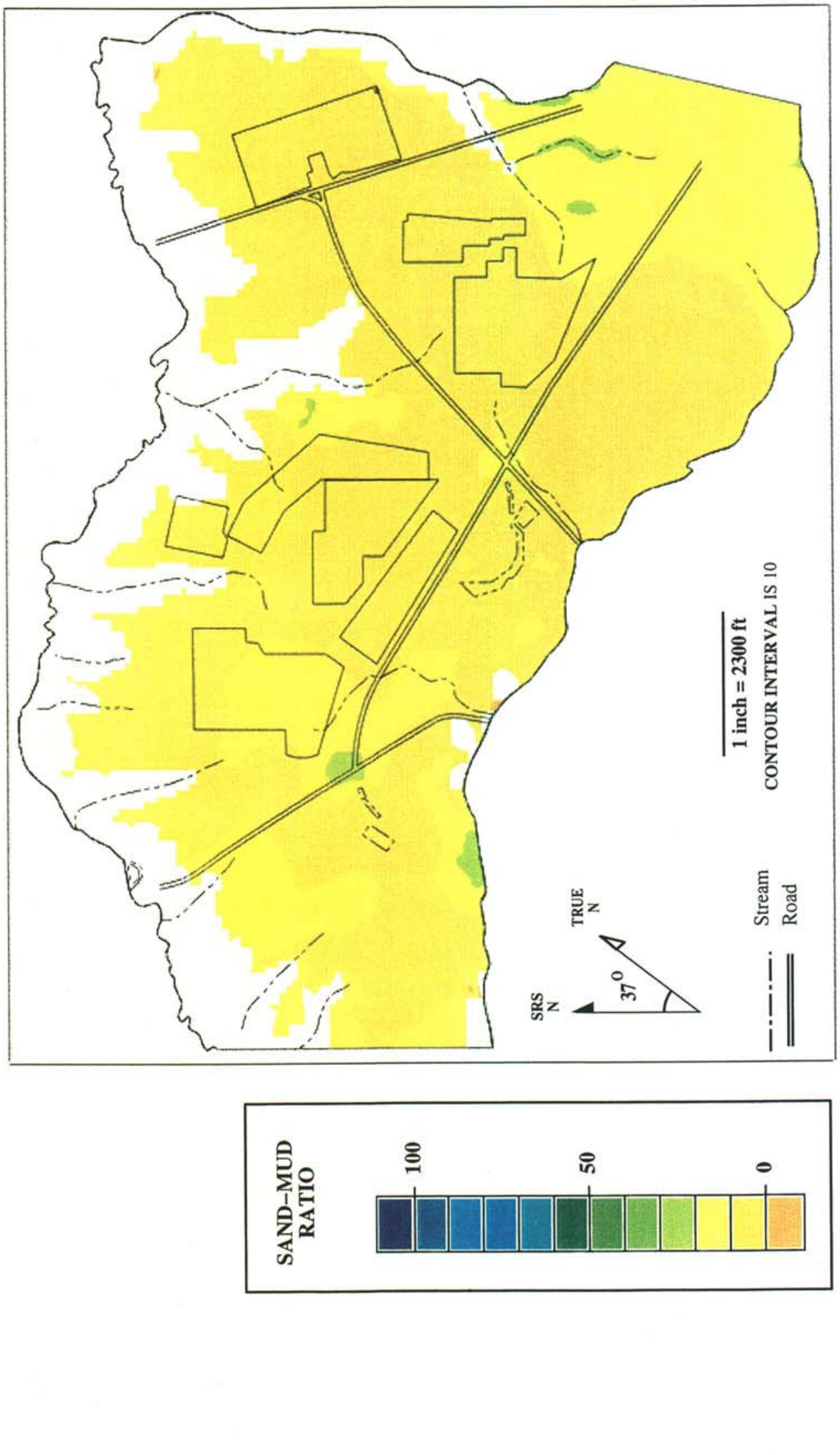

Figure 53. Map of Average Sand–Mud Ratios in the Saturated Zone within the "Upper" Aquifer Zone

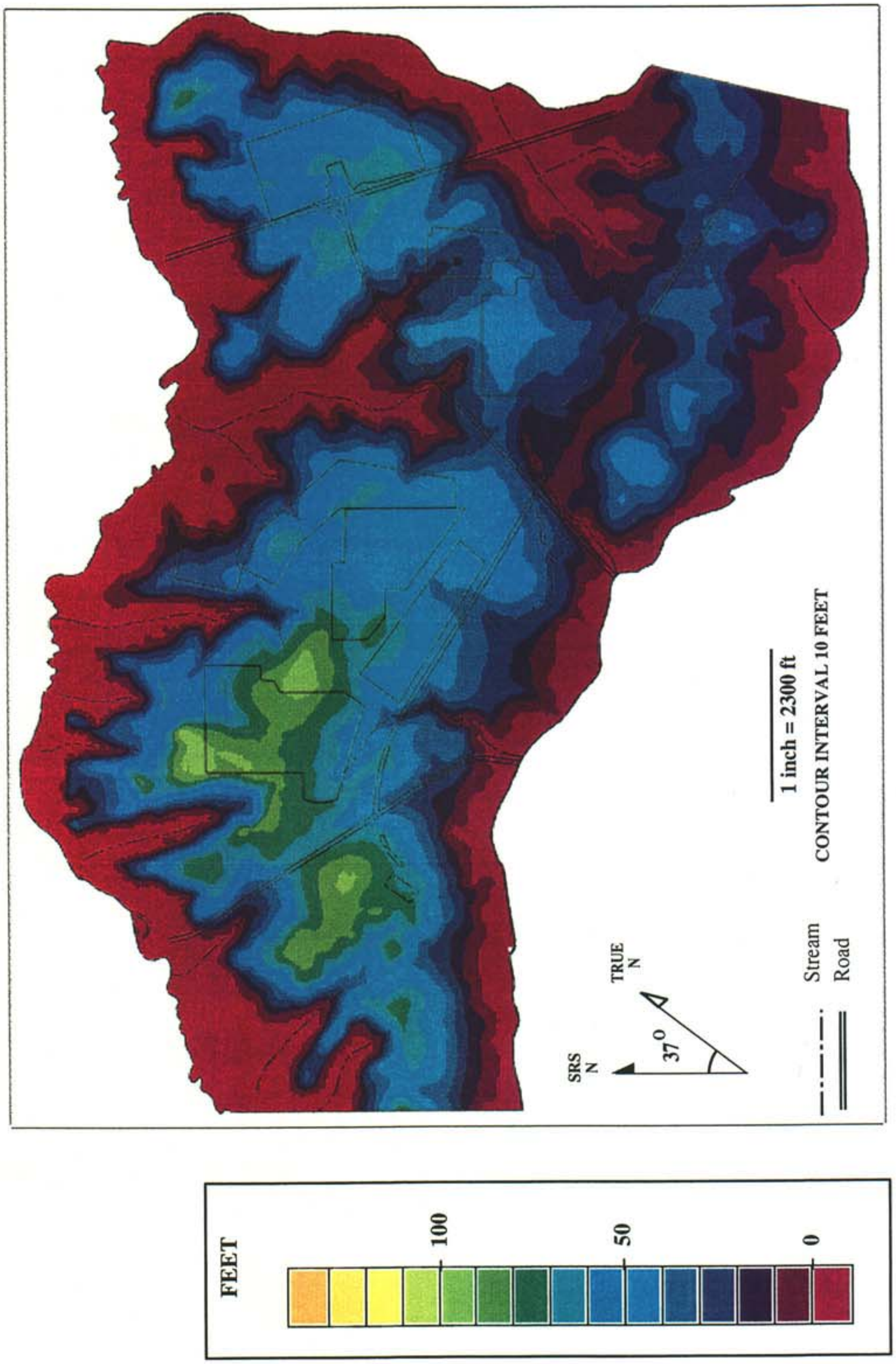

Figure 54. Isopach Map of the Vadose Zone within the "Upper" Aquifer Zone

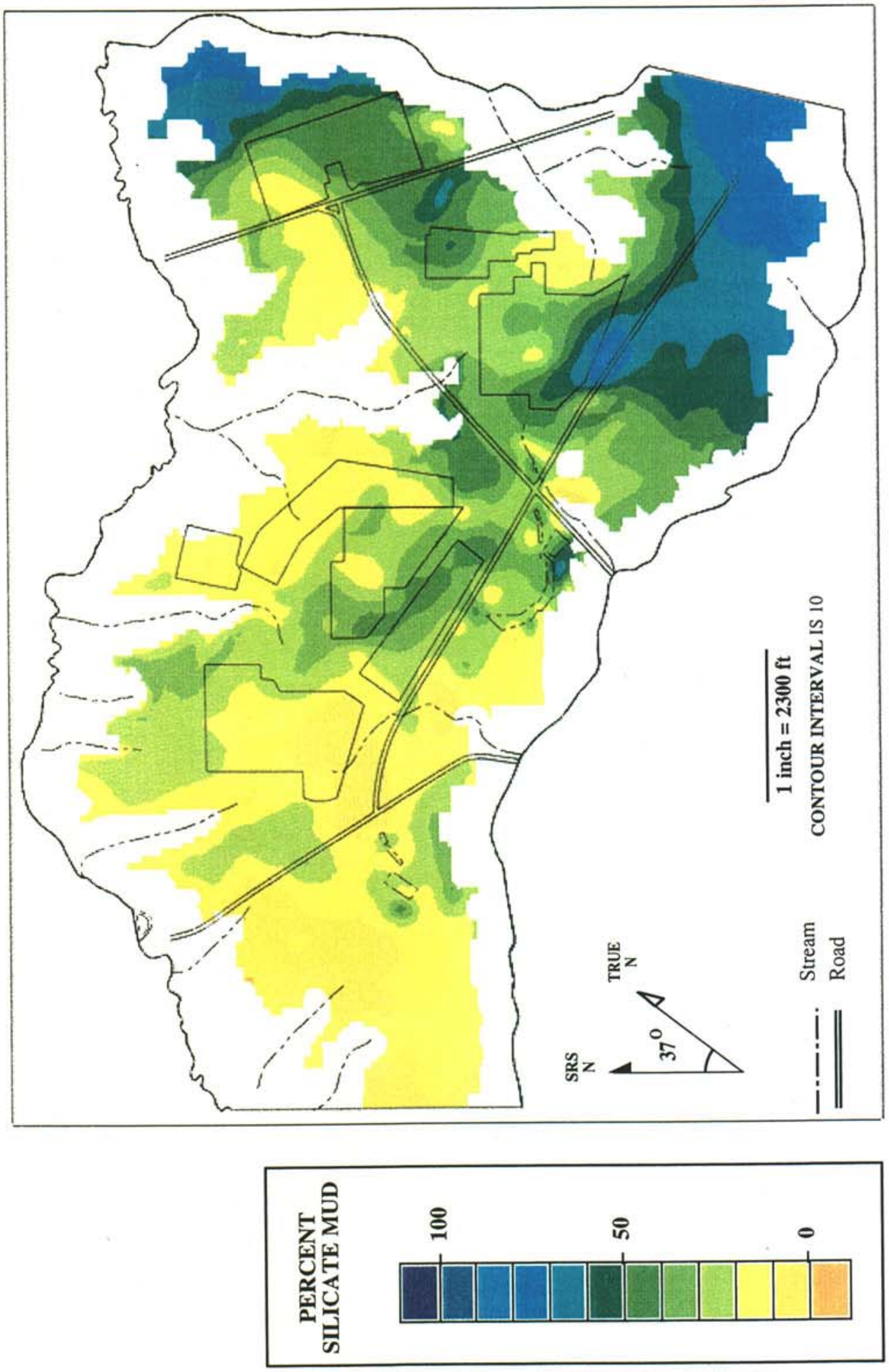

Figure 55. Average Percent Silicate Mud in the Vadose Zone within the "Upper" Aquifer Zone

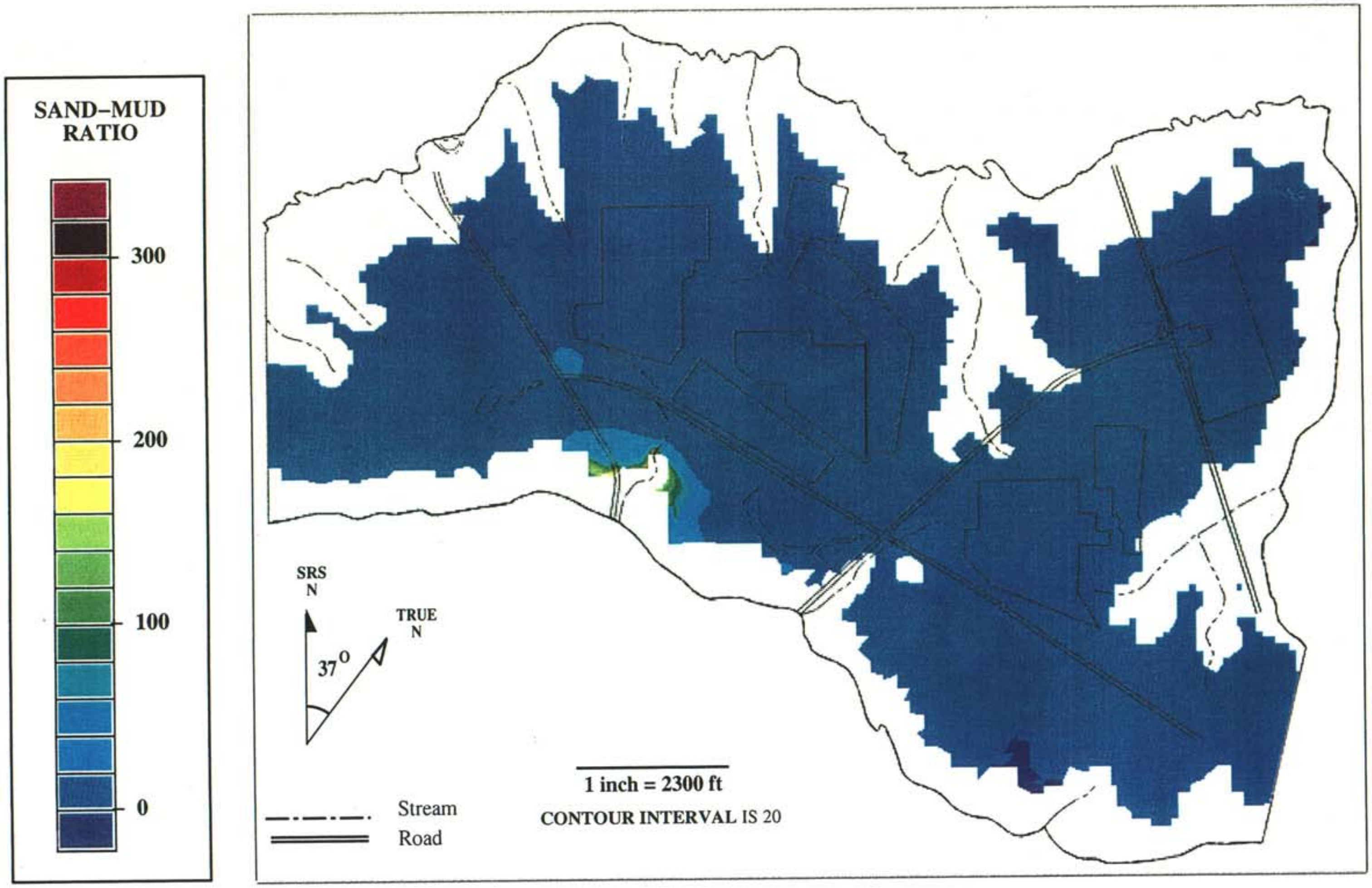

Figure 56. Map of Average Sand–Mud Ratios in the Vadose Zone within the "Upper" Aquifer Zone

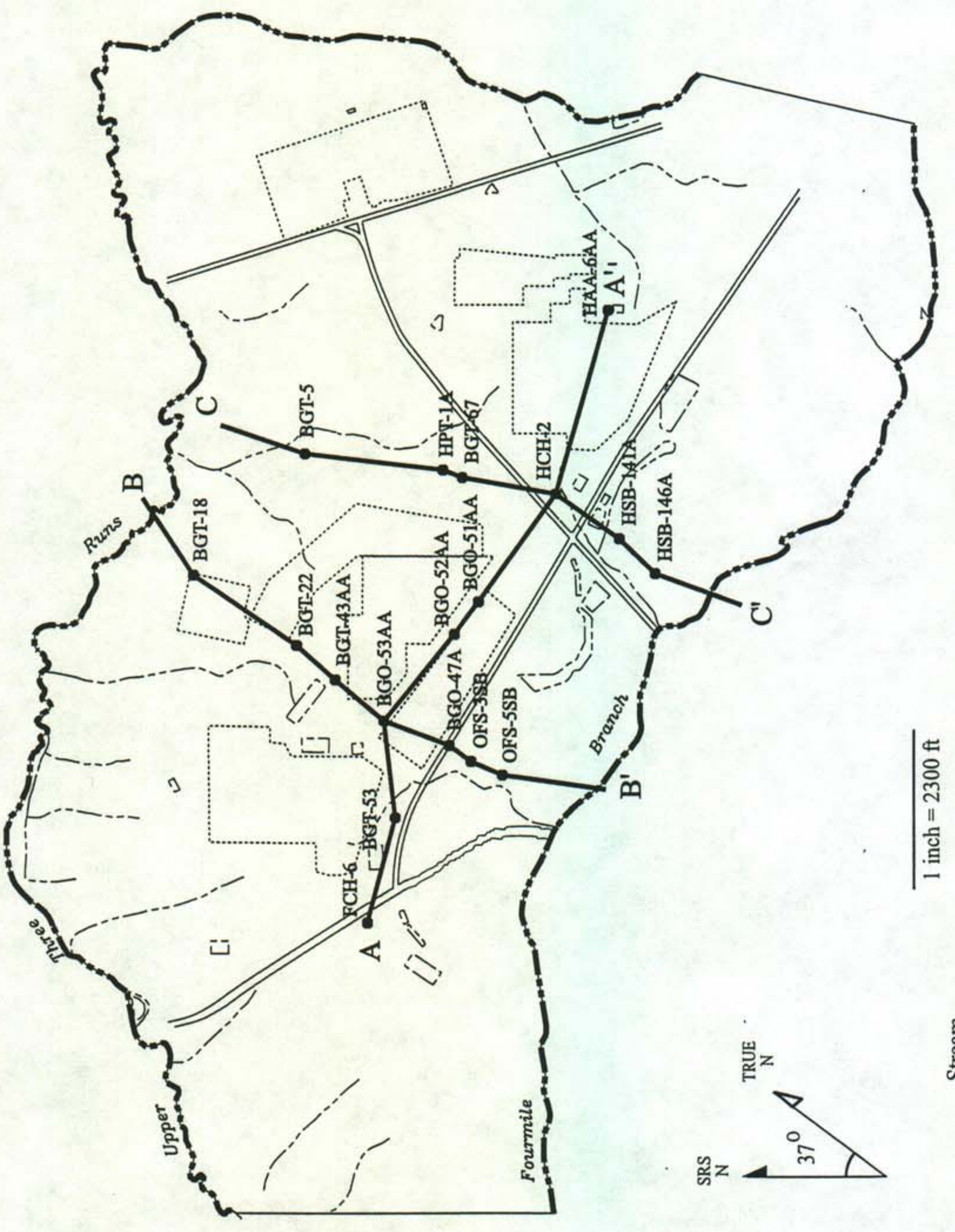

Figure 57. Locations of Cross-Sections

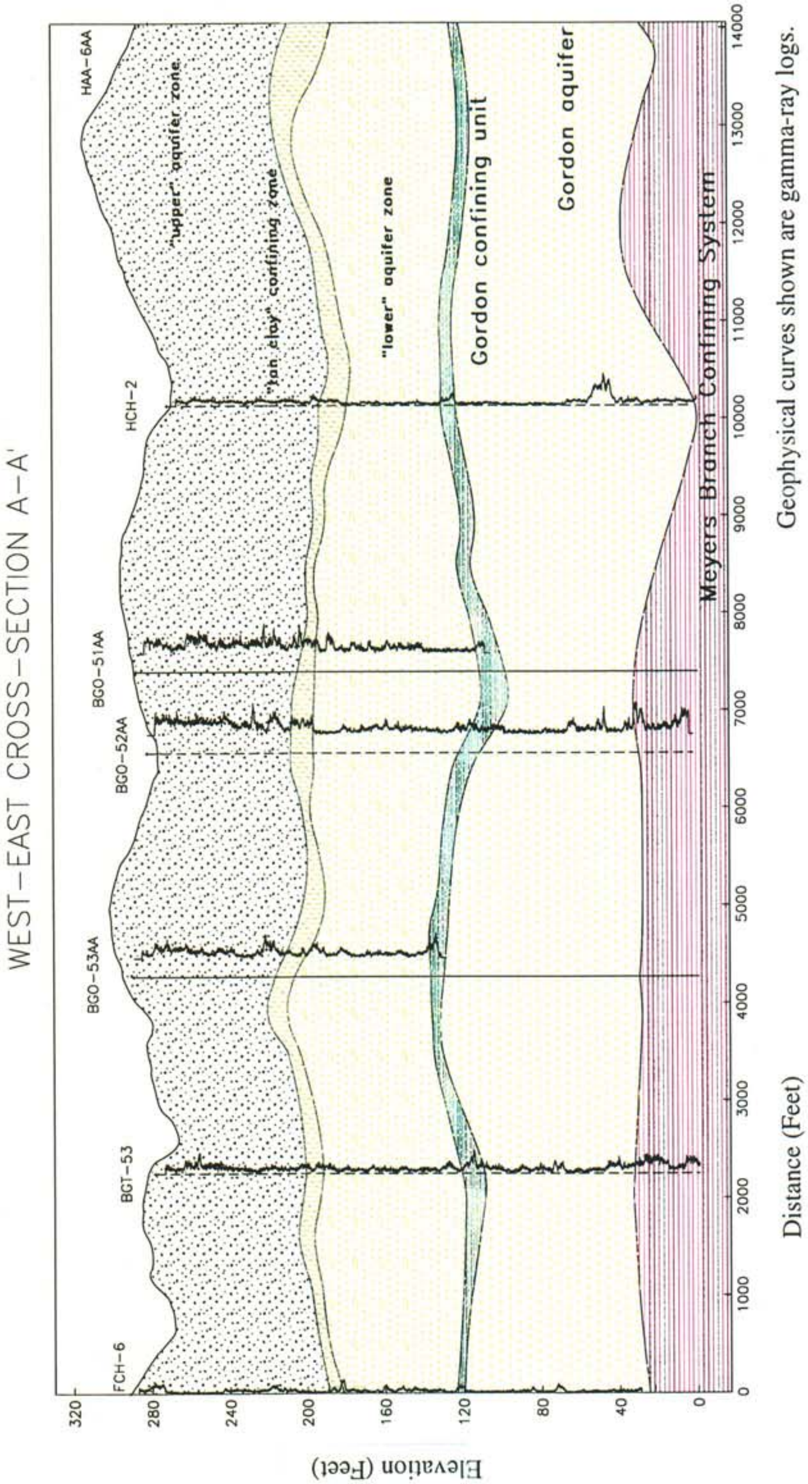

Figure 58. West-East Hydrostratigraphic Cross-Section AA

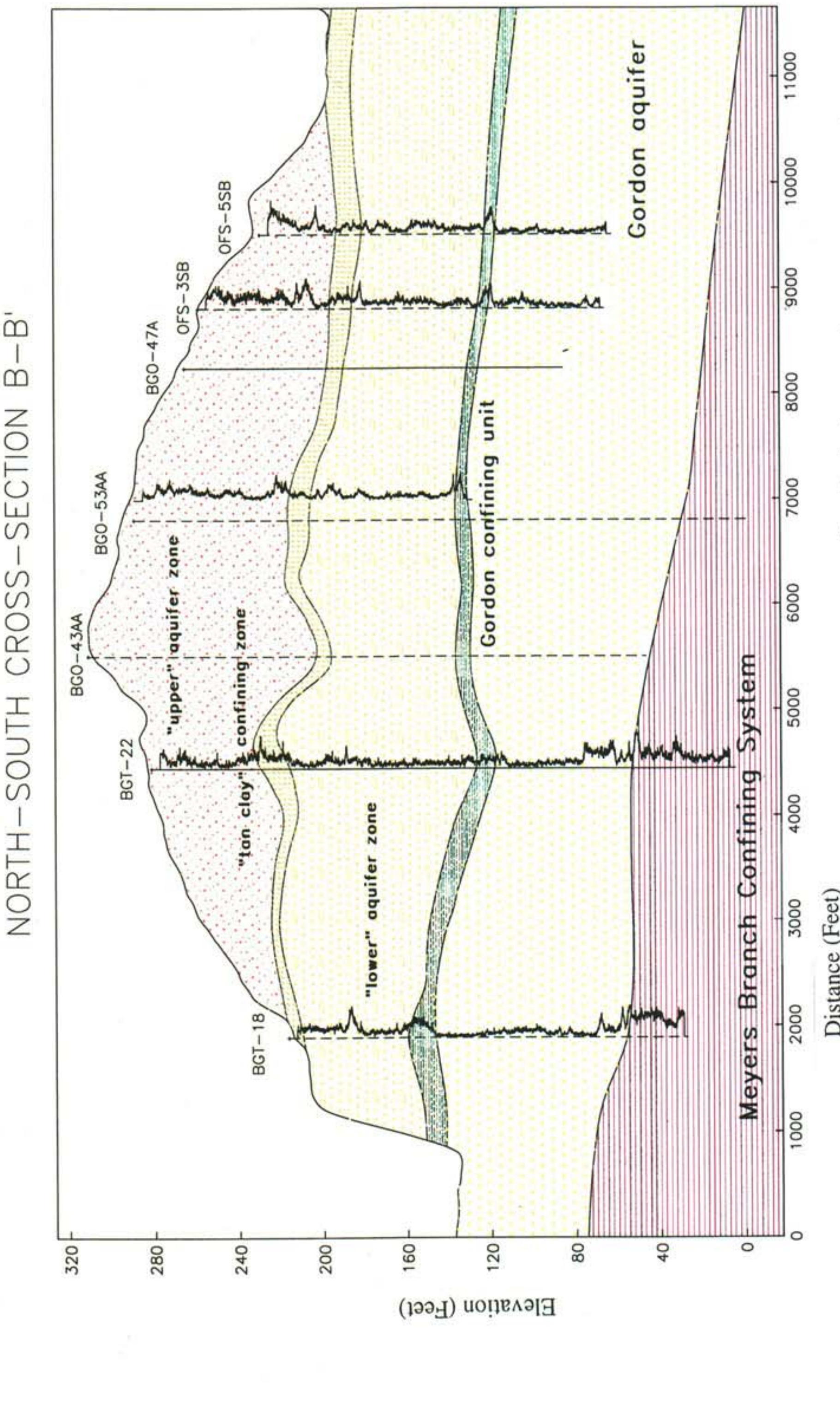

Geophysical curves shown are gamma-ray logs.

Figure 59. North-South Hydrostratigraphic Cross-Section BB'

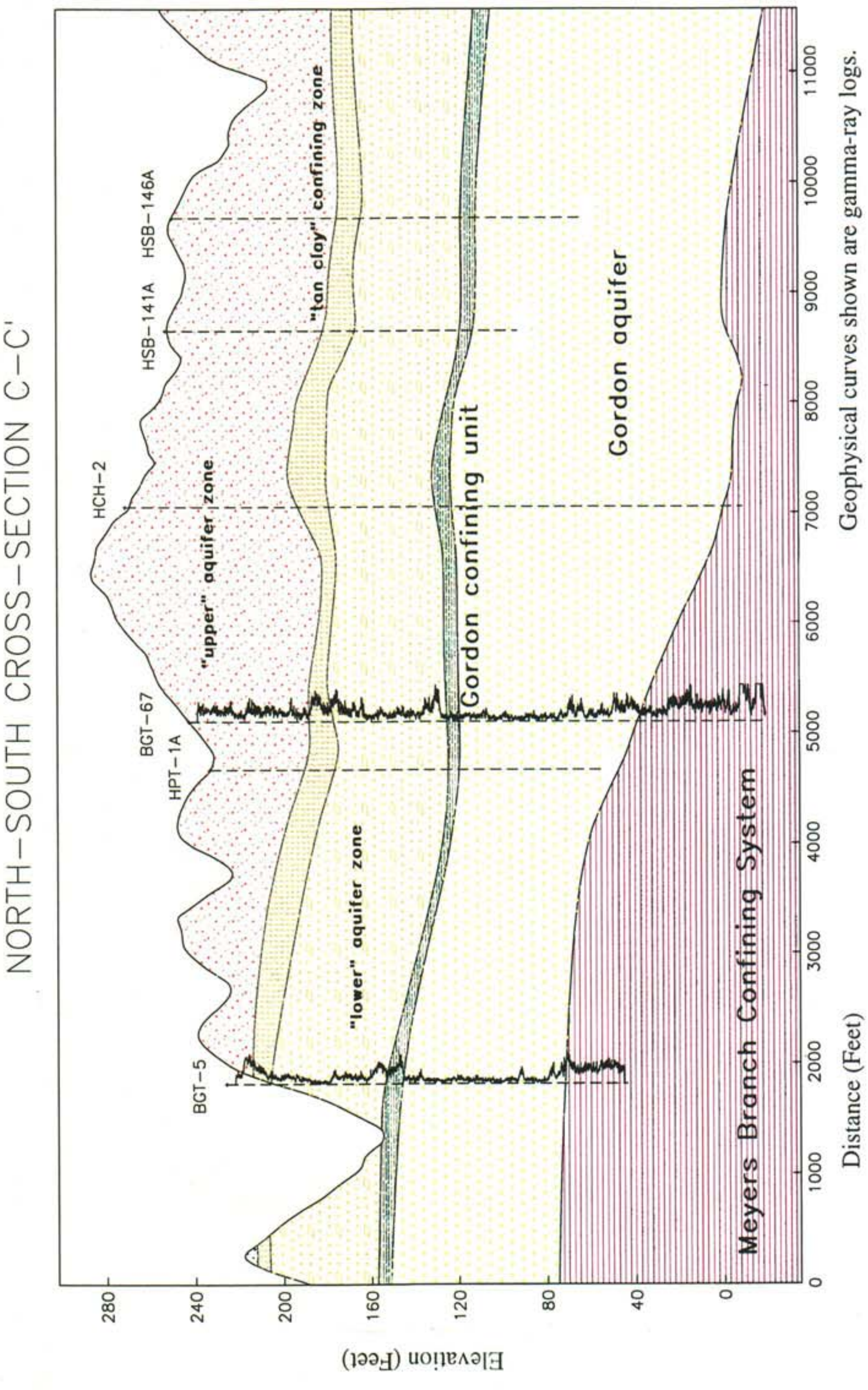

Geophysical curves shown are gamma-ray logs.

Figure 60. North-South Hydrostratigraphic Cross-Section CC'

Table 1. Lithologic and Hydrologic Parameters Calculated from Property Data Using EarthVision®

Average Percent Siliciclastic Mud	The average percentage of mud (silt + clay) within the hydrostratigraphic unit. Calculated over all 3-D grid nodes between the unit top and base.
Average Percent Calcareous Mud	The average percentage of calcareous mud within the hydrostratigraphic unit. Calculated from the 3-D (property) grid for "total percent carbonate" field of Core Description. The average is calculated over all 3-D grid nodes between the unit top and base; output as a 2-D grid with the average percentage as the Z values.
Average Percent Carbonate Sediment	The average node value for percentage of carbonate material within the hydrostratigraphic unit. Calculated over all 3-D grid nodes between the unit top and base. Output as a 2-D grid with the average percentage as the Z values .
Sand/Mud Ratio	The thickness ratio of sand to mud (silt + clay). Equals the total sand in the hydrostratigraphic unit divided by the total mud in the hydrostratigraphic unit. The numerical value of the sand/mud ratio varies from zero to infinity (∞). High values in sand-mud ratios represent high percentages of sand and decreasing percentages of mud. Values smaller than 1/32 or larger than 32 indicate that one of the components is present in amounts of about 3 percent, which probably approaches the limit of the accuracy of the data. The sand/mud ratio indicates the number of feet of sand per foot of mud. For example, a sand/mud ratio of 3.2 indicates that the hydrostratigraphic interval contains 3.2 feet of sand per foot of mud. A sand/mud ratio of infinity indicates that mud beds are not present. Calculated over all 3-D grid nodes between the unit top and base. Output as a 2-D grid with the average sand/mud ratio as Z values.

Table 1. Lithologic and Hydrologic Parameters Calculated from Property Data Using EarthVision® (Continued)

Clastic Ratio	The thickness ratio of terrigenous clastic sediment to carbonate sediment and limestone in the hydrostratigraphic unit. The clastic ratio is calculated by the formula (B + C)/A, where B represents the thickness of coarse detrital components, gravel and sand, and C includes the fine detrital sediment, silt and clay. Component A represents the thickness of chemically or biochemically precipitated carbonate in the hydrostratigraphic unit. The numerical value of the clastic ratio varies from zero to infinity. High clastic ratio values indicate increasing percentages of sand and mud and decreasing percentages of carbonate sediment. A clastic ratio of infinity indicates that limestone is not present. (Krumbein and Sloss, 1963). Calculated over all 3-D grid nodes between the unit top and base. Output as a 2-D grid with the average clastic ratio as Z values.
Vertical Hydraulic Conductivity Distribution	The coefficient of permeability for a sediment measured in the vertical direction. Output as a two-dimensional grid with the average conductivity as the Z values. Contoured using the base-10 logarithm for clarity.
Leakance Distribution	Distribution of this effective leakance. Computed over the thickness of an interval from the geometric means of the vertical hydraulic conductivity. Output as a 2-D grid with the leakance as the Z values. Contoured using the base-10 logarithm for clarity

Table 2. Limits and Characteristics of Lithologic Groups

Group Name	Value Ranges: Clastic Ratio	Value Ranges: Sand-Mud Ratio	Characteristics
Sand	>8	>8	Sand > 89%
Sand-mud	>8	8 - 1	Sand > mud; limestone < 11%
Mud-sand	>8	1 - 0.125	Mud > sand; limestone < 11%
Mud	>8	<0.125	Mud > 89%
Sand-carbonate	1 - 8	>1	Sand > mud; 11% < limestone < 50%
Mud-Carbonate	1 - 8	<1	Mud > sand; 11% < limestone < 50%
Carbonate-Sand	0.25 - 1	>1	Sand > mud; 50% < limestone < 80
Carbonate-Mud	0.25 - 1	<1	Mud > sand; 50% < limestone < 80
Limestone	<0.25	(any value)	Limestone > 80%

(Modified from Krumbein and Sloss, 1963)

Table 3. Summary of Grids Calculated for Lithostratigraphic Units

		Unit Top (ft m.s.l.)			Isopach (ft)		
Lithostratigraphic Unit	**Data Points**	Grid Minimum	Grid Maximum	Grid Average	Grid Minimum	Grid Maximum	Grid Average
"upland" unit	-	-	-	-	0.00*	138.18	32.90
Barnwell Group	108	147.72	317.76	240.38	0.00*	154.82	86.94
Santee Formation	164	55.67	200.85	153.72	0.00*	84.05	38.70
Congaree Formation	142	36.28	167.21	117.58	34.33	165.83	87.66
Lang Syne Formation	82	-66.85	91.74	29.65	-	-	-

* Thickness is zero at extent of unit outcrop.

Table 4. Summary of Grids Calculated for Potentiometric Surfaces

Figure Number	Potentiometric Surface	Number of Wells	Grid Minimum	Grid Maximum	Grid Mean
16	"Upper" Aquifer Zone	99	161.83	301.37	223.01
15	"Lower" Aquifer Zone	104	115.6	266.89	200.36
14	Gordon Aquifer	75	115.6	202.77	163.22

Table 5. Summary of Grids Calculated for Hydrostratigraphic Units

Hydrostratigraphic Unit	Data Points	Unit Top (ft m.s.l.)			Isopach (ft)		
		Grid Minimum	Grid Maximum	Grid Average	Grid Minimum	Grid Maximum	Grid Average
vadose zone	-	-	-	-	0.00	152.22	32.80
saturated zone,"upper" aquifer zone	-	-	-	-	0.00*	174.06	72.23
"tan clay" confining zone	225	150.60	239.63	197.96	0.00*	25.11	9.42
"lower" aquifer zone	222	143.04	230.55	188.68	0.00*	125.77	61.45
Gordon confining unit	161	90.02	181.70	128.51	0.00*	16.57	7.36
Gordon aquifer	146	80.89	168.18	120.93	53.00	153.14	92.87
Meyers Branch confining system	52	-59.00	86.63	26.73	-	-	-

* Thickness is zero at extent of unit outcrop.

Table 6. Summary of Grids Calculated for Lithologic Parameters in the Gordon Aquifer

Property	Minimum	Maximum	Average
Average % Mud	0.10	54.83	23.54
Average % Carbonate	0.00	2.90	0.10
Average Sand-Mud Ratio	0.00	84.15	16.31
Clastic Ratio	31.07	99.05	75.75
Vertical Hydraulic Conductivity (ft/d)	-	-	-
Leakance (ft/d/ft)	-	-	-

Table 7. Summary of Grids Calculated for Lithologic Parameters in the Gordon Confining Unit

Property	Minimum	Maximum	Average
Average % Mud	0.00	99.21	37.37
Average % Carbonate	0.00	57.75	0.627
Average Sand-Mud Ratio	0.00	24.24	4.68
Clastic Ratio	0.00	99.26	19.74
Vertical Hydraulic Conductivity ($\log_{10}$ [ft/d])	-8.15	-1.63	-4.89
Leakance ($\log_{10}$ [ft/d/ft])	-9.88	-2.09	-5.76

Table 8. Summary of Grids Calculated for Lithologic Parameters in the "Lower" Aquifer Zone

Property	Minimum	Maximum	Average
Average % Mud	0.90	44.85	20.75
Average % Carbonate	0.00	97.61	11.30
Average Sand-Mud Ratio	0.00	38.15	7.81
Clastic Ratio	0.00	95.30	20.73
Vertical Hydraulic Conductivity (ft/d)	-	-	-
Leakance (ft/d/ft)	-	-	-

Table 9. Summary of Grids Calculated for Lithologic Parameters in the "Tan Clay" Confining Zone

Property	Minimum	Maximum	Average
Average % Mud	0.41	98.98	38.64
Average % Carbonate	0.00	40.63	0.78
Average Sand-Mud Ratio	0.00	51.50	4.70
Clastic Ratio	0.00	99.35	28.57
Vertical Hydraulic Conductivity ($\log_{10}$ [ft/d])	-5.21	1.09	-2.15
Leakance ($\log_{10}$ [ft/d/ft])	-5.33	-0.01	-3.15

Table 10. Summary of Grids Calculated for Lithologic Parameters in the Saturated Zone

Property	Minimum	Maximum	Average
Average % Mud	0.00	76.09	23.05
Average % Carbonate	-	-	-
Average Sand-Mud Ratio	0.00	56.52	7.90
Clastic Ratio	-	-	-
Vertical Hydraulic Conductivity (ft/d)	-	-	-
Leakance (ft/d/ft)	-	-	-

Table 11. Summary of Grids Calculated for Lithologic Parameters in the Vadose Zone

Property	Minimum	Maximum	Average
Average % Mud	0.00	98.97	33.95
Average % Carbonate	-	-	-
Average Sand-Mud Ratio	0.00	346.36	6.54
Clastic Ratio	-	-	-
Vertical Hydraulic Conductivity (ft/d)	-	-	-
Leakance (ft/d/ft)	-	-	-

Plate 1. Gordon Aquifer. Lithology is moderately sorted, medium-grained sand from SRS core P-28TA, 165 feet. Length of sample is 12 cm.

Plate 2. Gordon Aquifer. Lithology is moderately sorted, medium-grained sand from SRS core YSC-5A, 150 feet. Length of sample is 8 cm.

Plate 3. Gordon Confining Unit. Lithology is fissile, sandy clay from SRS core YSC-5A, 140 feet. Length of sample is 7 cm.

Plate 4. Gordon Confining Unit. Lithology is poorly sorted, interbedded clayey shell limestone and sandy clay from SRS core BGO-9AA, 153 feet.

Plate 5. "Lower" Aquifer Zone. Lithology is well-sorted, fine- to medium-grained sand from SRS core BGO-9AA, 108 feet. Length of sample is 13 cm.

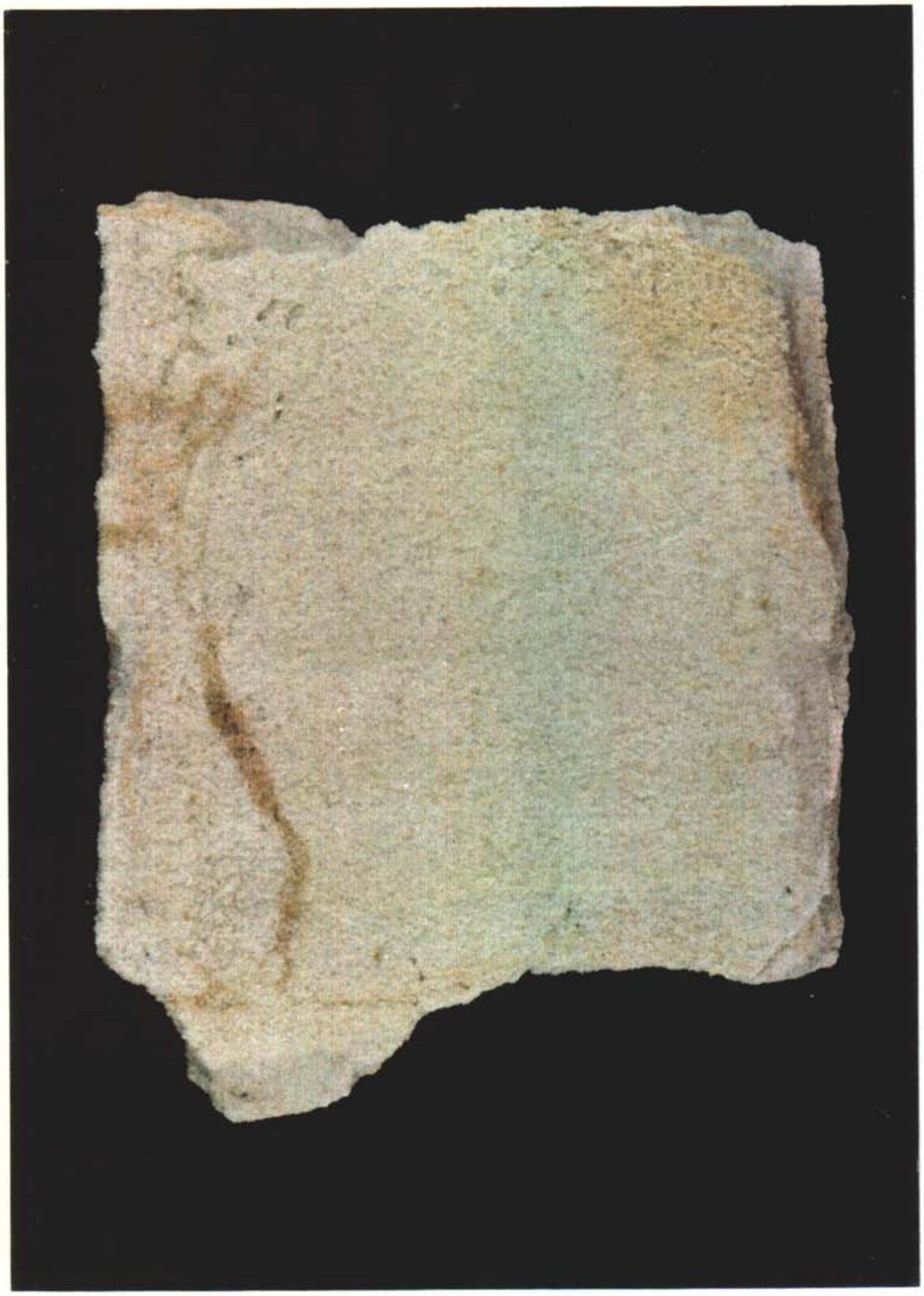

Plate 6. "Lower" Aquifer Zone. Lithology is well-sorted, fine- to medium-grained sand from SRS core P-28TA, 121 feet. Length of sample is 7 cm.

Plate 7. "Lower" Aquifer Zone. Lithology is poorly sorted, fine- to medium-grained clayey sand with minor interlaminated clay from SRS core FSB-116C, 80 feet. Length of sample is 8 cm.

Plate 8. "Lower" Aquifer Zone. Lithology is poorly sorted, coarse-grained clayey sand from SRS core P-28TA, 105 feet. Length of sample is 7 cm.

Plate 9. "Lower" Aquifer Zone. Lithology is moderately porous, moderately sorted, sandy biomoldic limestone from SRS core FSB-114A, 109 feet. Length of sample is 10 cm.

Plate 10. "Lower" Aquifer Zone. Lithology is moderately porous, moderately sorted, sandy biomoldic shell limestone from SRS core HMD-1C, 114 feet. Length of sample is 6 cm.

Plate 11. "Lower" Aquifer Zone. Lithology is poorly sorted, sandy calcarenite from SRS core BGO-9AA, 145 feet. Length of sample is 6 cm.

Plate 12. "Lower" Aquifer Zone. Lithology is moderately sorted, micritic, clayey sand from SRS core BGO-9AA, 144 feet.

Plate 13. "Lower" Aquifer Zone. Lithology is moderately sorted, silica-cemented, calcarenaceous sand from SRS core YSC-5A, 106 feet. Length of sample is 6.5 cm.

Plate 15. "Tan Clay" Confining Zone. Lithology is very poorly sorted, interbedded fissile clay and sand from SRS core BGO-9AA, 61 feet. Length of sample is 10 cm.

Plate 16. "Upper" Aquifer Zone. Lithology is moderately sorted, coarse-grained sand with clayey wisps from SRS core P-28TA, 43 feet. Length of sample is 7 cm.

APPENDIX A

STRATIGRAPHIC DATA

(This page intentionally left blank)

Appendix A-1

Index of Wells and Borings

(This page intentionally left blank)

Well ID	SRS Easting	SRS Northing	Surface Elevation	Location Map No.[1]
BGO-10A	57050.92	76805.18	299.10	B-2
BGO-10AA	56990.54	76997.88	298.80	B-2
BGO-12A	56250.68	76804.63	311.40	B-2
BGO-14A	55838.32	76377.54	300.20	B-2
BGO-16A	56194.15	75756.95	302.80	B-2
BGO-18A	56699.67	75599.89	292.90	B-2
BGO-20AA	57114.81	74953.76	280.88	B-2
BGO-25A	55668.08	76158.50	294.70	B-2
BGO-26A	55014.20	76144.60	285.10	B-2
BGO-27C	54671.40	75666.30	273.90	B-2
BGO-29A	54103.50	75560.00	262.10	B-2
BGO-31C	54816.20	74978.00	271.10	B-2
BGO-33C	55681.40	74479.70	277.40	B-2
BGO-35C	56545.70	73953.90	271.40	B-2
BGO-37C	57279.20	73498.20	284.30	B-2
BGO-39A	57821.93	73572.52	293.70	C-2
BGO-3A	58806.84	75561.71	288.20	C-2
BGO-41A	55403.69	76469.52	298.30	B-2
BGO-42C	55522.27	76404.71	295.90	B-2
BGO-43AA	56268.64	77066.01	312.20	B-2
BGO-44AA	57880.51	76757.02	283.30	C-2
BGO-45A	54550.14	75830.03	276.90	B-2
BGO-46B	54444.65	75012.10	263.40	B-2
BGO-47A	54914.04	74728.83	264.80	B-2
BGO-48C	55124.38	74599.64	274.70	B-2
BGO-49A	56205.08	73902.78	269.10	B-2
BGO-50A	54179.77	75201.16	253.50	B-2
BGO-51AA	57867.00	74113.10	287.20	C-2
BGO-52AA	57201.60	74617.30	281.60	B-2
BGO-53AA	55429.22	76068.96	288.90	B-2
BGO-5C	58794.50	76476.90	294.20	C-2
BGO-6A	58316.80	76487.20	283.80	C-2
BGO-6B	58346.46	76553.24	284.50	C-2
BGO-8A	57618.30	76569.00	281.30	C-2
BGO-9AA	57371.94	76975.69	282.80	B-2
BGT-1	59178.40	76700.60	282.90	C-2
BGT-10	59507.20	79104.60	215.20	C-1
BGT-11	59697.70	79566.90	222.50	C-1
BGT-12	58045.90	77291.20	284.20	C-2
BGT-13	58074.00	77488.90	287.80	C-2
BGT-14	58143.40	77984.00	280.70	C-1
BGT-15	58212.80	78479.20	277.50	C-1
BGT-16	58283.50	78974.10	250.70	C-1
BGT-17	58350.00	79469.70	240.70	C-1
BGT-18	58416.50	79965.30	216.50	C-1

Well ID	SRS Easting	SRS Northing	Surface Elevation	Location Map No.[1]
BGT-2	59607.20	76957.60	276.40	C-2
BGT-20	58549.60	80956.40	159.50	C-1
BGT-21	56952.50	77280.70	294.20	B-2
BGT-22	56970.30	77860.30	281.00	B-1
BGT-23	56997.00	78279.70	270.00	B-1
BGT-24	57019.20	78779.20	265.80	B-1
BGT-25	57041.40	79278.70	264.80	B-1
BGT-27	57085.90	80277.70	256.90	B-1
BGT-28	57108.10	80777.20	258.30	B-1
BGT-29	57130.40	81276.70	243.00	B-1
BGT-3	60045.90	77197.60	275.70	C-2
BGT-30	57150.40	81726.30	219.00	B-1
BGT-31	56189.75	77228.97	308.76	B-2
BGT-32	56121.10	77791.41	310.12	B-1
BGT-33	56037.17	78404.46	290.42	B-1
BGT-34	56027.45	78803.92	286.76	B-1
BGT-35	55929.89	79305.84	267.73	B-1
BGT-36	55867.47	79801.93	261.36	B-1
BGT-37	55805.00	80298.03	251.60	B-1
BGT-4	60484.50	77437.60	259.20	C-2
BGT-40	55644.42	77297.15	332.32	B-2
BGT-41	55490.12	77734.75	328.37	B-1
BGT-42	55313.07	78240.66	310.92	B-1
BGT-43	54816.04	79655.92	277.08	B-1
BGT-44	54650.36	80127.67	276.20	B-1
BGT-45	54533.05	80461.74	285.28	B-1
BGT-46	55354.96	76714.30	310.00	B-2
BGT-47	54986.57	77051.85	317.32	B-2
BGT-48	54895.09	77135.74	314.33	B-2
BGT-49	54946.30	76203.90	297.26	B-2
BGT-5	60924.10	77677.60	225.70	C-1
BGT-50	54756.20	76359.30	296.27	B-2
BGT-51	54505.65	75519.81	272.64	B-2
BGT-53	53422.04	75837.68	278.25	B-2
BGT-54	52889.14	75941.66	279.96	B-2
BGT-56	56265.77	73521.24	262.94	B-2
BGT-57	56104.24	73268.51	259.35	B-2
BGT-58	57399.60	73406.90	285.76	B-2
BGT-59	57123.20	72802.60	281.88	B-2
BGT-6	58746.70	77254.80	282.20	C-2
BGT-60	58057.22	73120.63	291.42	C-2
BGT-61	58490.09	72911.77	284.30	C-2
BGT-62	58609.00	72854.40	282.03	C-2
BGT-63	59146.34	73319.43	293.67	C-2
BGT-63A	58768.10	73646.40	290.79	C-2

Well ID	SRS Easting	SRS Northing	Surface Elevation	Location Map No.[1]
BGT-64	59499.95	73013.74	283.25	C-2
BGT-66	60033.67	74476.55	244.04	C-2
BGT-67	60426.74	74443.06	242.30	C-2
BGT-7	58935.70	77717.80	276.40	C-1
BGT-8	59118.60	78161.50	249.30	C-1
BGT-9	59316.70	78642.30	226.00	C-1
BGX-11D	59581.40	75300.70	273.80	C-2
BGX-1A	58590.35	76831.89	289.10	C-2
BGX-2B	58256.50	77203.40	289.20	C-2
BGX-4A	57215.60	77879.20	288.80	B-1
BGX-7D	58312.80	78349.30	277.10	C-1
BGX-9D	59522.10	76936.00	277.40	C-2
BRR-1D	50588.20	77365.20	293.80	A-2
BRR-3D	50203.50	77398.30	289.50	A-2
BRR-6B	51100.00	77054.60	293.90	A-2
BRR-7B	50707.50	77575.40	289.60	A-1
BRR-8B	50116.50	77634.70	276.70	A-1
CPC-1	47183.78	66855.77	285.10	A-3
FAC-1SB	55243.00	78138.00	312.00	B-1
FCH-1	52843.11	79488.82	316.80	B-1
FCH-2	52599.59	78500.00	288.70	B-1
FCH-3	52087.22	78059.22	307.20	B-1
FCH-4	52021.03	77514.56	297.50	B-1
FCH-5	51667.65	76992.12	284.20	B-2
FCH-6	51245.70	76410.33	291.50	A-2
FIW-1MC	51354.40	76165.30	293.30	B-2
FIW-2MA	51184.50	75930.80	290.50	A-2
FNB-1A	54288.80	80154.50	282.40	B-1
FNB-3A	54116.60	80557.20	282.20	B-1
FSB-100A	50958.40	75534.40	283.80	A-2
FSB-101A	51191.30	75719.00	282.90	A-2
FSB-112A	48809.10	74231.40	227.00	A-2
FSB-113A	51068.10	74167.50	221.30	A-2
FSB-114A	52046.60	75297.40	250.00	B-2
FSB-115C	49736.00	72515.50	205.80	A-2
FSB-116C	50645.90	72725.50	200.50	A-2
FSB-120A	49175.70	75538.90	278.00	A-2
FSB-121C	48413.10	75155.70	254.40	A-2
FSB-122C	48195.00	73881.80	216.00	A-2
FSB-123C	51750.50	74566.70	236.30	B-2
FSB-1TA	51658.30	75649.10	275.40	B-2
FSB-76A	51391.60	76131.90	291.50	B-2
FSB-78A	50172.80	74757.70	270.50	A-2
FSB-79A	50149.60	73664.50	216.10	A-2
FSB-87A	50115.80	75601.70	285.60	A-2

Well ID	SRS Easting	SRS Northing	Surface Elevation	Location Map No.[1]
FSB-89C	51345.20	75553.20	279.10	B-2
FSB-91C	50953.50	75213.30	277.00	A-2
FSB-93C	50458.30	74897.30	274.00	A-2
FSB-95C	50016.70	74971.70	281.80	A-2
FSB-96A	49778.70	74882.20	277.70	A-2
FSB-97A	49965.70	75171.20	283.80	A-2
FSB-98A	50121.60	75389.80	280.70	A-2
FSB-99A	50314.80	75675.60	285.30	A-2
FSB-PC	50140.00	74090.20	230.80	A-2
HAA-1TA	62953.30	69892.20	290.20	C-3
HAA-2AA	61285.10	70925.40	291.40	C-3
HAA-3AA	60201.90	71488.00	274.50	C-2
HAA-4AA	61929.60	72223.20	299.20	C-2
HAA-6AA	63860.20	71441.00	279.80	D-2
HC-12A	59504.00	73187.00	287.30	C-2
HCA-4AA	62942.50	72513.70	308.60	C-2
HCH-1	60923.42	72796.39	284.00	C-2
HCH-2	60091.79	72519.61	270.90	C-2
HCH-3	59917.33	71998.82	264.00	C-2
HCH-4	59139.93	72449.59	269.90	C-2
HCH-5	59331.53	71810.36	255.00	C-2
HIW-1BD	58342.20	72564.60	275.80	C-2
HIW-1MC	58471.80	72500.00	272.30	C-2
HIW-2A	56753.00	73249.70	276.30	B-2
HIW-2MC	56698.40	73226.40	269.00	B-2
HIW-4MC	56570.10	73160.10	263.40	B-2
HIW-5MC	56498.90	73557.90	266.10	B-2
HMD-1C	56973.30	78731.70	262.70	B-1
HMD-2C	57269.70	79665.80	259.30	B-1
HMD-3C	57745.20	79578.70	257.50	C-1
HMD-4C	58188.50	79160.40	248.50	C-1
HPC-1	62493.60	70395.40	293.50	C-3
HPT-1A	60587.00	74847.10	232.90	C-2
HPT-2A	60200.50	75061.80	257.80	C-2
HSB-101C	58604.40	72001.90	256.30	C-2
HSB-103C	58323.60	71593.90	245.20	C-2
HSB-104C	58082.60	71376.80	245.50	C-2
HSB-105C	57883.80	71447.30	247.20	C-2
HSB-106C	57651.50	71720.90	250.70	C-2
HSB-107C	57432.00	71698.50	259.30	B-2
HSB-109C	56895.60	71684.80	259.40	B-2
HSB-110C	56680.70	71779.30	253.40	B-2
HSB-111C	56501.90	71919.40	253.70	B-2
HSB-112C	56417.40	72156.40	252.60	B-2
HSB-113C	56160.40	72312.30	258.70	B-2

Well ID	SRS Easting	SRS Northing	Surface Elevation	Location Map No.[1]
HSB-115C	56043.20	72653.20	266.80	B-2
HSB-117A	55170.10	72733.60	234.80	B-2
HSB-118A	55775.60	72696.40	245.00	B-2
HSB-119A	56100.20	73082.50	254.80	B-2
HSB-120A	56431.90	73395.10	266.00	B-2
HSB-121A	57389.60	72024.80	272.30	B-2
HSB-122A	57747.40	72195.90	269.40	C-2
HSB-123A	58124.80	72189.80	263.60	C-2
HSB-124A	58514.60	72199.60	263.90	C-2
HSB-132C	58787.70	71472.40	238.30	C-2
HSB-139A	57365.40	71127.40	231.50	B-2
HSB-140A	56535.40	70050.30	234.00	B-3
HSB-141A	59168.70	71213.60	252.60	C-2
HSB-143C	52773.20	73738.20	220.10	B-2
HSB-144A	56200.50	71892.10	233.60	B-2
HSB-145C	57769.00	71098.90	233.70	C-2
HSB-146A	58454.00	70478.90	249.50	C-3
HSB-148C	55344.20	70151.50	248.90	B-3
HSB-151C	54014.90	72997.90	211.60	B-2
HSB-152C	54346.70	72012.00	212.10	B-2
HSB-65A	58436.00	72436.20	270.70	C-2
HSB-68A	56892.10	71526.90	247.40	B-2
HSB-69A	56465.10	71549.40	234.10	B-2
HSB-83A	58606.10	71648.60	234.90	C-2
HSB-84A	56359.10	71586.20	226.70	B-2
HSB-85A	58943.40	73791.90	292.10	C-2
HSB-86A	55985.90	72520.20	260.00	B-2
HSB-PC	55650.03	72119.31	227.80	B-2
HSB-TB	58696.10	72394.00	267.10	C-2
HSL-6AA	60555.70	72692.60	274.60	C-2
HSL-8AA	61113.80	72729.40	286.70	C-2
LWR-9SB	45406.62	71658.83	238.20	A-2
OFS-1SB	54032.60	74967.50	261.60	B-2
OFS-2SB	53848.00	74671.00	257.50	B-2
OFS-3SB	54579.00	74270.00	258.10	B-2
OFS-4SB	55188.00	73874.00	258.70	B-2
OFS-5SB	54298.00	73623.00	228.70	B-2
P-18TA	47652.70	67578.50	296.90	A-3
P-27TA	64022.90	70382.00	274.10	D-3
P-28TA	55441.10	79284.30	285.60	B-1
SDS-21	67087.00	78951.00	251.00	D-1
SDS-22	66304.00	76887.00	283.00	D-2
YSC-1A	65438.93	78039.90	268.90	D-1
YSC-1C	65855.46	78186.24	272.50	D-1
YSC-2A	66100.08	78311.53	281.70	D-1

Well ID	SRS Easting	SRS Northing	Surface Elevation	Location Map No.[1]
YSC-3SB	65920.00	77680.00	277.00	D-1
YSC-4A	65883.50	77050.08	287.50	D-2
YSC-5A	67134.90	74295.90	273.00	D-2

Notes:

[1] Numbers refer to grid in Figure A-1

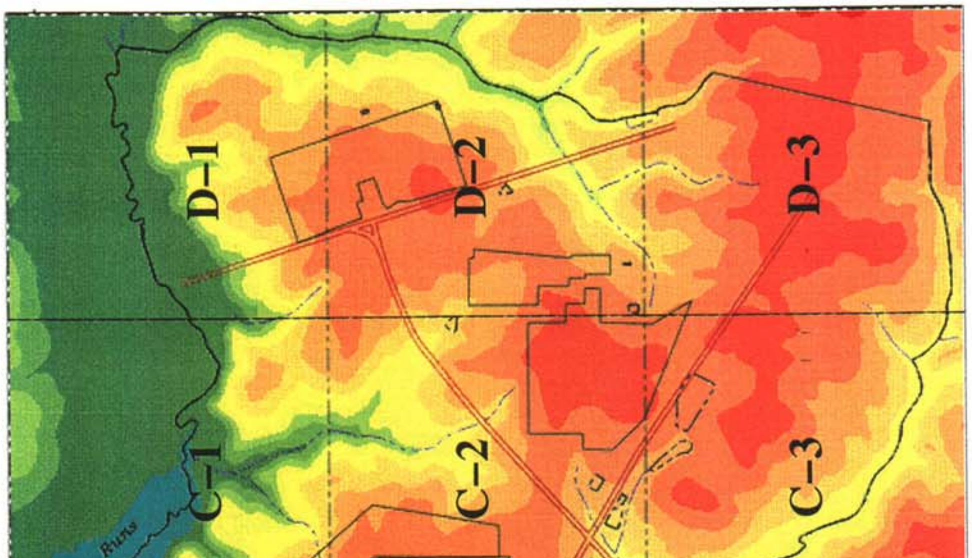

Figure A–1. Index Grid for Data Location Maps

Data Location Map A-1

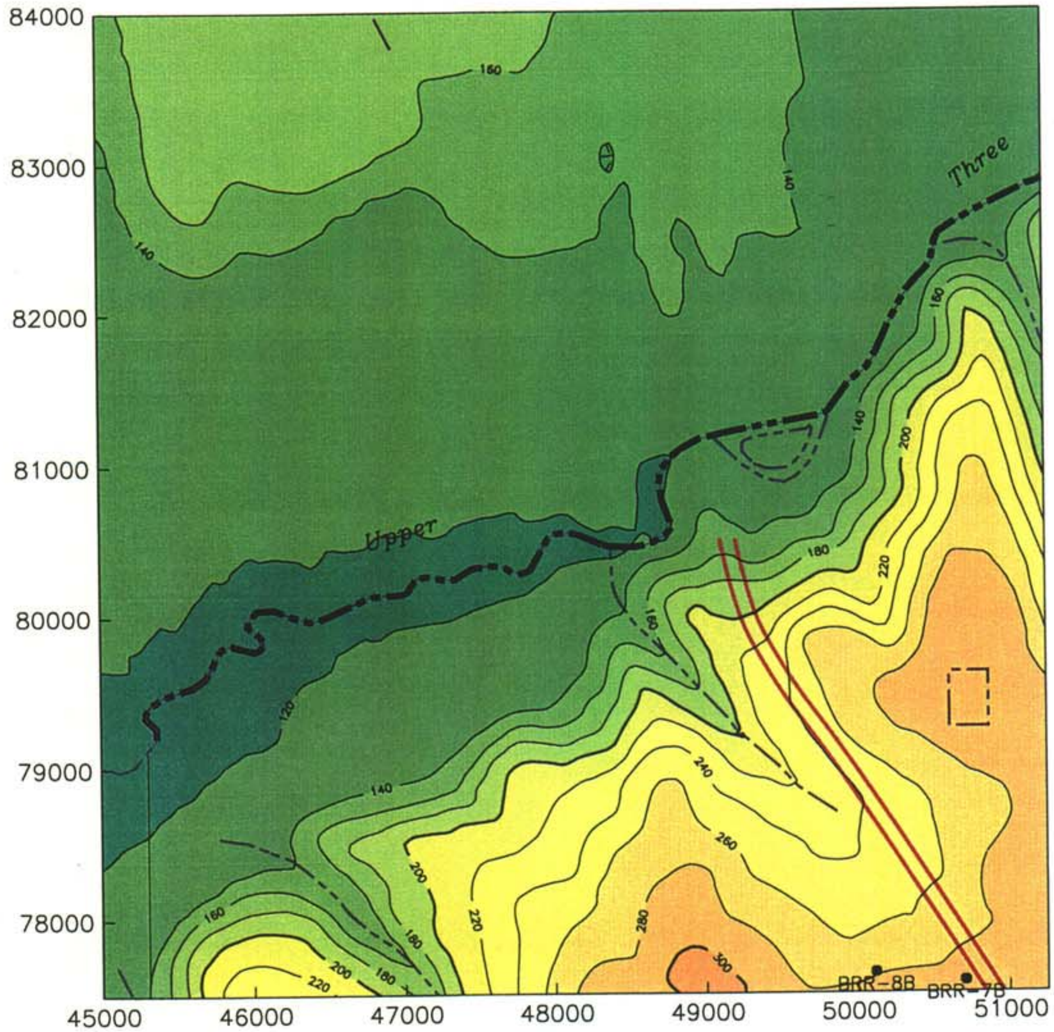

Data Location Map A-2

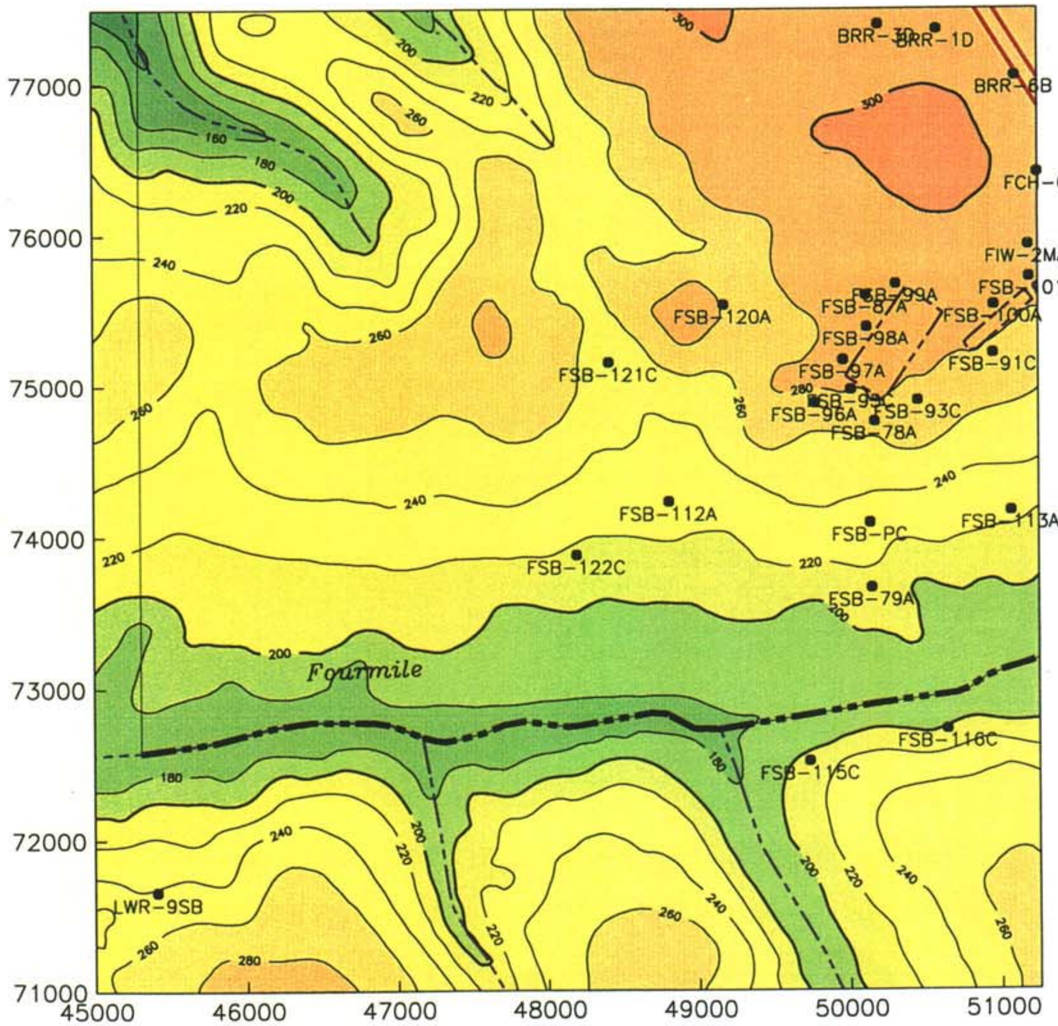

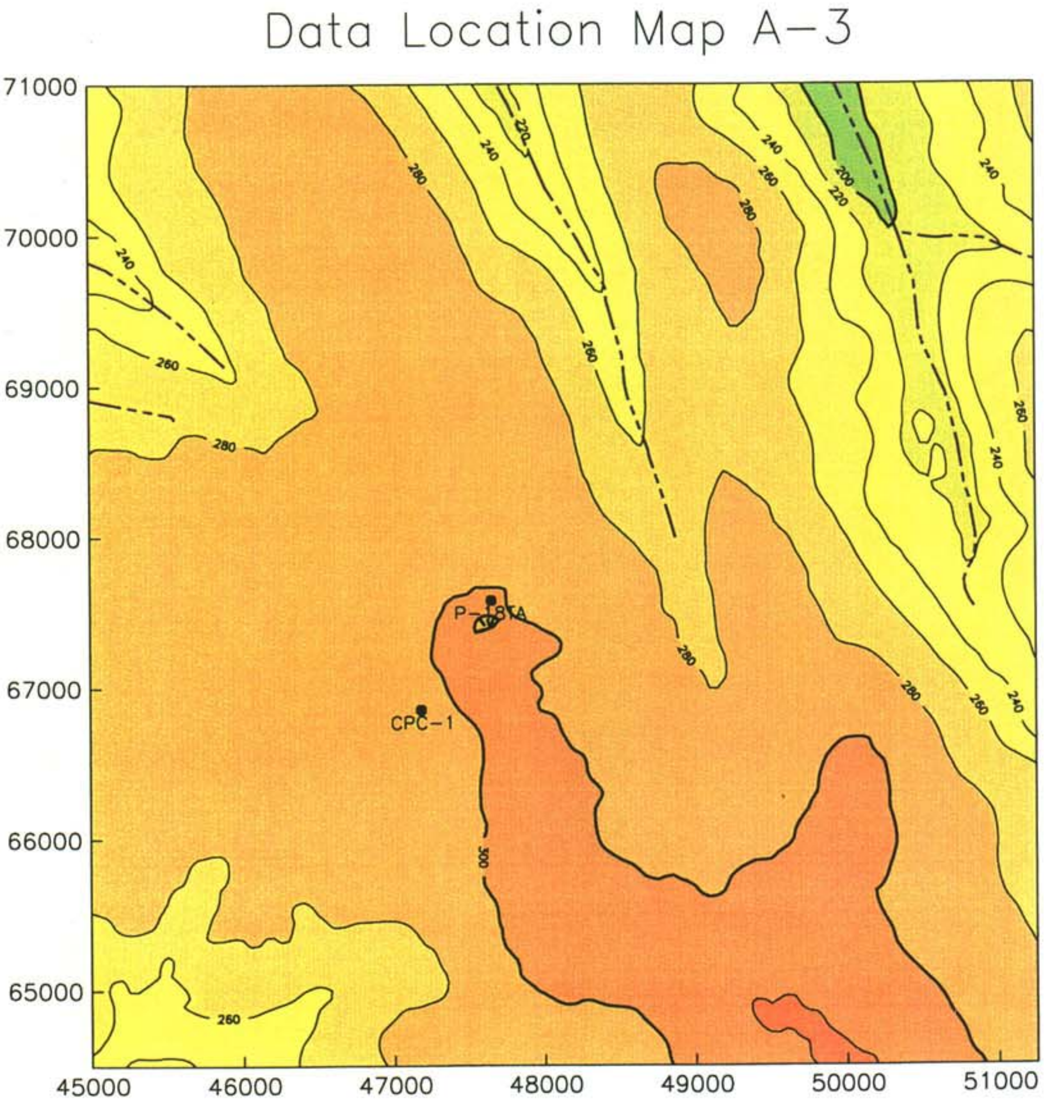

Data Location Map A-3
71000
70000
69000
68000
67000
66000
65000
45000
46000
47000
48000
49000
50000
51000
P-18TA
CPC-1
200
220
240
260
280
300

Data Location Map B−1

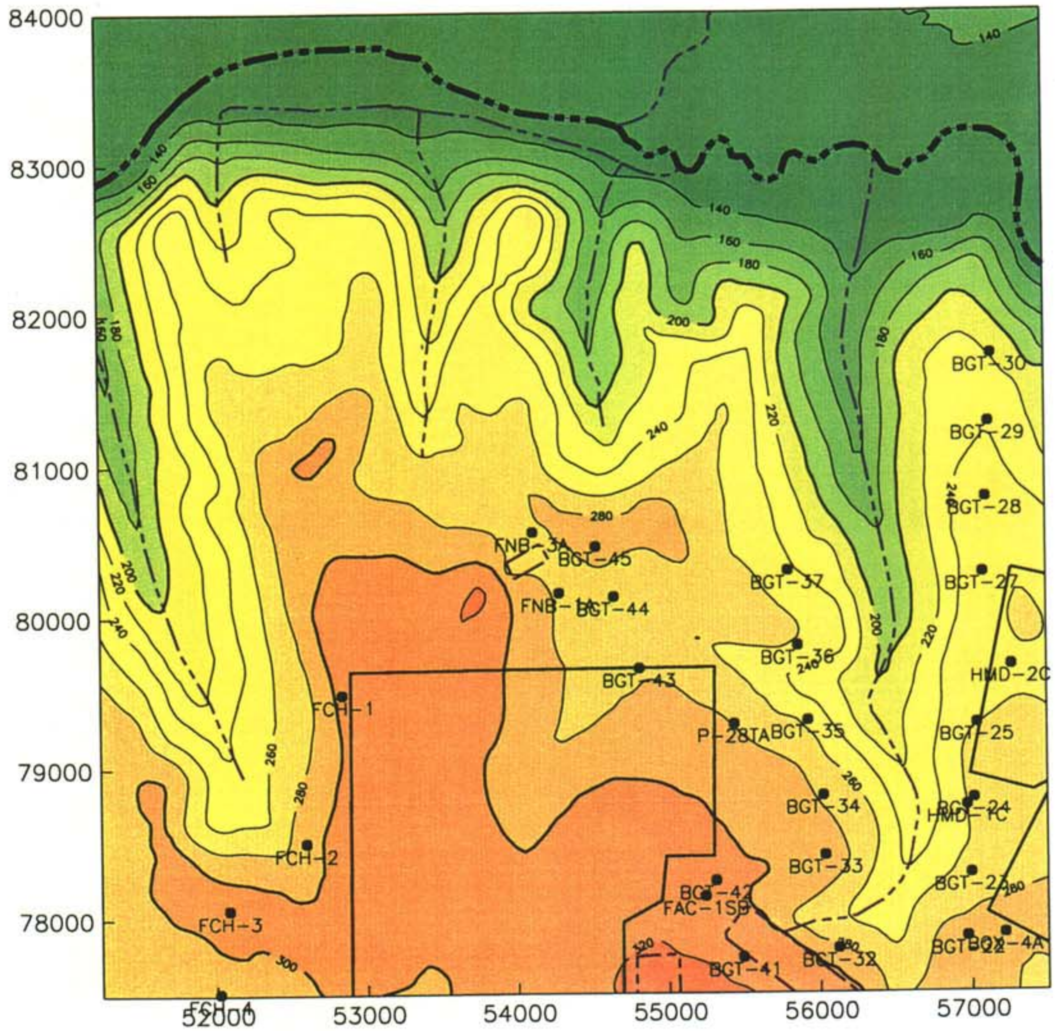

Data Location Map B-2

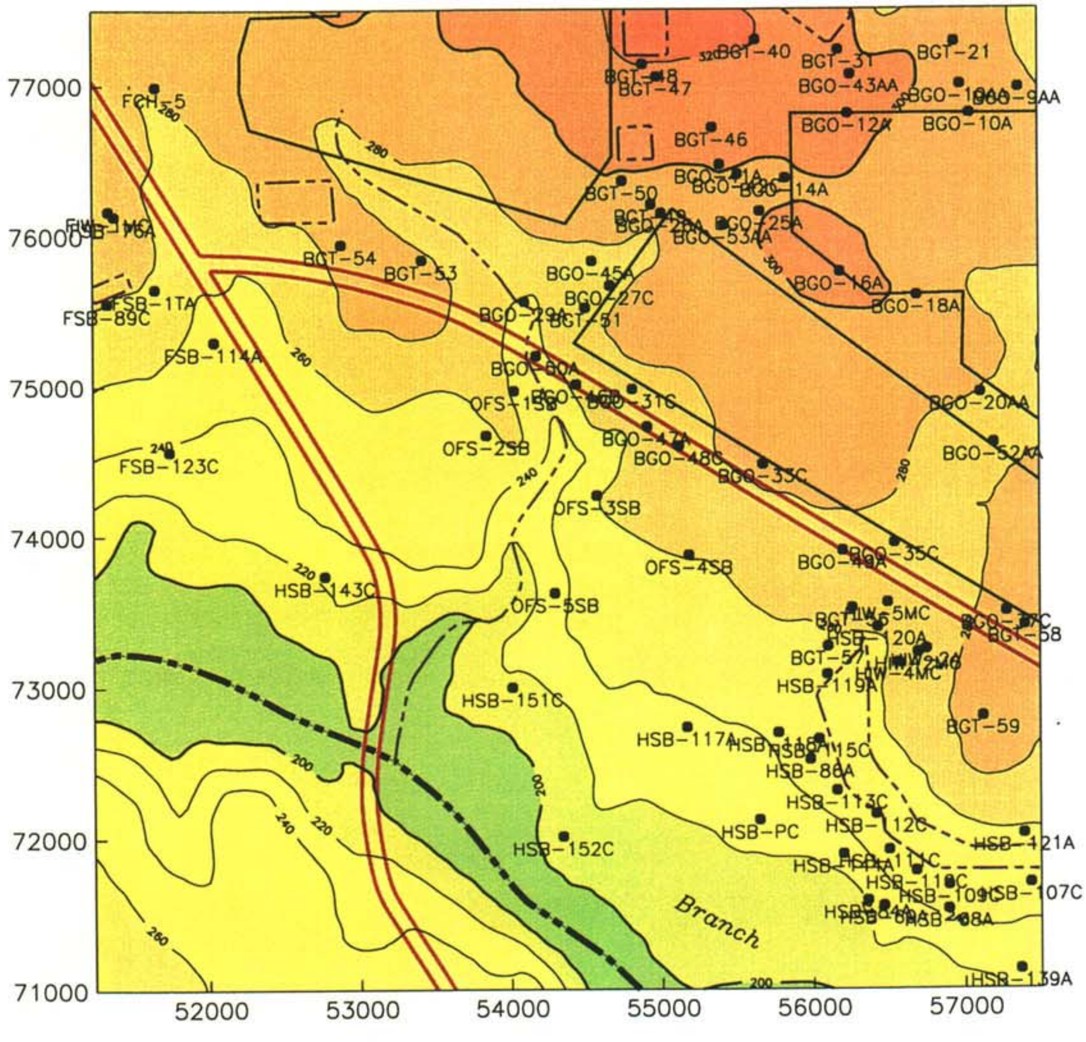

Data Location Map C−1

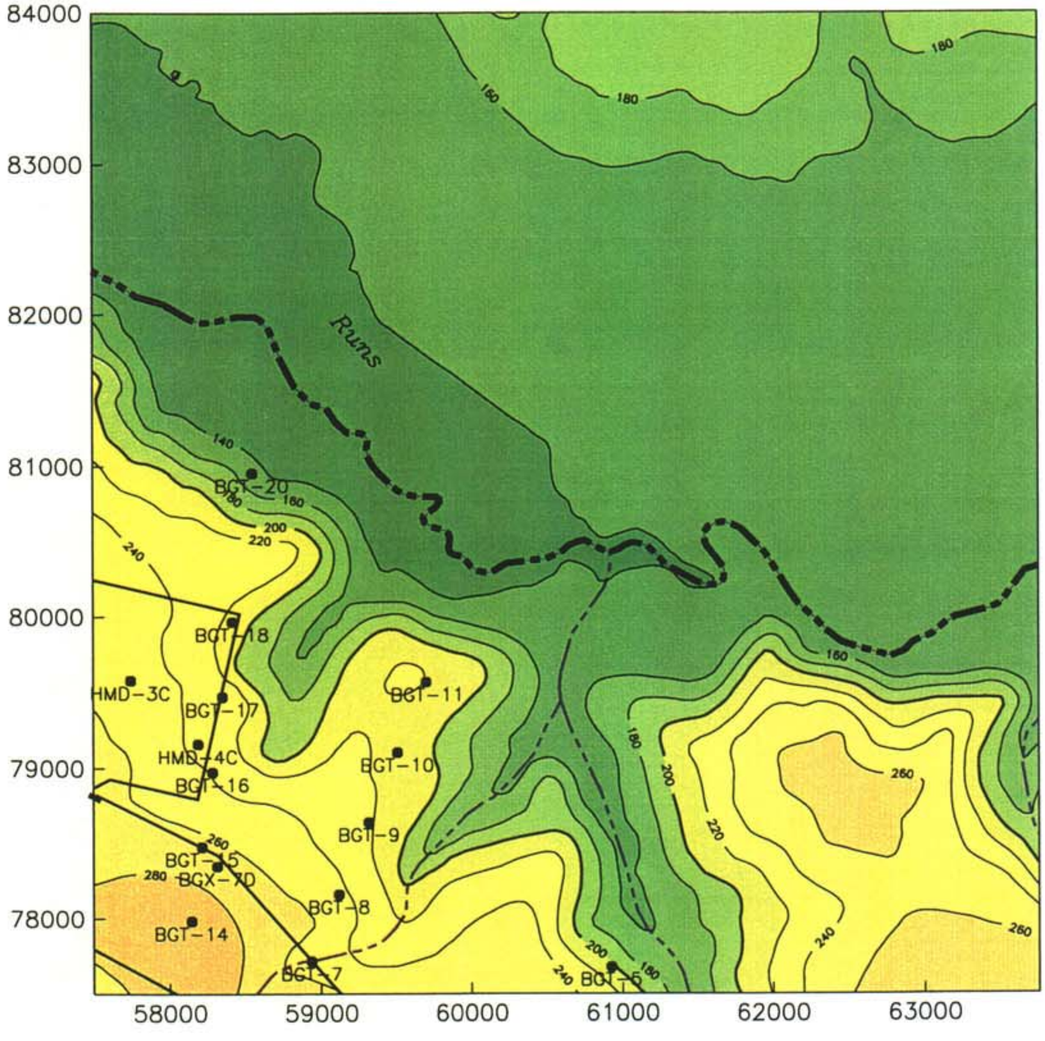

Data Location Map B-3

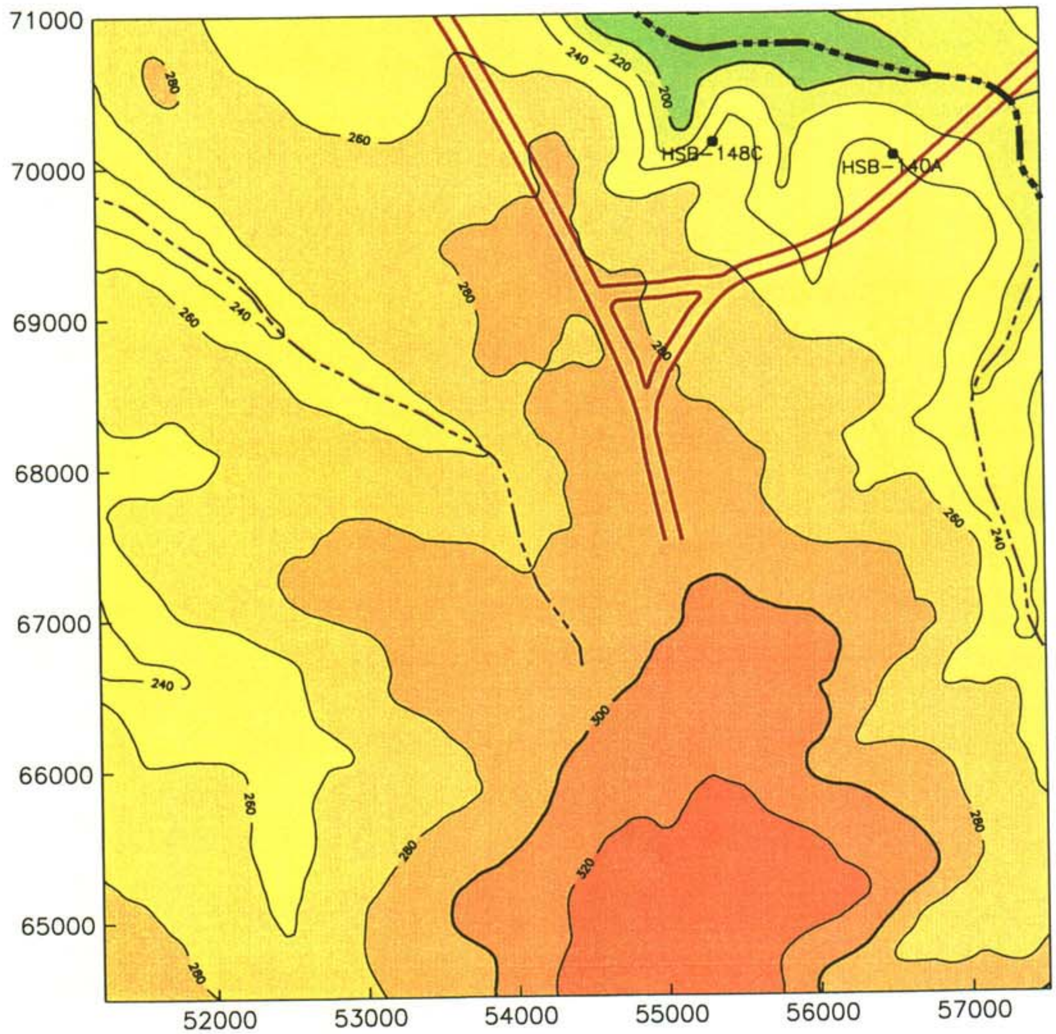

Data Location Map C-2

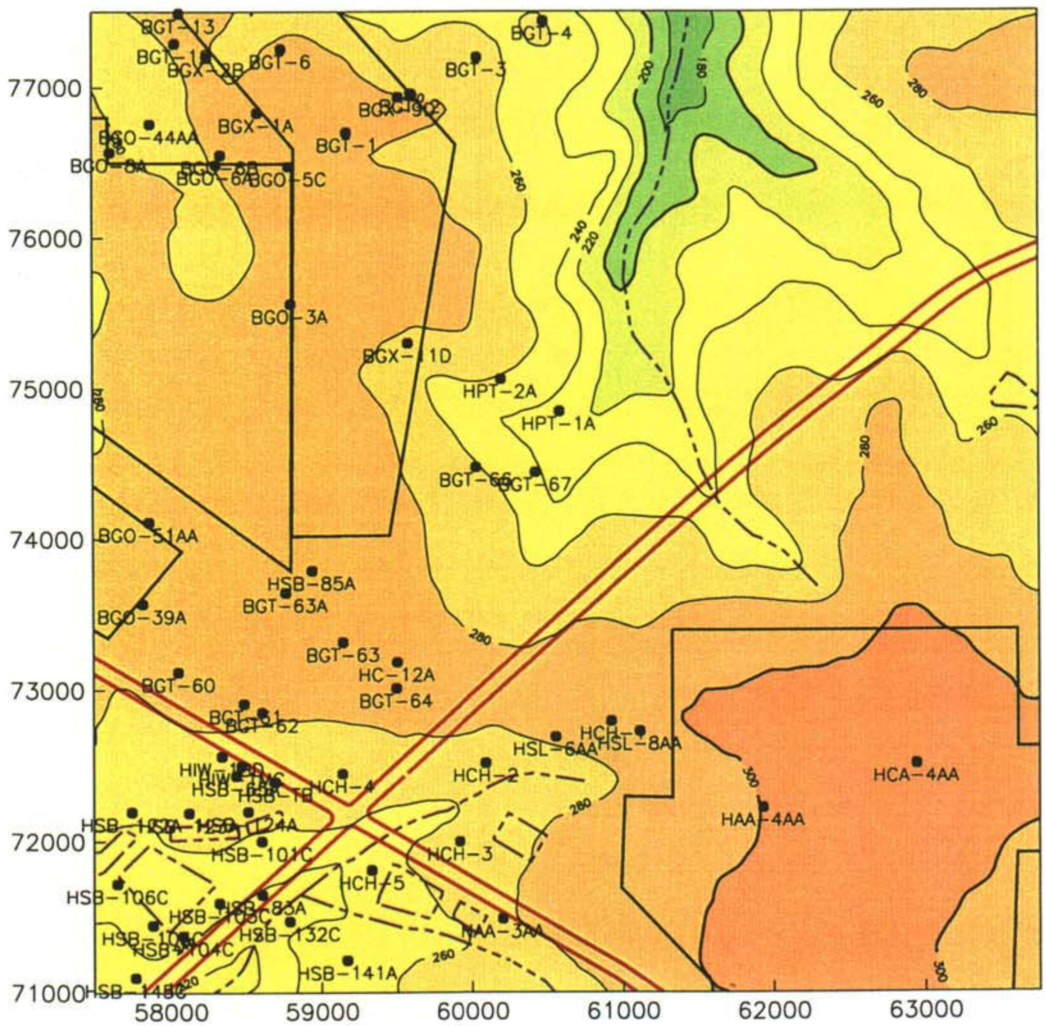

Data Location Map C-3

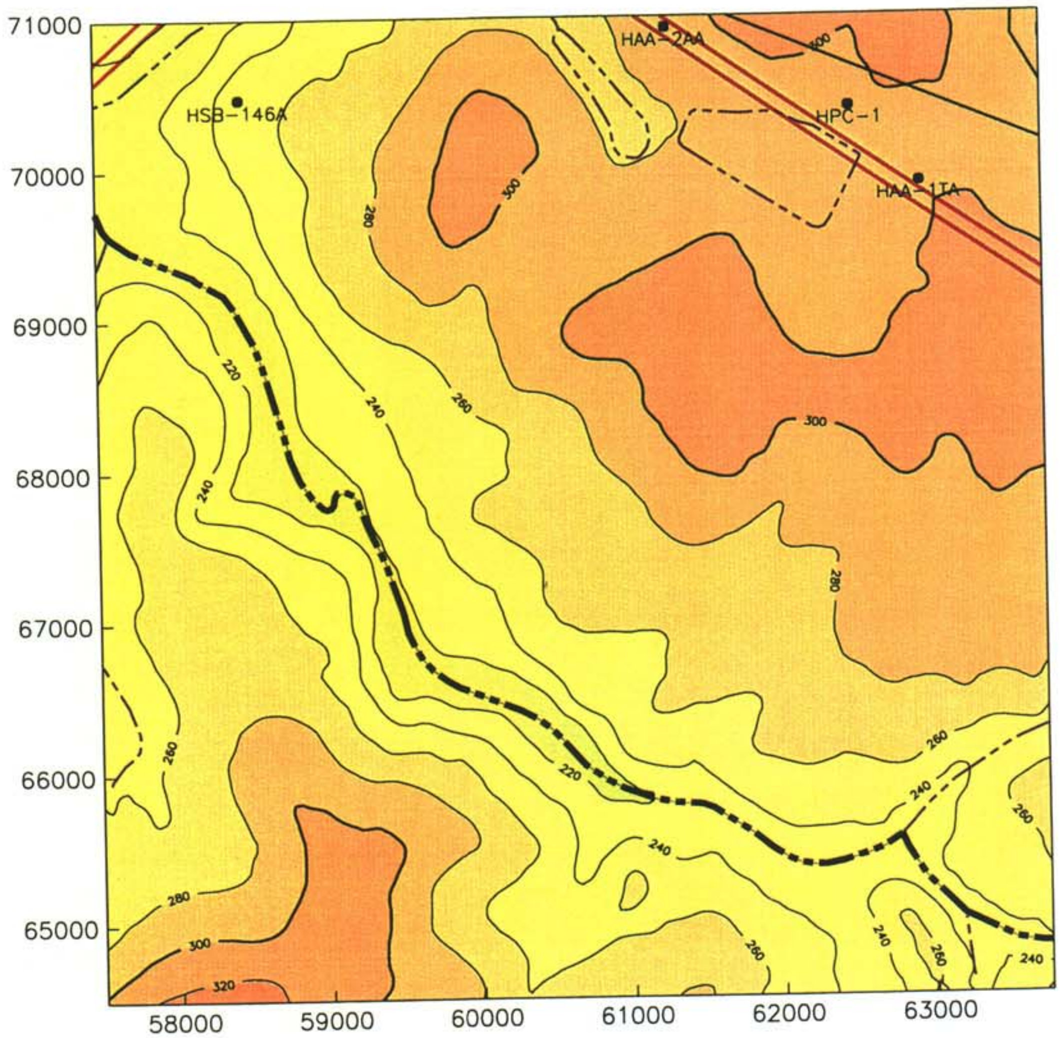

Data Location Map D-1

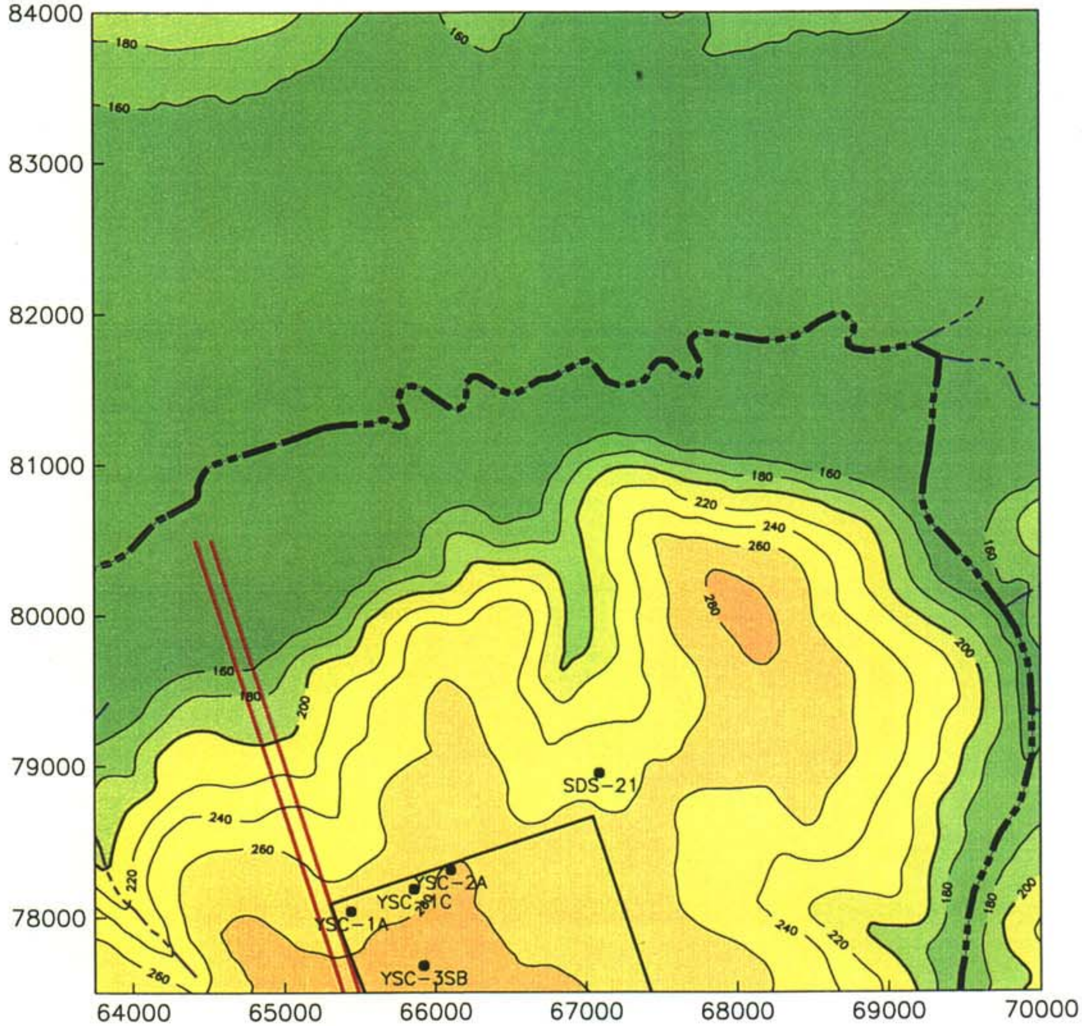

Data Location Map D-2

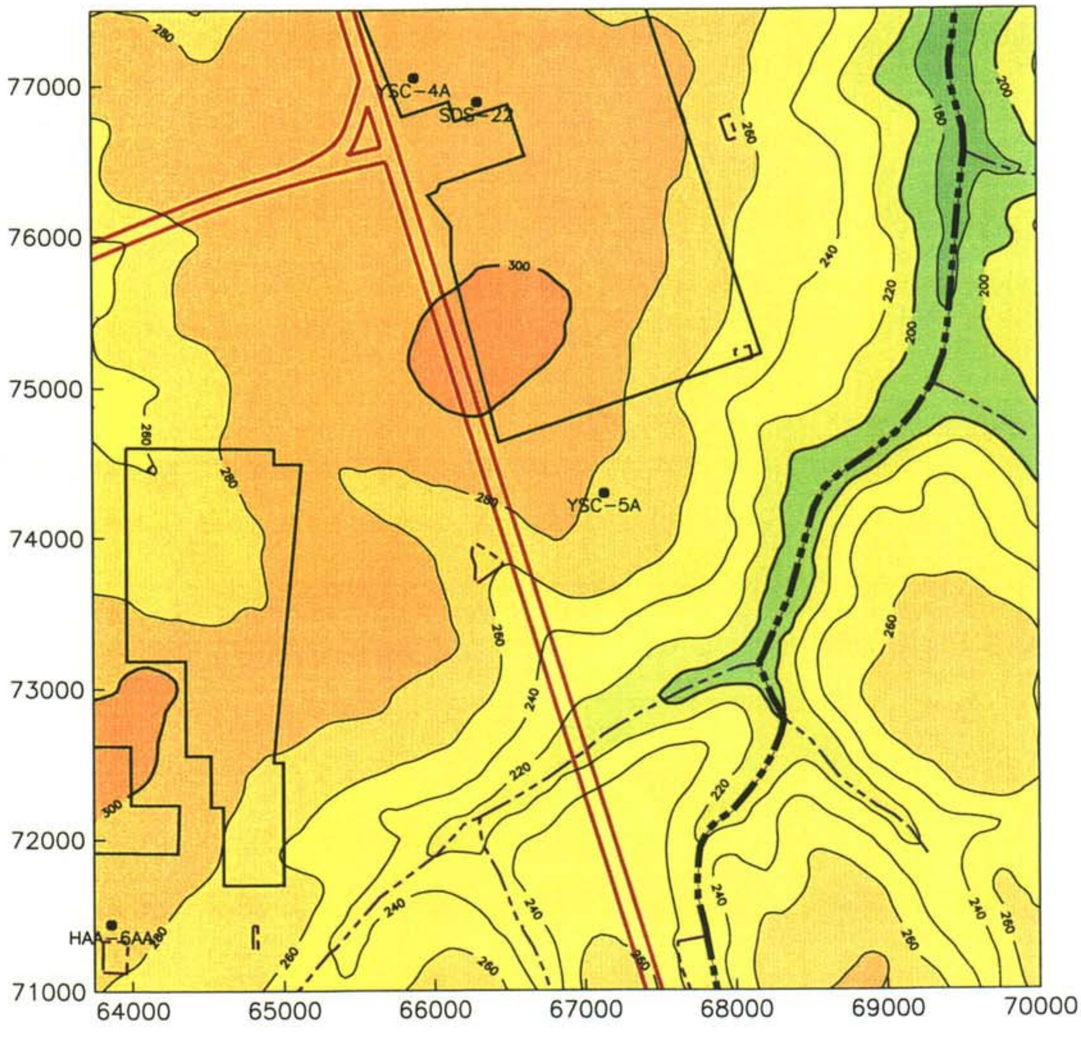

Data Location Map D−3

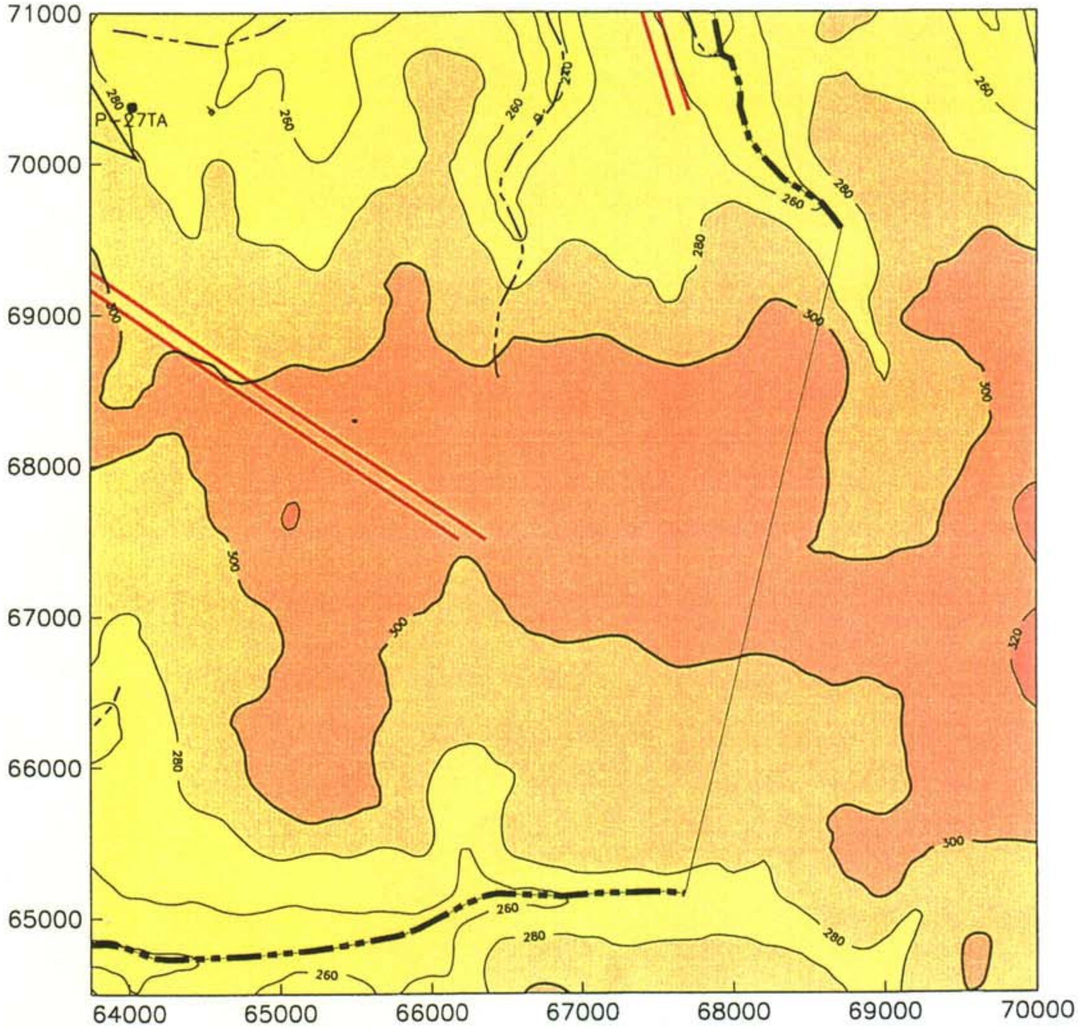

Appendix A-2

Lithostratigraphic Boundaries

(This page intentionally left blank)

Well ID	SRS Easting	SRS Northing	Surface Elevation	Barnwell		Santee		Congaree		Ellenton	
				Elev. (ft msl)	Depth (ft bgl)	Elev. (ft msl)	Depth (ft bgl)	Elev. (ft msl)	Depth (ft bgl)	Elev. (ft msl)	Depth (ft bgl)
BGO-10AA	56990.54	76997.88	298.80	271	28	168	131	120	179		
BGO-12A	56250.68	76804.63	311.40	273	38	164	147	130	181		
BGO-14A	55838.32	76377.54	300.20	280	21	180	120	130	171		
BGO-16A	56194.15	75756.95	302.80	297	6	161	142	126	177		
BGO-18A	56699.67	75599.89	292.90			160	133	125	168		
BGO-20AA	57114.81	74953.76	280.88			173	108	114	167	45	236
BGO-25A	55668.08	76158.50	294.70	278	17	177	118	128	167		
BGO-26A	55014.20	76144.60	285.10	253	33	178	108	128	158		
BGO-27C	54671.40	75666.30	273.90	254	20	162	112				
BGO-29A	54103.50	75560.00	262.10	246	17	157	106	114	148		
BGO-31C	54816.20	74978.00	271.10	247	25	161	111				
BGO-33C	55681.40	74479.70	277.40	252	25	164	113				
BGO-39A	57821.93	73572.52	293.70	278	16	153	141	104	190	37	257
BGO-3A	58806.84	75561.71	288.20	274	15	158	131	121	167	44	244
BGO-41A	55403.69	76469.52	298.30	275	23	169	130	117	181		
BGO-42C	55522.27	76404.71	295.90	273	23						
BGO-43AA	56268.64	77066.01	312.20	277	36	162	150	121	191		
BGO-44AA	57880.51	76757.02	283.30	248	35	160	123	120	163		
BGO-45A	54550.14	75830.03	276.90	252	25	171	106	126	151		
BGO-46B	54444.65	75012.10	263.40			153	110	123	140		
BGO-47A	54914.04	74728.83	264.80			153	112	123	142		
BGO-48C	55124.38	74599.64	274.70	253	22	168	107				
BGO-49A	56205.08	73902.78	269.10	247	22	152	118	105	164		
BGO-50A	54179.77	75201.16	253.50			157	97	115	139		
BGO-51AA	57867.00	74113.10	287.20	262	25	158	130	105	182	42	245
BGO-52AA	57201.60	74617.30	281.60			151	131	115	167	31	251
BGO-53AA	55429.22	76068.96	288.90	278	11	183	106	132	157	30	259
BGO-6B	58346.46	76553.24	284.50	273	12	162	123	128	157		
BGO-8A	57618.30	76569.00	281.30	265	16	180	101	120	161		
BGO-9AA	57371.94	76975.69	282.80	251	32	179	104	119	164		
BGT-11	59697.70	79566.90	222.50			183	40	145	78	68	155
BGT-18	58416.50	79965.30	216.50			178	39	147	70	70	147
BGT-20	58549.60	80956.40	159.50							76	84
BGT-22	56970.30	77860.30	281.00	270	12	182	99	115	166	49	232
BGT-28	57108.10	80777.20	258.30			177	82	134	124	77	181
BGT-3	60045.90	77197.60	275.70			175	101	140	136		
BGT-47	54986.57	77051.85	317.32	262	55	170	147	127	190		
BGT-5	60924.10	77677.60	225.70			179	47	146	80	71	155
BGT-53	53422.04	75837.68	278.25	254	24	153	125	109	169	33	246
BGT-61	58490.09	72911.77	284.30	266	19	145	139	100	184		
BGT-67	60426.74	74443.06	242.30			163	80	128	115	50	192
BGT-9	59316.70	78642.30	226.00			175	51	138	88	64	163

Well ID	SRS Easting	SRS Northing	Surface Elevation	Barnwell		Santee		Congaree		Ellenton	
				Elev. (ft msl)	Depth (ft bgl)	Elev. (ft msl)	Depth (ft bgl)	Elev. (ft msl)	Depth (ft bgl)	Elev. (ft msl)	Depth (ft bgl)
BGX-11D	59581.40	75300.70	273.80			156	118	117	157		
BGX-1A	58590.35	76831.89	289.10	256	33	166	124	127	163		
BGX-2B	58256.50	77203.40	289.20	242	48	167	123	125	164		
BGX-4A	57215.60	77879.20	288.80	258	31	166	123	118	171		
BGX-7D	58312.80	78349.30	277.10	253	24	183	94	144	134		
BGX-9D	59522.10	76936.00	277.40	249	28	170	107	130	147		
BH-1	64590.00	76000.00	283.30							83	200
BH-10	65000.00	74000.00	286.10							57	229
BH-11	65199.00	74301.00	285.00							68	217
BH-12	65998.00	74001.00	271.20							72	200
BH-13	64002.00	72999.00	305.20							18	288
BH-14	65018.00	72993.00	285.50							20	266
BH-15	66008.00	72992.00	268.10							62	207
BH-16	64592.00	72504.00	285.70							49	237
BH-2	64000.00	74999.00	260.90							73	188
BH-20A	65175.00	75025.00	283.50							75	209
BH-24	64600.00	73693.00	275.10							42	234
BH-3	64601.00	75003.00	276.40							61	216
BH-38	64590.00	74745.00	277.10							57	220
BH-4	65305.00	75106.00	283.90							75	209
BH-5	66001.00	75001.00	295.00							69	226
BH-50A	65790.00	74590.00	283.10							70	213
BH-6	64586.00	74500.00	276.50							58	219
BH-63B	65640.00	74459.00	278.40							72	206
BH-64A	65790.00	74405.00	276.60							77	200
BH-7	63015.00	73995.00	285.90							26	260
BH-72	65502.00	74332.00	275.50							68	208
BH-8	63995.00	73994.00	272.30							61	211
BH-9	64601.00	74011.00	273.20							37	237
BH-90A	64591.00	73851.00	275.30							27	249
BPC-1	42023.04	86417.06	281.50	262	20	195	87	153	129	37	245
BRR-1D	50588.20	77365.20	293.80	259	35						
BRR-3D	50203.50	77398.30	289.50	260	30						
BRR-6B	51100.00	77054.60	293.90	270	24	140	154	113	181		
BRR-7B	50707.50	77575.40	289.60	273	17	158	132	122	168		
BRR-8B	50116.50	77634.70	276.70	272	5	159	118	127	150		
CPC-1	47183.78	66855.77	285.10	229	57	94	191	65	220	-9	294
FAC-1SB	55243.00	78138.00	312.00	281	31	177	135				
FC-3A	57620.00	78726.60	269.50							42	228
FC-4A	53896.50	82242.50	239.00							73	166
FC-5A	54671.70	87988.10	204.40							91	114
FCH-1	52843.11	79488.82	316.80	291	26	163	154	129	188	65	252
FCH-2	52599.59	78500.00	288.70	276	13	164	125	130	159	63	226

Well ID	SRS Easting	SRS Northing	Surface Elevation	Barnwell		Santee		Congaree		Ellenton	
				Elev. (ft msl)	Depth (ft bgl)	Elev. (ft msl)	Depth (ft bgl)	Elev. (ft msl)	Depth (ft bgl)	Elev. (ft msl)	Depth (ft bgl)
FCH-3	52087.22	78059.22	307.20	269	39	156	151	131	176	52	256
FCH-4	52021.03	77514.56	297.50	264	34	153	145	122	176	45	253
FCH-5	51667.65	76992.12	284.20	250	34	163	122	125	159	36	248
FCH-6	51245.70	76410.33	291.50	244	48	155	137	121	171	29	263
FIW-1MC	51354.40	76165.30	293.30	276	17	153	140				
FIW-2MA	51184.50	75930.80	290.50	267	24	153	138	117	174		
FNB-1A	54288.80	80154.50	282.40			175	107	113	169		
FNB-3A	54116.60	80557.20	282.20			169	113				
FSB-100A	50958.40	75534.40	283.80	261	23	150	134	114	170		
FSB-101A	51191.30	75719.00	282.90	263	20	143	140	116	167		
FSB-112A	48809.10	74231.40	227.00			131	96	101	126		
FSB-113A	51068.10	74167.50	221.30			142	80	107	114	22	199
FSB-114A	52046.60	75297.40	250.00			148	102	110	140		
FSB-115C	49736.00	72515.50	205.80			140	66	88	118	9	197
FSB-120A	49175.70	75538.90	278.00	235	43	139	139	111	168		
FSB-1TA	51658.30	75649.10	275.40	260	16	147	128	114	161	26	249
FSB-76A	51391.60	76131.90	291.50	276	16	145	147	117	175		
FSB-78A	50172.80	74757.70	270.50	228	43						
FSB-79A	50149.60	73664.50	216.10			134	83	100	117	18	198
FSB-87A	50115.80	75601.70	285.60	255	31	135	151	107	179		
FSB-96A	49778.70	74882.20	277.70	234	44	143	135	106	172		
FSB-97A	49965.70	75171.20	283.80	248	36	144	140	107	177		
FSB-98A	50121.60	75389.80	280.70	242	39	135	146	106	175		
FSB-99A	50314.80	75675.60	285.30	247	38	137	148	110	176		
FSB-PC	50140.00	74090.20	230.80			129	102				
HAA-1TA	62953.30	69892.20	290.20	245	45	150	140	110	181	-13	303
HAA-2AA	61285.10	70925.40	291.40	272	20	157	134	119	172	30	262
HAA-3AA	60201.90	71488.00	274.50	247	28	155	120	111	164	25	250
HAA-4AA	61929.60	72223.20	299.20	247	52	156	143	119	180		
HAA-6AA	63860.20	71441.00	279.80	259	21	153	127	120	160	20	260
HC-10A	61593.40	75806.70	228.00			161	68	119	109		
HC-11A	62147.00	74519.00	263.80			165	99				
HC-12A	59504.00	73187.00	287.30			154	133				
HC-13A	63610.00	73394.00	291.30	276	16	158	133				
HC-14A	60658.00	67560.00	268.50			156	113	108	161		
HC-16A	65462.00	72596.00	262.60			161	102	127	136		
HC-17A	61700.00	73200.00	294.00	263	31	154	141				
HC-18A	63409.00	71560.00	293.00	276	17	149	144				
HC-1A	61867.00	71755.00	299.50			155	145	119	181		
HC-2A	61866.00	71794.00	298.70	282	17	161	138	118	181		
HC-35D	58548.00	71918.00	253.80			148	106	111	143		
HC-3A	62266.00	71742.00	300.60	285	16	158	143	115	186		
HC-4A	63409.00	71606.00	293.00	273	20	149	144				

Well ID	SRS Easting	SRS Northing	Surface Elevation	Barnwell		Santee		Congaree		Ellenton	
				Elev. (ft msl)	Depth (ft bgl)	Elev. (ft msl)	Depth (ft bgl)	Elev. (ft msl)	Depth (ft bgl)	Elev. (ft msl)	Depth (ft bgl)
HC-5A	61710.00	73265.00	294.00	275	19	155	139				
HC-7A	66992.00	74352.00	277.00			178	99				
HC-8A	60058.50	77481.80	262.30			185	77	140	122	74	188
HC-9A	64084.00	75135.00	269.30			164	105	130	139		
HCA-4AA	62942.50	72513.70	308.60	291	18	150	159	116	193		
HCH-1	60923.42	72796.39	284.00	267	17	170	115	127	158	48	237
HCH-2	60091.79	72519.61	270.90	231	40	166	105	122	149	50	221
HCH-3	59917.33	71998.82	264.00			155	109	123	141	26	238
HCH-4	59139.93	72449.59	269.90			153	117	115	155		
HCH-5	59331.53	71810.36	255.00			158	98	119	136	14	242
HIW-2A	56753.00	73249.70	276.30	257	19	144	133	109	168		
HIW-2MC	56698.40	73226.40	269.00	254	15	145	124				
HIW-4MC	56570.10	73160.10	263.40	246	17	141	123				
HIW-5MC	56498.90	73557.90	266.10			142	124				
HMD-1C	56973.30	78731.70	262.70	240	23	175	88	124	139		
HMD-2C	57269.70	79665.80	259.30	235	24	185	75	137	122		
HMD-3C	57745.20	79578.70	257.50	240	18	178	80	148	110		
HMD-4C	58188.50	79160.40	248.50	234	15	176	73	141	108		
HPC-1	62493.60	70395.40	293.50	239	55	148	146	108	186	-7	300
HPT-1A	60587.00	74847.10	232.90			153	80	115	118	53	180
HPT-2A	60200.50	75061.80	257.80	249	9	157	101	117	141		
HSB-117A	55170.10	72733.60	234.80			138	97	118	117		
HSB-118A	55775.60	72696.40	245.00	227	18	147	99	104	142		
HSB-119A	56100.20	73082.50	254.80			142	113	111	144		
HSB-120A	56431.90	73395.10	266.00			140	126	109	157		
HSB-121A	57389.60	72024.80	272.30			148	124	106	167		
HSB-122A	57747.40	72195.90	269.40			150	119	104	165		
HSB-123A	58124.80	72189.80	263.60	253	11	161	103	110	154		
HSB-124A	58514.60	72199.60	263.90			148	116	110	154		
HSB-139A	57365.40	71127.40	231.50			160	72	114	118		
HSB-140A	56535.40	70050.30	234.00	223	11	142	93	105	130		
HSB-141A	59168.70	71213.60	252.60			149	104	113	140		
HSB-144A	56200.50	71892.10	233.60			141	93	103	131		
HSB-145C	57769.00	71098.90	233.70			159	75				
HSB-146A	58454.00	70478.90	249.50			148	102	112	138		
HSB-65A	58436.00	72436.20	270.70	255	16	161	110	111	160	35	236
HSB-68A	56892.10	71526.90	247.40	230	17	157	90	110	137	24	223
HSB-69A	56465.10	71549.40	234.10			148	86	109	125		
HSB-83A	58606.10	71648.60	234.90	209	26	142	93	106	129		
HSB-84A	56359.10	71586.20	226.70			145	82	110	117		
HSB-85A	58943.40	73791.90	292.10	274	18	162	130	118	174		
HSB-86A	55985.90	72520.20	260.00			142	118	108	152		
HSB-PC	55650.03	72119.31	227.80			142	86				

Well ID	SRS Easting	SRS Northing	Surface Elevation	Barnwell		Santee		Congaree		Ellenton	
				Elev. (ft msl)	Depth (ft bgl)	Elev. (ft msl)	Depth (ft bgl)	Elev. (ft msl)	Depth (ft bgl)	Elev. (ft msl)	Depth (ft bgl)
HSB-TB	58696.10	72394.00	267.10			160	107	108	159	35	232
HSL-6AA	60555.70	72692.60	274.60	240	35	160	115	121	154		
HSL-8AA	61113.80	72729.40	286.70	260	27	170	117	125	162	47	240
IDB-2A	75391.13	77284.38	301.79	288	14	195	107	137	165	-14	316
IDP-3A	37781.10	85104.30	282.20			180	102	140	142	36	247
LWR-9SB	45406.62	71658.83	238.20	226	13	139	99	109	129	12	226
MWD-1A	75121.90	69592.80	327.50	268	60	162	166	129	199	41	287
NPN-1A	70856.20	66632.10	335.90	320	16	174	162	103	233	2	334
OFS-1SB	54032.60	74967.50	261.60			146	116	123	139		
OFS-2SB	53848.00	74671.00	257.50	222	36	152	106	121	137		
OFS-3SB	54579.00	74270.00	258.10			165	93	119	139		
OFS-4SB	55188.00	73874.00	258.70			147	112	121	138		
OFS-5SB	54298.00	73623.00	228.70			136	93	118	111		
P-14TA	76439.60	72444.90	294.40			166	128	126	168	26	269
P-18TA	47652.70	67578.50	296.90	280	17	127	170	88	209	-2	299
P-27TA	64022.90	70382.00	274.10	260	15	158	116	127	148	48	226
P-28TA	55441.10	79284.30	285.60			169	117	134	152	63	223
SDS-21	67087.00	78951.00	251.00			191	61	147	105		
SDS-22	66304.00	76887.00	283.00	270	13	183	100				
SSW-3	40532.31	70517.63	178.70			123	56	88	91	7	172
YSC-1A	65438.93	78039.90	268.90	251	18	189	80	147	122	69	200
YSC-1C	65855.46	78186.24	272.50	254	19	185	88				
YSC-2A	66100.08	78311.53	281.70	259	23	192	90	150	132	53	229
YSC-3SB	65920.00	77680.00	277.00	250	27	187	90	138	140	55	222
YSC-4A	65883.50	77050.08	287.50	249	39	187	101	140	148	66	222
YSC-5A	67134.90	74295.90	273.00	246	28	175	98	128	145		
ZBG-1	65584.10	76584.20	288.90	272	17						
ZBG-2	67472.90	76170.50	275.80	266	10						

(This page intentionally left blank)

Appendix A-3

Hydrostratigraphic Boundaries

(This page intentionally left blank)

Well ID	SRS Easting	SRS Northing	Surface Elevatio n	TCCZ		LAZ		GCU		GAU		MBCS	
				Elev. (ft msl)	Depth (ft bgl)	Elev. (ft msl)	Depth (ft bgl)	Elev. (ft msl)	Depth (ft bgl)	Elev. (ft msl)	Depth (ft bgl)	Elev. (ft msl)	Depth (ft bgl)
BGO-10A	57050.92	76805.18	299.10	209	90	207	92	131	168	124	175		
BGO-10A	56990.54	76997.88	298.80	219	80	207	92	130	169	126	173		
BGO-12A	56250.68	76804.63	311.40	199	112	186	125	137	174	132	179		
BGO-14A	55838.32	76377.54	300.20	220	80	212	88	133	167	127	173		
BGO-16A	56194.15	75756.95	302.80	196	107	183	120	131	172	126	177		
BGO-18A	56699.67	75599.89	292.90	194	99	199	94	131	162	126	167		
BGO-20A	57114.81	74953.76	280.88	206	75	194	87	125	156	114	167	43	238
BGO-25A	55668.08	76158.50	294.70	212	83	201	94	138	157	128	167		
BGO-26A	55014.20	76144.60	285.10	219	66	205	80	133	152	129	156		
BGO-27C	54671.40	75666.30	273.90	199	75	192	82						
BGO-29A	54103.50	75560.00	262.10	196	66	185	77	124	138	113	149		
BGO-31C	54816.20	74978.00	271.10	198	73	188	83						
BGO-33C	55681.40	74479.70	277.40	200	77	191	86						
BGO-35C	56545.70	73953.90	271.40	204	67	197	74						
BGO-37C	57279.20	73498.20	284.30	199	85	191	93						
BGO-39A	57821.93	73572.52	293.70	204	90	202	92	113	181	102	192	29	265
BGO-3A	58806.84	75561.71	288.20	197	91	188	100	130	158	121	167	40	248
BGO-41A	55403.69	76469.52	298.30	217	81	208	90	138	160	131	167		
BGO-42C	55522.27	76404.71	295.90	216	80	209	87						
BGO-43A	56268.64	77066.01	312.20	195	117	187	125	135	177	127	185		
BGO-44A	57880.51	76757.02	283.30	222	61	199	84	131	152	120	163		
BGO-45A	54550.14	75830.03	276.90	207	70	201	76	134	143	130	147		
BGO-46B	54444.65	75012.10	263.40	199	64	193	70	128	135	126	137		
BGO-47A	54914.04	74728.83	264.80	198	67	190	75	131	134	125	140		
BGO-48C	55124.38	74599.64	274.70	198	77	192	83						
BGO-49A	56205.08	73902.78	269.10	201	68	192	77	119	150	115	154		
BGO-50A	54179.77	75201.16	253.50	194	60	184	70	133	121	129	125		
BGO-51A	57867.00	74113.10	287.20	205	82	194	93	107	180	93	194	32	255
BGO-52A	57201.60	74617.30	281.60	207	75	197	85	125	157	116	166	18	264
BGO-53A	55429.22	76068.96	288.90	223	66	216	73	138	151	132	157	29	260
BGO-5C	58794.50	76476.90	294.20	218	76	201	93						
BGO-6A	58316.80	76487.20	283.80	210	74	195	89	121	163	120	164		
BGO-6B	58346.46	76553.24	284.50	203	82	192	93	137	148	123	162		
BGO-8A	57618.30	76569.00	281.30	213	68	199	82	130	151	120	161		
BGO-9AA	57371.94	76975.69	282.80	224	59	211	72	135	148	125	158		
BGT-1	59178.40	76700.60	282.90	222	61	208	75						
BGT-10	59507.20	79104.60	215.20	201	14	194	21	156	59	147	68		
BGT-11	59697.70	79566.90	222.50					151	72	146	77	68	155
BGT-12	58045.90	77291.20	284.20	225	59	214	70						
BGT-13	58074.00	77488.90	287.80	224	64	216	72						
BGT-14	58143.40	77984.00	280.70	215	66	209	72						
BGT-15	58212.80	78479.20	277.50	209	69	201	77	150	128				
BGT-16	58283.50	78974.10	250.70					151	100				
BGT-17	58350.00	79469.70	240.70					150	91				
BGT-18	58416.50	79965.30	216.50					162	55	147	70	55	162
BGT-2	59607.20	76957.60	276.40	213	63	198	78						
BGT-20	58549.60	80956.40	159.50					151	9	140	20	70	90
BGT-21	56952.50	77280.70	294.20	223	71	216	78						
BGT-22	56970.30	77860.30	281.00	231	50	216	65	126	155	114	167	53	228
BGT-23	56997.00	78279.70	270.00	216	54	210	60						

Well ID	SRS Easting	SRS Northing	Surface Elevation	TCCZ		LAZ		GCU		GAU		MBCS	
				Elev. (ft msl)	Depth (ft bgl)	Elev. (ft msl)	Depth (ft bgl)	Elev. (ft msl)	Depth (ft bgl)	Elev. (ft msl)	Depth (ft bgl)	Elev. (ft msl)	Depth (ft bgl)
BGT-24	57019.20	78779.20	265.80	227	39	220	46						
BGT-25	57041.40	79278.70	264.80	229	36	224	41						
BGT-27	57085.90	80277.70	256.90	217	40	207	50	152	105				
BGT-28	57108.10	80777.20	258.30	216	42	194	64	156	102	150	108	48	210
BGT-29	57130.40	81276.70	243.00	219	24	215	28						
BGT-3	60045.90	77197.60	275.70	212	64	198	78	143	133	141	135	65	211
BGT-30	57150.40	81726.30	219.00					147	72	141	78		
BGT-31	56189.75	77228.97	308.76	220	89	215	94						
BGT-32	56121.10	77791.41	310.12	237	73	234	76						
BGT-33	56037.17	78404.46	290.42	239	51	223	67						
BGT-34	56027.45	78803.92	286.76	228	59	218	69						
BGT-35	55929.89	79305.84	267.73	217	51	212	56						
BGT-36	55867.47	79801.93	261.36	226	35	215	46	148	113				
BGT-37	55805.00	80298.03	251.60	222	30	215	37	133	119				
BGT-4	60484.50	77437.60	259.20	213	46	204	55	149	110				
BGT-40	55644.42	77297.15	332.32	209	123	203	129						
BGT-41	55490.12	77734.75	328.37	224	104	219	109	149	179	142	186		
BGT-42	55313.07	78240.66	310.92	224	87	219	92						
BGT-43	54816.04	79655.92	277.08	205	72	201	76						
BGT-44	54650.36	80127.67	276.20	214	62	209	67						
BGT-45	54533.05	80461.74	285.28	218	67	209	76	150	135				
BGT-46	55354.96	76714.30	310.00	213	97	205	105	134	176	125	185		
BGT-47	54986.57	77051.85	317.32	214	103	210	107	137	180	128	189		
BGT-48	54895.09	77135.74	314.33	217	97	209	105						
BGT-49	54946.30	76203.90	297.26	222	75	214	83	135	162	126	171		
BGT-5	60924.10	77677.60	225.70	214	12	206	20	154	72	146	80	72	154
BGT-50	54756.20	76359.30	296.27	221	75	214	82	132	164	124	172		
BGT-51	54505.65	75519.81	272.64	193	80	186	87						
BGT-53	53422.04	75837.68	278.25	200	78	191	87	120	158	109	169	32	246
BGT-54	52889.14	75941.66	279.96	205	75	196	84						
BGT-56	56265.77	73521.24	262.94	182	81	175	88						
BGT-57	56104.24	73268.51	259.35	179	80	169	90						
BGT-58	57399.60	73406.90	285.76	192	94	190	96	112	174	103	183		
BGT-59	57123.20	72802.60	281.88	182	100	173	109						
BGT-6	58746.70	77254.80	282.20	218	64								
BGT-60	58057.22	73120.63	291.42	186	105	176	115						
BGT-61	58490.09	72911.77	284.30	184	100	178	106	108	176	101	183		
BGT-62	58609.00	72854.40	282.03	190	92	176	106						
BGT-63	59146.34	73319.43	293.67	195	99	189	105						
BGT-63A	58768.10	73646.40	290.79	198	93	194	97						
BGT-64	59499.95	73013.74	283.25	195	88	188	95	123	160				
BGT-66	60033.67	74476.55	244.04	195	49	188	56						
BGT-67	60426.74	74443.06	242.30	186	57	174	69	135	107	128	115	27	215
BGT-7	58935.70	77717.80	276.40	212	64	199	77						
BGT-8	59118.60	78161.50	249.30	221	28	217	32	149	100				
BGT-9	59316.70	78642.30	226.00	210	16	205	21	149	77	141	85	64	162
BGX-11D	59581.40	75300.70	273.80	193	81	177	97	126	148	117	157		
BGX-1A	58590.35	76831.89	289.10	211	78	198	91	132	157	127	162		
BGX-2B	58256.50	77203.40	289.20	216	73	198	91	140	149	127	162		
BGX-4A	57215.60	77879.20	288.80	225	64	213	76	130	159	124	165		

Well ID	SRS Easting	SRS Northing	Surface Elevation	TCCZ		LAZ		GCU		GAU		MBCS	
				Elev. (ft msl)	Depth (ft bgl)	Elev. (ft msl)	Depth (ft bgl)	Elev. (ft msl)	Depth (ft bgl)	Elev. (ft msl)	Depth (ft bgl)	Elev. (ft msl)	Depth (ft bgl)
BGX-7D	58312.80	78349.30	277.10	225	52	220	57	157	120	144	133		
BGX-9D	59522.10	76936.00	277.40	207	70	202	75	139	138	131	146		
BPC-1	42023.04	86417.06	281.50	193	89	186	96	155	127	151	131	37	245
BRR-1D	50588.20	77365.20	293.80	195	99								
BRR-3D	50203.50	77398.30	289.50	208	82	194	96						
BRR-6B	51100.00	77054.60	293.90	178	116	166	128	123	171	108	186		
BRR-7B	50707.50	77575.40	289.60	202	88	190	100	135	155	122	168		
BRR-8B	50116.50	77634.70	276.70	205	72	200	77	131	146	126	151		
CPC-1	47183.78	66855.77	285.10	166	120	156	129	96	190	87	199	-8	294
FAC-1SB	55243.00	78138.00	312.00	224	88	217	95	149	163				
FCH-1	52843.11	79488.82	316.80	214	103	202	115	142	175	126	191	67	250
FCH-2	52599.59	78500.00	288.70	213	76	197	92	142	147	130	159	58	231
FCH-3	52087.22	78059.22	307.20	207	100	196	111	140	167	131	176	59	248
FCH-4	52021.03	77514.56	297.50	197	101	187	111	128	170	121	177	42	256
FCH-5	51667.65	76992.12	284.20	196	88	191	93	129	155	128	156	36	248
FCH-6	51245.70	76410.33	291.50	189	103	182	110	124	168	121	171	25	267
FIW-1MC	51354.40	76165.30	293.30	190	103	185	108	121	172				
FIW-2MA	51184.50	75930.80	290.50	189	102	180	111	121	170	117	174		
FNB-1A	54288.80	80154.50	282.40	208	74	202	80	151	131	138	145		
FNB-3A	54116.60	80557.20	282.20	211	71	208	75	146	136	140	142		
FSB-100A	50958.40	75534.40	283.80	185	99	183	101	118	166	114	170		
FSB-101A	51191.30	75719.00	282.90	191	92	183	100	119	164	116	167		
FSB-112A	48809.10	74231.40	227.00	164	63	144	83	103	124	98	129		
FSB-113A	51068.10	74167.50	221.30	178	43	171	50	109	112	104	117	22	199
FSB-114A	52046.60	75297.40	250.00	178	72	173	77	114	136	110	140		
FSB-115C	49736.00	72515.50	205.80	181	25	165	41	101	105	86	120	6	200
FSB-116C	50645.90	72725.50	200.50	176	25	171	30						
FSB-120A	49175.70	75538.90	278.00	181	97	165	113	112	166	110	168		
FSB-121C	48413.10	75155.70	254.40	173	81	162	92						
FSB-122C	48195.00	73881.80	216.00	164	52	148	68	104	112				
FSB-123C	51750.50	74566.70	236.30	183	53	172	64						
FSB-1TA	51658.30	75649.10	275.40	191	84	187	88	117	158	115	160	24	251
FSB-76A	51391.60	76131.90	291.50					121	171	117	175		
FSB-78A	50172.80	74757.70	270.50	163	108	147	124	105	166	100	171		
FSB-79A	50149.60	73664.50	216.10	173	43	164	52	103	113	100	116	18	198
FSB-87A	50115.80	75601.70	285.60	176	110	173	113	115	171	109	177		
FSB-89C	51345.20	75553.20	279.10	186	93	180	99						
FSB-91C	50953.50	75213.30	277.00	168	109	161	116						
FSB-93C	50458.30	74897.30	274.00	166	108	151	123						
FSB-95C	50016.70	74971.70	281.80	174	108	158	124						
FSB-96A	49778.70	74882.20	277.70	167	111	154	124	109	169	101	177		
FSB-97A	49965.70	75171.20	283.80	163	121	152	132	111	173	107	177		
FSB-98A	50121.60	75389.80	280.70	172	109	160	121	109	172	107	174		
FSB-99A	50314.80	75675.60	285.30	178	107	173	112	115	170	112	173		
FSB-PC	50140.00	74090.20	230.80	161	70	157	74						
HAA-1TA	62953.30	69892.20	290.20	208	83	204	86	117	173	110	181	-12	303
HAA-2AA	61285.10	70925.40	291.40	190	102	186	106	125	167	119	173	30	262
HAA-3AA	60201.90	71488.00	274.50	191	84	179	96	128	147	123	152	10	265
HAA-4AA	61929.60	72223.20	299.20	202	97	194	106	125	175	119	181		
HAA-6AA	63860.20	71441.00	279.80	210	70	183	97	125	155	120	160	23	257

Well ID	SRS Easting	SRS Northing	Surface Elevation	TCCZ		LAZ		GCU		GAU		MBCS	
				Elev. (ft msl)	Depth (ft bgl)	Elev. (ft msl)	Depth (ft bgl)	Elev. (ft msl)	Depth (ft bgl)	Elev. (ft msl)	Depth (ft bgl)	Elev. (ft msl)	Depth (ft bgl)
HC-12A	59504.00	73187.00	287.30	195	92	190	97						
HCA-4AA	62942.50	72513.70	308.60	234	75	230	79	124	185	117	192		
HCH-1	60923.42	72796.39	284.00	202	82	187	97	135	149	126	158	18	266
HCH-2	60091.79	72519.61	270.90	196	75	180	91	131	140	123	148	0	271
HCH-3	59917.33	71998.82	264.00	197	67	179	85	130	134	123	141		
HCH-4	59139.93	72449.59	269.90	193	77	183	87	123	147	114	156		
HCH-5	59331.53	71810.36	255.00	192	63	180	75	123	132	119	136	-10	265
HIW-1BD	58342.20	72564.60	275.80	205	71								
HIW-1MC	58471.80	72500.00	272.30	187	86	180	93						
HIW-2A	56753.00	73249.70	276.30	202	75	195	81	116	160	110	166		
HIW-2MC	56698.40	73226.40	269.00	199	70	194	76						
HIW-4MC	56570.10	73160.10	263.40	197	66	190	73	112	151				
HIW-5MC	56498.90	73557.90	266.10	184	82	178	88						
HMD-1C	56973.30	78731.70	262.70	229	34	226	37	139	124	127	136		
HMD-2C	57269.70	79665.80	259.30	222	37	216	43	143	116	138	121		
HMD-3C	57745.20	79578.70	257.50	224	34	219	39	155	103	150	108		
HMD-4C	58188.50	79160.40	248.50	224	25	220	29	153	96	141	108		
HPC-1	62493.60	70395.40	293.50	195	99	188	106	116	178	110	184	28	266
HPT-1A	60587.00	74847.10	232.90					119	114	115	118	53	180
HPT-2A	60200.50	75061.80	257.80					121	137	118	140	57	201
HSB-101C	58604.40	72001.90	256.30	195	61	189	67						
HSB-103C	58323.60	71593.90	245.20	195	50	181	64						
HSB-104C	58082.60	71376.80	245.50	194	52	185	61						
HSB-105C	57883.80	71447.30	247.20	190	57	183	64						
HSB-106C	57651.50	71720.90	250.70	192	59	184	67						
HSB-107C	57432.00	71698.50	259.30	199	60	191	68						
HSB-109C	56895.60	71684.80	259.40	203	56	189	70						
HSB-110C	56680.70	71779.30	253.40	192	61	188	65						
HSB-111C	56501.90	71919.40	253.70	188	66	172	82						
HSB-112C	56417.40	72156.40	252.60	191	62	186	67						
HSB-113C	56160.40	72312.30	258.70	188	71	174	85						
HSB-115C	56043.20	72653.20	266.80	209	58	197	70						
HSB-117A	55170.10	72733.60	234.80	216	19	192	43	123	112	117	118		
HSB-118A	55775.60	72696.40	245.00	183	62	173	72	119	126	114	131		
HSB-119A	56100.20	73082.50	254.80	213	42	195	60	115	140	111	144		
HSB-120A	56431.90	73395.10	266.00	203	63	196	70	112	154	110	156		
HSB-121A	57389.60	72024.80	272.30	197	75	184	88	113	159	109	163		
HSB-122A	57747.40	72195.90	269.40	188	81	177	92	110	159	108	161		
HSB-123A	58124.80	72189.80	263.60	196	68	186	78	114	150	108	156		
HSB-124A	58514.60	72199.60	263.90					118	146				
HSB-132C	58787.70	71472.40	238.30	163	75	158	80						
HSB-139A	57365.40	71127.40	231.50	190	42	179	53	119	113	115	117		
HSB-140A	56535.40	70050.30	234.00	194	40	181	53	111	123	105	129		
HSB-141A	59168.70	71213.60	252.60	181	72	167	86	119	134	113	140		
HSB-143C	52773.20	73738.20	220.10	198	22	179	41						
HSB-144A	56200.50	71892.10	233.60	186	48	179	55	109	125	104	130		
HSB-145C	57769.00	71098.90	233.70	184	50	175	59						
HSB-146A	58454.00	70478.90	249.50	174	76	163	87	119	131	112	138		
HSB-148C	55344.20	70151.50	248.90	187	62	175	74						
HSB-151C	54014.90	72997.90	211.60	193	19	183	29						

Well ID	SRS Easting	SRS Northing	Surface Elevation	TCCZ		LAZ		GCU		GAU		MBCS	
				Elev. (ft msl)	Depth (ft bgl)	Elev. (ft msl)	Depth (ft bgl)	Elev. (ft msl)	Depth (ft bgl)	Elev. (ft msl)	Depth (ft bgl)	Elev. (ft msl)	Depth (ft bgl)
HSB-152C	54346.70	72012.00	212.10	198	14	186	26						
HSB-65A	58436.00	72436.20	270.70	204	67	199	72	119	152	113	158		
HSB-68A	56892.10	71526.90	247.40	198	49	193	54	116	131	110	137		
HSB-69A	56465.10	71549.40	234.10	187	47	181	53	115	119	112	122		
HSB-83A	58606.10	71648.60	234.90	195	40	188	47	114	121	104	131	12	223
HSB-84A	56359.10	71586.20	226.70	205	22	181	46	119	108	111	116		
HSB-85A	58943.40	73791.90	292.10	204	88	200	92	126	166	119	173		
HSB-86A	55985.90	72520.20	260.00	185	75	178	82	112	148	109	151		
HSB-PC	55650.03	72119.31	227.80	188	40	178	50						
HSB-TB	58696.10	72394.00	267.10	207	60	199	68	110	157	106	161	9	258
HSL-6AA	60555.70	72692.60	274.60	174	101	169	106	126	149	121	154	9	266
HSL-8AA	61113.80	72729.40	286.70	193	94	186	101	137	150	129	158	46	241
IDB-2A	75391.13	77284.38	301.79	245	57	228	74	142	160	138	164	-14	316
IDP-3A	37781.10	85104.30	282.20	190	92	182	100	161	121	140	142	36	246
LWR-9SB	45406.62	71658.83	238.20	179	59	161	77	110	128	108	130		
MWD-1A	75121.90	69592.80	327.50	218	110	211	117	133	195	130	198	22	306
NPN-1A	70856.20	66632.10	335.90	235	101	224	112	110	226	105	231	2	334
OFS-1SB	54032.60	74967.50	261.60	196	66	186	76	129	133	126	136		
OFS-2SB	53848.00	74671.00	257.50	198	60	188	70	125	133	121	137		
OFS-3SB	54579.00	74270.00	258.10	196	62	185	73	125	133	120	138		
OFS-4SB	55188.00	73874.00	258.70	196	63	192	67	127	132	122	137		
OFS-5SB	54298.00	73623.00	228.70	189	40	178	51	122	107	117	112		
P-14TA	76439.60	72444.90	294.40	213	81	203	92	139	155	131	163	26	269
P-18TA	47652.70	67578.50	296.90	175	122	167	130	91	206	86	211	-17	314
P-27TA	64022.90	70382.00	274.10	180	94	169	105	129	145	127	147	49	225
P-28TA	55441.10	79284.30	285.60	215	71	211	75	141	145	133	153	64	222
SDS-21	67087.00	78951.00	251.00	205	47	199	53	163	89	148	104		
SDS-22	66304.00	76887.00	283.00	191	93	188	96	149	134	138	145		
SSW-3	40532.31	70517.63	178.70	139	40	134	45	89	90	84	95		
YSC-1A	65438.93	78039.90	268.90	210	59	199	70	159	110	154	115	69	200
YSC-1C	65855.46	78186.24	272.50	215	58	213	60	164	109	157	116		
YSC-2A	66100.08	78311.53	281.70	220	62	215	67	162	120	151	131		
YSC-3SB	65920.00	77680.00	277.00	211	66	205	72	149	128	140	137		
YSC-4A	65883.50	77050.08	287.50	223	65	214	74	160	128	145	143	87	201
YSC-5A	67134.90	74295.90	273.00	221	52	209	64	136	137	128	145		

Notes:

TCCZ - "tan clay" confining zone

LAZ - "lower" aquifer zone

GCU - Gordon confining unit

GAU - Gordon aquifer unit

MBCS - Meyers Branch confining system

(This page intentionally left blank)

APPENDIX B

LITHOLOGIC DATA

(This page intentionally left blank)

Appendix B-1 Sediment Types Recorded in Core Descriptions

	Abbreviation	Lithology
Sand	BLSD	Sand with biomoldic limestone
	CASD	calcarenaceous Sand
	CACLSD	calcarenaceous, clayey Sand
	CLSD	clayey Sand
	MCCLSD	micritic, clayey Sand
	MCSD	micritic Sand
	PB	Gravel
	PBSD	gravelly Sand
	SD	Sand
	SDPB	sandy Gravel
	SLCLSD	shelly, clayey Sand
	SLSD	shelly, siliciclastic Sand
	STSD	silty Sand
Mud	CACL	calcarenaceous Clay
	CASDCL	calcarenaceous, sandy Clay
	CL/ST/STCL	Clay (mud-sized material)
	MCCL	micritic Clay
	MCSDCL	micritic, sandy Clay
	PBCL	gravelly Clay
	SDCL/SDST	sandy Clay/sandy Silt
	SLCL	shelly Clay
	SLSDCL	shelly, sandy Clay
Limestone	BL	Biomoldic Limestone
(Carbonate >49%)	CA	Calcarenite
	CLMC	clayey Micrite
	CLSL	clayey, Shell Limestone
	MC	Micrite
	SDBL	sandy Biomoldic Limestone
	SDCA	sandy Calcarenite
	SDMC	sandy Micrite
	SDSL	sandy Shell Limestone
	SDXL	sandy Crystalline Limestone
	SDVL	sandy Vuggy Limestone
	SL	Shell Limestone
	XL	Crystalline Limestone

(This page intentionally left blank)

Appendix B-2 Lithologic Parameters Determined from Core Descriptions

No Recovery — The number of feet of missing or non-recovered core within the measured hydrostratigraphic interval.

Estimated Mud — The estimated number of feet of mud (silt + clay) in the interval of non-recovered core. Determined by examination of geophysical logs, including gamma-ray, SP, and resistivity curves.

Estimated Sand — The estimated number of feet of sand in the interval of non-recovered core. Determined by examination of geophysical logs, including gamma-ray, SP, and resistivity curves.

Estimated Calcareous Sand/Mud — The estimated number of feet of calcareous sand or mud in the interval of non-recovered core. Determined by examination of geophysical logs, including gamma-ray, SP, and resistivity curves. Estimated to be primarily terrigenous sand or mud with 1 - 49% carbonate material.

Estimated Limestone — The estimated number of feet of limestone in the interval of non-recovered core. Determined by examination of geophysical logs, including gamma-ray, SP, and resistivity curves. Estimated to be primarily carbonate material with <50% terrigenous sediment.

Average Percent Mud — The average percentage of mud (silt + clay) within the hydrostratigraphic unit.

Percent Calcareous Sand/Mud — The percentage of calcareous sand or mud in the hydrostratigraphic unit. Equals the total thickness divided by the thickness of the hydrostratigraphic unit or zone, multiplied by 100.

Average Percent Sand — The percentage of sand in the hydrostratigraphic unit.

Average Percent Limestone — The percentage of limestone in the hydrostratigraphic unit.

Sand/Mud Ratio

The thickness ratio of sand to mud (silt + clay). Equals the total sand in the hydrostratigraphic unit divided by the total mud in the hydrostratigraphic unit. The numerical value of the sand/mud ratio varies from zero to infinity (∞). High values in sand-mud ratios represent high percentages of sand and decreasing percentages of mud. Values smaller than 1/32 or larger than 32 indicate that one of the components is present in amounts of about 3 percent, which probably approaches the limit of the accuracy of the data. The sand/mud ratio indicates the number of feet of sand per foot of mud. For example, a sand/mud ratio of 3.2 indicates that the hydrostratigraphic interval contains 3.2 feet of sand per foot of mud. A sand/mud ratio of infinity indicates that mud beds are not present.

Clastic Ratio

The thickness ratio of terrigenous clastic sediment to limestone in the hydrostratigraphic unit. The clastic ratio is calculated by the formula (B + C)/A, where B represents the thickness of coarse detrital components, gravel and sand, and C includes the fine detrital sediments, silt and clay. Component A represents the thickness of chemically or biochemically precipitated limestone in the hydrostratigraphic unit. The numerical value of the clastic ratio varies from zero to infinity. High clastic ratio values indicate increasing percentages of sand and mud and decreasing percentages of carbonate sediment. A clastic ratio of infinity indicates that limestone is not present. (Krumbein and Sloss, 1963).

Appendix B-3 Lithologic Data from Core Descriptions

Lithologic data from core descriptions are included on the 3.5-inch IBM-compatible diskette.

(This page intentionally left blank)

Appendix B-4 SRS Core Logging Format

NOTE:
This appendix presents an explanation of all data fields in the description code used at SRS. Database fieldnames are indicated with underlined, boldface type. Superheadings (groups of related fields) are indicated in italics with underlined, boldface type. Content is adapted from WSRC ESSOP-2-15, *Binocular Examination of Sediment Core Samples*. Refer to Appendix B-*Lithologic Descriptions* for a listing of specific data fields used in the Earth Vision® dataset.

GENERAL

1). Make letters and numbers clear and unambiguos. Use standard, block, uppercase letters. Use letters and numbers only; no symbols.

2). Left justify letters; Right Justify numbers.

3). Estimating percentages

-If constituent <10% or 90%, use increments of 1%
-If constituent between 10% and 90% use increments of 5%
-Highest value is 99%
-Use .1 for trace quantities (<1%)

4). Core Description

Log core from bottom up. Slice core to observe sedimentary structures. Thin layers or laminae, less than a few inches, should be noted under "Structure".

Certain properties are best determined in hand specimen: color, structure, maximum size, roundness, sorting, etc., are best determined with a binocular microscope.

5). If there is sediment, especially pebbles and sand, in the top few inches of a core that is obviously different from the underlying material, it probably fell down ("caved") from up the hole and should not be described.

6). Put your initials (e.g., LOGGED BY: PAT) and date (DD-MM-YY format) in upper left corner of the log sheet. Fill in the page numbers in upper right corner (e.g., 1 of 8). Check in lower right corner of log sheet whether core is WET or DRY. Log core in sequence and record all page numbers in sequence.

WE*LL* (Cols. 1-8)

Record only on top line of sheet.

Cols 1-3 [**Well Series**] Letter or letters. Left justify (LJ).
Cols. 4-6 [**Well Number**] Number. Right justify (RJ).
Cols. 7-8 [**Screen Zone**] Letter. Left Justify (LJ).

Examples: P_18TA
CMP_09_

DEPTH (Cols. 9-12)

Starting at bottom of core, describe in one-foot increments. Assume that missing core results from failure to sample bottom of interval. Record on computer load sheets from the bottom of the sheet upward.

(Right Justify) (RJ).

Examples: 115
89
7
127

RECOVERY [INDUR] (Col. 14) = Degree of Lithification

1 = Loose	Core unlithified.
2 = Friable	Core coherent, but easily disaggregated.
3 = Hard	Core firm, but grains can be dislodged.
4 = Very Hard	Hard rock (some carbonates, silicified rock, or iron oxides).

COLOR (Cols. 15-19)

Left Justify (LJ).

Use most common or overall color. Prefix main rock color with shade. (i.e., light, medium, or dark).

Colors: Use first two letters of color:

BR = Brown
OR = Orange

PI = Pink
PU = Purple
RE = Red
TA = Tan
WH = White
YE = Yellow

Exceptions:

BE = Blue
BK = Black
GN = Green
GY = Gray
MT = Mottled
VAR = Variegated

STRUCTURE (Cols. 20-27) = Sedimentary Structures

Left Justify.

Leave BLANK for massive, structureless beds.

B = Color banded (B + color; e.g., BGY = banded gray)
BR = Brecciated
BU = Burrow
CLB = Clay balls (Any gravel sized clay)
CTN = Chert Nodule
FE = Iron oxide nodule
FR = Fracture
FS = Fissile
ICA = Interbedded or interlaminated calcarenite
ICL = Interbedded or interlaminated clay (silt + clay)
IMC = Interbedded or interlaminated micrite
IPB = Interbedded or interlaminated pebbles
ISD = Interbedded or interlaminated sand
MCB = Micrite balls or fragments (gravel sized)
MT = Mottled
PE = Pelleted
PY = Pyrite
RT = Root structure (cast or mold)
VN = Mineral vein
WSP = Wispy laminations or bedding
XB = Cross bedded

Examples: IPBCLB = Interbedded pebbles and clay balls
PYVN = Pyrite Vein

SILICATE **[Use only for siliciclastic fraction]** (Cols. 28-38)

PERCENT GRAVEL, SAND, MUD [%GR % SD % MD] (Cols. 28-38)

Normalize estimated percent siliciclastic gravel, sand and mud (silt + clay) to 100 % and record in appropriate column.

Right Justify.

%GR (Cols. 28-29) = **% GRAVEL (>2mm)**
%SD (Cols. 30-31) = **% SAND (2mm - 0.0625mm)**
%MD (Cols. 32-33) = **% MUD (<0.0625mm)**

SIZE (Cols. 34-37)

MX (Cols. 34-35 = **MAXIMUM SIZE**

Left Justify.

Record maximum size of siliciclastic fraction using following abbreviations:

BO = Boulder (> 256mm)
UC = Upper Cobble (128-256mm)
LC = Lower Cobble (64-128mm)
UP = Upper Cobble (16-64mm)
LP = Lower Pebble (4-16mm)
GR = Granule (2-4mm)
VC = Very Coarse Sand (1-2mm)
C = Coarse Sand (0.5-1mm)
M = Medium Sand (0.25-0.5mm)
F = Fine Sand (0.125-0.25)
VF = Very Fine Sand (0.0625-0.125mm)
CL = Silt and Clay (<0.0625mm)

MD (Cols. 36-37) = **MODAL SIZE**

Modal Size = Most Abundant Size Fraction

Left Justify.

May not be applicable to some carbonates (i.e., those that contain little or no siliciclastic material).

Record modal size using following abbreviations:

BO = Boulder (> 256mm)
UC = Upper Cobble (128-256mm)
LC = Lower Cobble (64-128mm)
UP = Upper Cobble (16-64mm)
LP = Lower Pebble (4-16mm)
GR = Granule (2-4mm)
VC = Very Coarse Sand (1-2mm)
C = Coarse Sand (0.5-1mm)
M = Medium Sand (0.25-0.5mm)
F = Fine Sand (0.125-0.25)
VF = Very Fine Sand (0.0625-0.125mm)
CL = Silt and Clay (<0.0625mm)

ROUNDNESS [RND] (Col. 38)

Record Average Roundness of Quartz grains only, using following scale:

1 = Very Angular
2 = Angular
3 = Subangular
4 = Subrounded
6 = Rounded
9 = Well Rounded

CARBONATE LITHOLOGY **[Use only for carbonate fraction]** (Cols. 39-48)

PERCENT (CARBONATE) **GRAVEL, SAND, MUD [%GR, %SD, %MD]** (Cols. 39-44)

Normalize estimated percent carbonate gravel, sand, and mud to 100%, and record in appropriate column.

Right Justify.

%GR (Cols. 39-40) **= % CARBONATE GRAVEL (>2mm)**
%SD (Cols. 41-42) **= % CARBONATE SAND (>2mm-0.0625mm)**
%MD (Cols. 43-44) **= % CARBONATE MUD (>0.0625mm)**

PERCENT CEMENT [%CMT] (Cols. 45-46)

Record total percent carbonate plus other cement (silica, iron sulfides, iron oxides, phosphate, glauconite, etc.).

Right Justify.

PERCENT CARBONATE [%CAR] (Cols. 47-48)

Check any suspicious sample with 10% hydrochloric acid, and estimate total percent carbonate.

Record total percent carbonate (Sum of matrix, cement, fossils, and other carbonate grains), with-out normalizing to 100%.

Right Justify.

ROCK NAME [%NAME] (Cols. 49-56)

Left Justify.

I. No Carbonate Present (<1% Carbonate)

A. If one size fraction 75% or greater, use following:

PB = Pebbles
SD = Sand
ST = Silt
CL = Clay

B. If another fraction is 25% or greater, use as a modifier with most abundant fraction last.

Example: SDCL = Sandy Clay

C. If **two or more** components are 25% or greater, list the **most abundant fraction last.**

Example: PBSDCL =Pebbly, Sandy Clay

Note: In most clastic sediments it is difficult to distinguish silt from clay. Generally, use CL (clay) for mixtures of clay and silt. Use ST (silt) only for silt or siltstone that is highly porous.

II. Carbonate Present (<1% Carbonate)

A. If Carbonate 75% or greater:

BL = Biomoldic Limestone (numerous megafossil molds)
CA= Calcarenite (granular, sand-sized carbonate)
GM= Green Micrite (looks like green clay)
MC= Micrite (lime mud; chalk)
SL = Shell Limestone (shells &/or shell fragments)
VL = Vuggy Limestone (numerous vugs)
XL = Crystalline Limestone (hard, massive)

B. If Carbonate 50-75%:

Prefix carbonate rock name with other constituent(s), least abundant first.

Examples: SDSL = Sandy, shell limestone
GLSDMC = Glauconitic, sandy micrite

C. If Carbonate 1-50%:

Prefix main rock name with carbonate modifier.

Examples: CM = Carbonated cemented
CMSD = Carbonate-cemented siliciclastic sand
MCCL = Micritic clay (clay is silicate)
SLSD = Shelly, siliciclastic sand

III. Other Lithologic Types

Must be 25% or greater in siliciclastic to be used as a modifier.

Use the following abbreviations:

AR = Arkosic (feldspathic)
CT = Chert cement or replacement (Use for any silica)
FE = Iron oxides (cement or replacement)
GL = Glauconite (green grains or cement)
LG = Lignite (soft, brown to black, woody fragments)
MU = Muscovite
PH = Phosphate (brown to black shell, bone, or tooth)
PY = Iron sulfides (pyrite or marcasite)

Examples:

PHMC	= phosphatic micrite
CTSLMC	= shelly micrite with chert

SORTING [SORT] (Col. 57)

Record overall sorting of rock using following scale:

W (Well sorted)	If 90% within 2 size classes
M (Moderately sorted)	If 90% within 4 size classes
P (Poorly sorted)	If 90% > 4 size classes
V (Very poorly sorted)	If 90% > 6 size classes

If a sand contains >25% CL (silt + clay) or MC, use P or V.

PERCENT POROSITY [%POR] (COL. 58-59)

Use for all lithologies. Left Justify (LJ).

Estimate percent of large pores by looking at whole core; estimate percent of small pores (2mm) using binocular microscope. Total porosity is sum of large and small pores.

Use following scale:

P (Poor)	= <5% porosity
M (Moderate)	= 5-15% porosity
G (Good)	= 15-30% porosity
E (Excellent)	= >30% porosity

PORE TYPE [PORE TYPE] (Cols. 60-61)

Use for all lithologies.

Record most abundant pore type in Cols. 60-61 using the following abbreviations:

BP =	Between Particle (Interparticle) Pore
CH=	Channel Pore
MI =	Micropore
MO=	Moldic Pore
VU=	Vug Pore
WP=	Within Particle (Intraparticle) Pore

PERCENT MUSCOVITE [%MUSC] (Cols. 62-63)

Record estimated volume percent muscovite.

Right Justify.

PERCENT GLAUCONITE [%GLAU] (Cols. 64-65)

Record estimated volume percent glauconite (As grains, matrix, or cement).

Right Justify.

PERCENT LIGNITE [%LIGN] (Cols. 66-67)

Record estimated volume percent lignite (As dark, soft, woody, peaty or coaly material).

Right Justify.

PERCENT SULPHIDES [%SULP] (Cols. 68-69)

Record estimated volume percent marcasite or pyrite.

Right Justify.

HEAVY MINERALS [HEAV] (Col. 70)

Record estimated volume percent heavy minerals (opaque and nonopaque) using the following scale:

R (Rare)	= Very few heavy mineral grains
C (Common)	= Heavy mineral grains easy to find
A (Abundant)	= "Loaded" with heavy mineral grains

FOSSILS (Cols. 71-80)

List most abundant first. Do not skip spaces between abbreviations.

If fossils are present, but you can't identify, note YE for YES.

If silicified, note CT first, then type(s).

Left justify.

Use the following abbreviations (for FOSSILS):

BA = Barnacle
BR = Bryozoan
ES = Echinoid Spine
FO = Foraminifer
GA = Gastropod
GI = *Crassostrea gigantissima*
OS = Ostracode
PL = Pelecypod
SA = Echinoderm (Sand Dollar)
SP = Sponge Spicule

Examples: CTPLGA = Silicified pelecypods & gastropods
BRFO = Bryozoans and foraminifers